

AFFDL-TR-76-66

AD-A031965

FIDY

# COMPARISON OF THE SONIC FATIGUE CHARACTERISTICS OF FOUR STRUCTURAL DESIGNS

*AERO-ACOUSTICS BRANCH  
STRUCTURES DIVISION*

SEPTEMBER 1976

TECHNICAL REPORT AFFDL-TR-76-66  
FINAL REPORT FOR PERIOD JANUARY 1972 THROUGH DECEMBER 1975

20070919101

Approved for public release; distribution unlimited

Best Available Copy

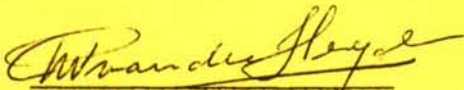
AIR FORCE FLIGHT DYNAMICS LABORATORY  
AIR FORCE WRIGHT AERONAUTICAL LABORATORIES  
AIR FORCE SYSTEMS COMMAND  
WRIGHT-PATTERSON AIR FORCE BASE, OHIO 45433

NOTICE

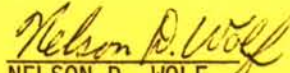
When Government drawings, specifications, or other data are used for any purpose other than in connection with a definitely related Government procurement operation, the United States Government thereby incurs no responsibility nor any obligation whatsoever; and the fact that the government may have formulated, furnished, or in any way supplied the said drawings, specifications, or other data, is not to be regarded by implication or otherwise as in any manner licensing the holder or any other person or corporation, or conveying any rights or permission to manufacture, use, or sell any patented invention that may in any way be related thereto.

This report has been reviewed by the Information Office (OI) and is releasable to the National Technical Information Service (NTIS). At NTIS, it will be available to the general public, including foreign nations.

This technical report has been reviewed and is approved for publication.

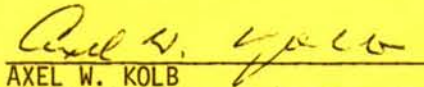


ROELOF C.W. VAN DER HEYDE  
Project Engineer



NELSON D. WOLF  
Project Engineer

FOR THE COMMANDER



AXEL W. KOLB  
Chief, Aero-Acoustics Branch  
Structures Division

Copies of this report should not be returned unless return is required by security considerations, contractual obligations, or notice on a specific document.



UNCLASSIFIED

SECURITY CLASSIFICATION OF THIS PAGE (When Data Entered)

REPORT DOCUMENTATION PAGE		READ INSTRUCTIONS BEFORE COMPLETING FORM
1. REPORT NUMBER AFFDL-TR-76-66	2. GOVT ACCESSION NO.	3. PERFORMER'S CATALOG NUMBER
4. TITLE (and Subtitle) COMPARISON OF THE SONIC FATIGUE CHARACTERISTICS OF FOUR STRUCTURAL DESIGNS		5. TYPE OF REPORT & PERIOD COVERED Final Report January 72 through December 75
		6. PERFORMING ORG. REPORT NUMBER
7. AUTHOR(s) Roelof C. W. van der Heyde Nelson D. Wolf		8. CONTRACT OR GRANT NUMBER(s)
9. PERFORMING ORGANIZATION NAME AND ADDRESS Air Force Flight Dynamics Laboratory Sonic Test Branch (AFFDL/FBF) Wright-Patterson AFB, Ohio 45433		10. PROGRAM ELEMENT, PROJECT, TASK AREA & WORK UNIT NUMBERS 62201F 14710107 1471 14710133
11. CONTROLLING OFFICE NAME AND ADDRESS Air Force Flight Dynamics Laboratory Sonic Test Branch (AFFDL/FBF) Wright-Patterson AFB, Ohio 45433		12. REPORT DATE September 1976
		13. NUMBER OF PAGES 98
14. MONITORING AGENCY NAME & ADDRESS (if different from Controlling Office)		15. SECURITY CLASS. (of this report) Unclassified
		15a. DECLASSIFICATION/DOWNGRADING SCHEDULE
16. DISTRIBUTION STATEMENT (of this Report)  Approved for public release; distribution unlimited.		
17. DISTRIBUTION STATEMENT (of the abstract entered in Block 20, if different from Report)		
18. SUPPLEMENTARY NOTES		
19. KEY WORDS (Continue on reverse side if necessary and identify by block number) Sonic Fatigue                      Panel Damping Sonic Fatigue Testing          Sonic Fatigue Design Acoustic Fatigue Dynamic Response		
20. ABSTRACT (Continue on reverse side if necessary and identify by block number) An experimental program was conducted under which the response and sonic fatigue resistance of four lightweight (1 lb/sq ft) aircraft structural panel types were investigated. Specifically, six sets of 20 aluminum alloy (7075-T 6) panels were tested: one design of skin-stringer, three designs of bonded-beaded, one design of chem-milled, and one design of corrugated panels. Each set of 20 panels was tested in four groups of five panels to obtain results with high statistical confidence levels. The data gathered included		

UNCLASSIFIED

SECURITY CLASSIFICATION OF THIS PAGE(When Data Entered)

panel damping ratios, rms stress, fatigue life and failure types. For some panel types, fatigue data in excess of  $10^8$  cycles were obtained. A comparison of the sonic fatigue resistance of the four structural designs was made and sonic fatigue design charts for bonded beaded panels developed.

UNCLASSIFIED

SECURITY CLASSIFICATION OF THIS PAGE(When Data Entered)



## FOREWORD

This report was prepared in the Aero-Acoustics Branch, Structures Division, Air Force Flight Dynamics Laboratory (AFFDL/FBF), Wright-Patterson Air Force Base, Ohio. The work was conducted under Project 1471, "Aero-Acoustic Problems in Air Force Flight Vehicles", Task 147101, "Sonic Fatigue". The work described herein has been a continuing effort under the Air Force Flight Dynamics Laboratory's exploratory development program to establish design criteria and tolerance levels for sonic fatigue prevention of structural components for flight vehicles.

The testing work including data analyses, instrumentation, and facility operation was conducted by personnel of the Instrumentation and Data Analysis Group and the Facilities Engineering Group of the AFFDL. The engineering development work including the technical aspects of the sonic fatigue testing, engineering analysis of the test results, criteria development, and reporting was performed by various personnel of the Sonic Fatigue and Acoustic Groups. Mr. R. C. W. van der Heyde was the Work Unit Engineer. Appreciation is extended to all personnel of the Aero-Acoustics Branch who contributed to the developments reported in this report and especially to Mr. A. W. Kolb who made many helpful recommendations and provided encouragement during the course of the program. The work was essentially completed during the period of January 1972 through December 1975.

## TABLE OF CONTENTS

SECTION	PAGE
I INTRODUCTION	1
II SUMMARY AND DISCUSSION OF EXPERIMENTAL RESULTS	3
1. Panel Damping Ratios and Modal Frequencies	4
a. Skin-Stringer Panels	19
b. Bonded-Beaded Panels	19
(1) Type I	19
(2) Type II	20
(3) Type III	20
c. Chem-Milled Panels	21
d. Corrugated Panels	22
2. Panel Stress and Life Data	22
3. Description of Panel Failures	29
a. Skin-Stringer Panels	39
b. Bonded-Beaded Panels	40
c. Chem-Milled Panels	41
d. Corrugated Panels	41
III DESIGN CHART FOR THE BONDED-BEADED PANELS	45
1. Theory	46
2. Analysis	46
a. Static Stress	50
b. Natural Frequency	51
c. Dynamic Stress	52

## TABLE OF CONTENTS (Contd)

SECTION	PAGE
IV CONCLUSIONS	55
1. Peak Frequency Response Variations	55
2. Panel Damping Ratio Comparison	56
3. Comparison of Four Designs	56
a. Skin-Stringer Panels	56
b. Bonded-Beaded Panels	61
c. Chem-Milled Panels	61
d. Corrugated Panels	66
APPENDIX A - DESCRIPTION OF TEST SPECIMENS	69
APPENDIX B - DESCRIPTION OF THE AFFDL WIDE BAND NOISE CHAMBER AND INSTRUMENTATION SYSTEM	79
1. Test Facility	79
a. The Reverberation Chamber	79
b. Noise Source Area	81
c. Control Room	81
d. Noise Sources	81
e. Horn System	84
f. Test Fixture	84
g. Location of the Test Fixture	85
2. Instrumentation and Data Analysis	85
APPENDIX C - STATISTICAL TECHNIQUES	89
REFERENCES	91



## LIST OF ILLUSTRATIONS

FIGURE	PAGE
1. Typical Strain Frequency Response, Filter Bandwidth 2 Hz	6
2. Damping Ratio Versus Frequency (Panel Type - Skin-Stringer)	13
3. Damping Ratio Versus Frequency (Panel Type - Bonded-Beaded, Type I)	14
4. Damping Ratio Versus Frequency (Panel Type - Bonded-Beaded, Type II)	15
5. Damping Ratio Versus Frequency (Panel Type - Bonded-Beaded, Type III)	16
6. Damping Ratio Versus Frequency (Panel Type - (Chem-Milled)	17
7. Damping Ratio Versus Frequency (Panel Type - Corrugated)	18
8. Spectrum Level - Life Relation (Panel Type - Skin-Stringer)	30
9. Spectrum Level - Life Relation (Panel Type - Bonded-Beaded, Type I)	31
10. Spectrum Level - Life Relation (Panel Type - Bonded-Beaded, Type II)	32
11. Spectrum Level - Life Relation (Panel Type - Bonded-Beaded, Type III)	33
12. Spectrum Level - Life Relation (Panel Type - Chem-Milled)	34
13. Spectrum Level - Life Relation (Panel Type - Corrugated)	35
14. RMS Stress - Life Relation (Panel Type - Skin-Stringer)	36
15. RMS Stress - Life Relation (Panel Type - Bonded-Beaded, Type I)	36
16. RMS Stress - Life Relation (Panel Type - Bonded-Beaded, Type II)	37

## LIST OF ILLUSTRATIONS (Contd)

FIGURE	PAGE
17. RMS Stress - Life Relation (Panel Type - Bonded-Beaded, Type III)	37
18. RMS Stress - Life Relation (Panel Type - Chem-Milled)	38
19. RMS Stress - Life Relation (Panel Type - Corrugated)	38
20. Typical Failure in Skin-Stringer Panels	40
21. Failures in Bonded-Beaded Panels	42
22. Typical Failures in Chem-Milled Panels	43
23. Failures in Corrugated Panels	44
24. Bonded-Beaded Panel Nomenclature	48
25. Design Chart for Bonded-Beaded Panel	54
26. Comparison Between Damping Ratios for All Panel Configurations	57
27. S/N Curves for Skin-Stringer Panels	58
28. Stress Range Versus Acoustic Loading	62
29. RMS Stress - Life Relation (Comparison Between All Panel Types)	63
30. RMS Stress - Life Relation (Comparison, Bonded-Beaded Panels)	63
31. Panel Selection Criteria	64
32. Spectrum Level - Life Relation	65
A-1. Skin-Stringer Panel	70
A-2. Chem-Milled Panel	72
A-3. Bonded-Beaded Panel Type I and Type II	73
A-4. Bonded-Beaded Panel Type III	74
A-5. Corrugated Panel	78

LIST OF ILLUSTRATIONS (Contd)

FIGURE		PAGE
B-1.	Floor Plan of the Wideband Acoustic Fatigue Facility	79
B-2.	Wall Detail for the Wideband Chamber	80
B-3.	Controls for the Siren and Air Modulator	82
B-4.	Wideband Siren with Three Horn System	82
B-5.	Air Modulator with Two Horn System	83
B-6.	Test Fixture	86
B-7.	Data Collection and Monitoring System	88
B-8.	Data Reduction System	88



## LIST OF TABLES

TABLE		PAGE
1	Panel Types Tested	4
2	Damping Ratios (Skin-Stringer Panels)	7
3	Damping Ratios (Bonded-Beaded Panels Type I)	8
4	Damping Ratios (Bonded-Beaded Panels Type II)	9
5	Damping Ratios (Bonded-Beaded Panels Type III)	10
6	Damping Ratios (Chem-Milled Panels)	11
7	Damping Ratios (Corrugated Panels)	12
8	Skin-Stringer Panels	23
9	Bonded-Beaded Panels Type I	24
10	Bonded-Beaded Panels Type II	25
11	Bonded-Beaded Panels Type III	26
12	Chem-Milled Panels	27
13	Corrugated Panels	28
14	Panel Dimensions Used for Development of Finite Element Models	47
15	Results of Nastran Calculations	49
16	Regression Coefficients	51
17	Regression Coefficients	51
18	Values of $X$ and $K_D$	52
A-1	Detail Test Specimen Dimensions	76
C-1	Calculated Values of $\epsilon$	90

## LIST OF SYMBOLS

D	Distance between bead sections, in (See Figure 24)
F	Natural frequency of first mode, Hz
$f_i$	Center frequency of ith mode, Hz
$\Delta f_i$	Frequency bandwidth, Hz
G(F)	Spectral density of acoustic excitation at the frequency F, $(\text{psi})^2/\text{Hz}$
H	Bead height, in
$K_D$	Constant, (See Eq. 4)
L	Bead length, in
N	Number of repeating bead sections (See Figure 24)
$T_B$	Bead thickness, in
$T_S$	Skin thickness, in
W	Bead width, in
X	Constant for each bonded-beaded panel type
$\delta_i$	Damping ratio for ith mode
$\zeta$	Damping ratio (1st mode)
$\sigma^2(t)$	Mean square dynamic stress, $(\text{psi})^2$
$\sigma_C$	Static stress at panel center, psi
$\sigma_D$	Dynamic stress, psi
$\sigma_0$	Static stress caused by uniform unit static pressure load, psi/psi
SPL	$20 \log_{10} \frac{P}{P_{\text{ref}}}$

SECTION I  
INTRODUCTION

The sonic fatigue failures which occurred in aircraft structural components in the late 1950's and early 1960's caused a large maintenance burden for the Air Force. This expense was estimated to be sixty million dollars over a five year period. The development of sonic fatigue data and design techniques were required to reduce the cost. Numerous investigations were initiated to study the mechanisms which cause sonic fatigue and to develop methods to obtain practical solutions to prevent sonic fatigue failures. Design criteria for many types of aircraft structures have been developed under Air Force sponsorship and by the industry in the past fifteen years. Reference 1 has a complete list of the reports describing these efforts. This research led to sonic fatigue design criteria and design charts which are widely used during the design of an aircraft. In general, this information enables the designer to select structural design parameters which result in conservative lightweight structures capable of withstanding the noise levels generated by the jet engines presently in operation. The development of new structural concepts and materials requires continuous updating of sonic fatigue design information. At the same time, existing design data require further refinement and verification. The effort described in this report falls into both categories.

The Air Force Flight Dynamics Laboratory (AFFDL) Sonic Fatigue Facility offered the capability to conduct a complete set of sonic



fatigue experiments under closely controlled conditions and with sufficient numbers of specimens to provide a high assurance of accurate results. Since sonic fatigue is normally a low-stress high-cycle phenomenon, the capability was also required for conducting tests with a very high number of load reversals (ideally  $10^9$  and higher). The purpose of the experiments reported herein was to: (1) determine the response parameters for four different structural panel types and (2) establish life curves for these types to provide a comparable basis for their sonic fatigue resistivity on an equal weight basis.

Since the program was designed to make a comparison between the panel structural types, in general only one panel design (i.e. the panel dimensions were the same), was tested for each type. The bonded-beaded panels were the exception. For this configuration three types were tested. The lack of design parameters prevented the construction of design charts for each panel type. The data obtained during the bonded-beaded panel test were supplemented with data obtained by using the technique described in Section III to obtain adequate information for the construction of a design chart. In brief, the technique described in Section III consists of developing a finite element model that was adjusted with the test data. Additional panel data were then generated by using the model and the NASTRAN digital computer program for calculating panel stress and frequency response for other panel designs. This technique enabled equations to be formulated for use in developing the design chart.

## SECTION II

### SUMMARY AND DISCUSSION OF EXPERIMENTAL RESULTS

The overall experimental program consisted of a series of tests on structural panels of four different types. These tests consisted of the following types:

1. The frequency response tests, used to determine the panel natural frequencies and the panel mode shape at each of these frequencies.
2. The static load response tests, used to provide panel stress data for uniform pressure loading for panel stiffness comparison and bonded-beaded panel design chart development.
3. The dynamic load response tests, used to determine the linearity of the stress response of the panel to increasing acoustic loading.
4. The endurance tests, used to determine the fatigue life of the panel as a function of the acoustic loading and the type and location of the panel failure. Panel response data from these tests were also used to calculate panel damping ratios. The complete results from the above tests for all panel types have been documented in References 2, 3, 4, and 5. Panel damping ratios, stress, life data, and panel failure types have been summarized in this section.

Four different structural panel types were tested under this program. All panels were constructed of 7075-T6 aluminum alloy. The types and the number of panels endurance tested are given in

Table 1. All panels had a uniform surface weight of 1 lb/sq ft. A description of the panels is given in Appendix A with the addition of the background which led to the various designs.

TABLE 1  
PANEL TYPES TESTED

<u>PANEL TYPE</u>	<u>NR ENDURANCE TESTED</u>
Skin-stringer	20
Bonded-beaded (3 designs)	60
Chem-milled	20
Corrugated	20

All tests were conducted in the AFFDL Sonic Fatigue Facility located at Wright-Patterson Air Force Base, Ohio. A detailed description of the facilities and the instrumentation used for the tests is given in Appendix B. The test procedures and instrumentation used are described in detail in References 2, 3, 4, and 5.

#### 1. PANEL DAMPING RATIOS AND MODAL FREQUENCIES

Total panel damping includes the acoustic radiation damping, panel edge damping, and damping in the panel itself. For small damping ( $\delta \ll 1$ ) the damping ratio  $\delta_i$  for the  $i$ th mode is approximately equal to one-half the ratio of frequency bandwidth  $\Delta f_i$  at the half-power point and the center frequency  $f_i$  of the mode. In equation form

$$\delta_i = 1/2 \Delta f_i / f_i$$

These data were obtained from the strain amplitude-frequency plots recorded from strain gages during the initial endurance test runs. Figure 1 shows a typical strain-frequency response curve. The frequencies ( $f_i$ ) of strain peaks greater than  $7\text{-}1/2\mu\text{in/in}$  were selected from the plots and the bandwidths ( $\Delta f_i$ ) measured at 3 dB down from the peak. The damping ratios for all panels are given in Tables 2 through 7.

Panel damping data have also been plotted in Figures 2 through 7. A least squares fit curve was calculated for all panels.

Correlation of the specific damping ratios given in Tables 2 through 7 with panel mode shapes reported in References 2, 3, 4, and 5 was not entirely possible because of the techniques used in obtaining the experimental data. Mode shapes reported in References 2, 3, 4 and 5 were determined by exciting the panel with a low level pure tone (approximately 100 dB) and adjusting the excitation frequency to peak up the response of each panel or panel bay until a maximum response was obtained. Node lines were determined by sprinkling a granular substance on the surface and letting it accumulate at the node lines by lightly exciting the panel. The mode shapes of the skin-stringer panel were obtained by recording accelerometer data (amplitude and phase) at each grid point on the panel. Mode shapes and node lines were determined from this data. Damping ratios reported in Tables 2 through 7 were determined as previously described at the higher spectrum levels given later in Subsection II-2, Tables 8 through 13. The zero crossings per second are also given in these tables.



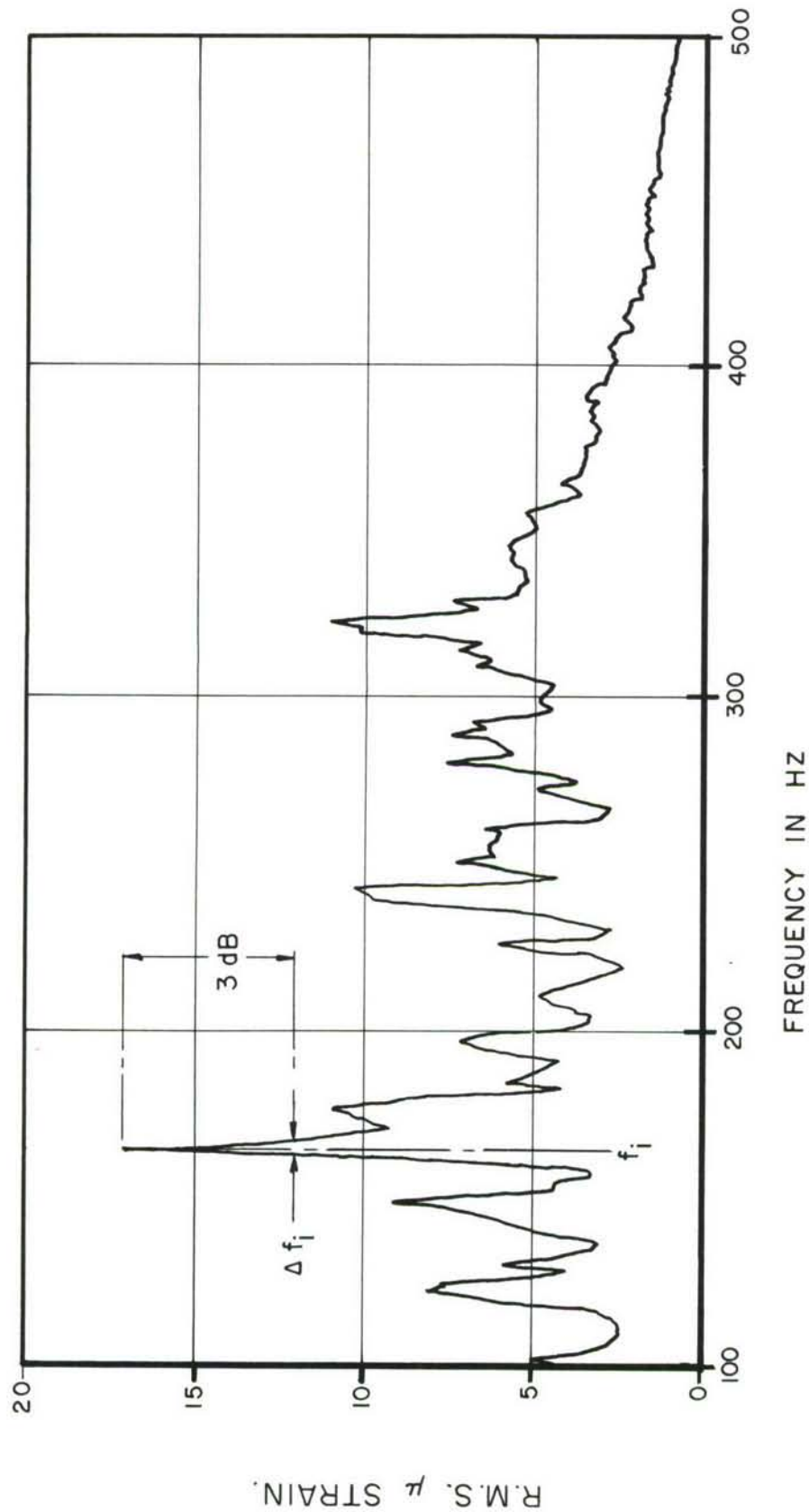


Figure 1. Typical Strain Frequency Response, Filter  
Bandwidth 2 Hz



TABLE 2  
DAMPING RATIOS (SKIN-STRINGER PANELS)

GROUP 1		GROUP 2		GROUP 3		GROUP 4	
FREQUENCY HZ	DAMPING RATIO	FREQUENCY HZ	DAMPING RATIO	FREQUENCY HZ	DAMPING RATIO	FREQUENCY HZ	DAMPING RATIO
PANEL A							
139	.0180	148	.0186	125	.0425	127	.0236
152	.0230	163	.0184	135	.0405	148	.0439
185	.0168	176	.0199	166	.0210	163	.0215
197	.0173	191	.0157	179	.0250	171	.0292
230	.0239			193	.0180	183	.0273
332	.0218			332	.0215	219	.0239
						220	.0136
						338	.0074
PANEL B							
137	.0292	101	.0325	126	.0260	102	.0392
148	.0135	124	.0351	148	.0185	133	.0263
152	.0214	127	.0275	163	.0165	145	.0345
166	.0226	147	.0187	194	.0140	165	.0242
176	.0202	163	.0190	210	.0215	183	.0164
194	.0155	193	.0233	320	.0185	193	.0207
210	.0167					208	.0192
228	.0154					222	.0225
328	.0198						
PANEL C							
130	.0250	129	.0337	168	.0145	149	.0168
149	.0235	138	.0243	187	.0235	161	.0248
168	.0208	149	.0252	208	.0140	175	.0220
175	.0143	164	.0198	229	.0130	201	.0124
195	.0231	182	.0198	240	.0160	212	.0165
207	.0181	203	.0160	264	.0170	230	.0174
229	.0153	224	.0161	354	.0210	337	.0223
239	.0167						
257	.0195						
PANEL D							
103	.0267	131	.0259	102	.0295	152	.0230
131	.0305	148	.0186	126	.0315	177	.0226
198	.0202	164	.0183	133	.0225		
PANEL E							
131	.0420	100	.0340	102	.0295	102	.0294
154	.0260	127	.0303	135	.0335	127	.0354
165	.0197	139	.0288	141	.0185	151	.0232
176	.0199	153	.0229	162	.0155	193	.0155
184	.0190	173	.0245	177	.0180	227	.0176
207	.0145	183	.0224	199	.0160	321	.0140
312	.0232	193	.0197	323	.0215		
		205	.0171				

NOTE: ALL TESTS CONDUCTED WITH WIDE BAND SIREN.

TABLE 3  
DAMPING RATIOS (BONDED-BEADED PANELS TYPE I)

GROUP 1		GROUP 2		GROUP 3		GROUP 4	
FREQUENCY HZ	DAMPING RATIO	FREQUENCY HZ	DAMPING RATIO	FREQUENCY HZ	DAMPING RATIO	FREQUENCY HZ	DAMPING RATIO
PANEL A							
139	.0180	125	.0176	140	.0143	153	.0098
153	.0131	142	.0239	200	.0100	203	.0123
171	.0132	164	.0171	210	.0072	227	.0111
183	.0109	176	.0312	218	.0092		
		195	.0113				
		230	.0139				
PANEL B							
144	.0244	124	.0282	126	.0178	139	.0162
172	.0088	132	.0227	142	.0228	146	.0106
		146	.0274	167	.0105	155	.0097
		164	.0158	175	.0100	166	.0210
		176	.0227			170	.0220
		196	.0102			220	.0088
		211	.0132			223	.0101
		226	.0080			292	.0086
		238	.0126				
PANEL C							
139	.0144	138	.0145	124	.0121	136	.0148
154	.0122	192	.0104	154	.0164	144	.0242
		238	.0088	168	.0149	153	.0115
				202	.0074	166	.0090
						175	.0115
						184	.0082
PANEL D							
134	.0205	102	.0196	134	.0206	133	.0195
146	.0154	132	.0303	145	.0138	137	.0237
153	.0114	148	.0135	154	.0097	146	.0154
		162	.0185			155	.0081
		196	.0112				
PANEL E							
140	.0142	102	.0294	125	.0280	140	.0214
150	.0216	126	.0254	141	.0177	155	.0113
		164	.0201	154	.0130		
		186	.0134				
		192	.0125				

TABLE 4  
DAMPING RATIOS (BONDED-BEADED PANELS TYPE II)

GROUP 1		GROUP 2		GROUP 3		GROUP 4	
FREQUENCY HZ	DAMPING RATIO	FREQUENCY HZ	DAMPING RATIO	FREQUENCY HZ	DAMPING RATIO	FREQUENCY HZ	DAMPING RATIO
PANEL A							
141	.0150	143	.0146	142	.0155	128	.0219
182	.0159	163	.0154	181	.0315	144	.0218
208	.0079	184	.0176	226	.0124	167	.0060
		200	.0096			182	.0187
		221	.0102				
PANEL B							
112	.0357	112	.0292	115	.0129	126	.0254
140	.0121	140	.0116	168	.0208	148	.0216
165	.0303	176	.0099	173	.0173	167	.0084
176	.0114	196	.0115	222	.0099	180	.0144
197	.0112	209	.0084	283	.0141	242	.0132
208	.0077	220	.0110			326	.0086
226	.0124	230	.0109				
231	.0130	238	.0084				
237	.0089						
PANEL C							
168	.0149	110	.0204	138	.0181	104	.0308
204	.0134	141	.0142	155	.0181	141	.0156
217	.0083	168	.0133	168	.0131	157	.0166
		203	.0123	176	.0176	168	.0131
		217	.0092	186	.0116		
				322	.0062		
				336	.0119		
PANEL D							
162	.0123	163	.0123	126	.0318	103	.0214
183	.0109	183	.0094	135	.0111	132	.0189
				142	.0246	169	.0122
				156	.0141		
				173	.0202		
PANEL E							
163	.0129	162	.0123	136	.0294	103	.0196
186	.0164	187	.0160	146	.0206	164	.0219
232	.0121	220	.0125	156	.0128		
		233	.0107	223	.0134		
				279	.0108		

NOTE: GROUP 3 PANELS TESTED WITH WIDE BAND SIREN.

TABLE 5  
DAMPING RATIOS (BONDED-BEADED PANELS TYPE III)

GROUP 1		GROUP 2		GROUP 3		GROUP 4	
FREQUENCY HZ	DAMPING RATIO	FREQUENCY HZ	DAMPING RATIO	FREQUENCY HZ	DAMPING RATIO	FREQUENCY HZ	DAMPING RATIO
PANEL A							
225	.0111	112	.0180	108	.0162	108	.0116
		225	.0100	125	.0160	116	.0064
				210	.0107	125	.0110
				220	.0125	210	.0084
						220	.0091
PANEL B							
224	.0156	163	.0108	164	.0107	104	.0144
233	.0097	224	.0145	210	.0114	111	.0130
				226	.0111	125	.0110
						145	.0086
						165	.0121
						212	.0076
						252	.0054
						328	.0092
PANEL C							
126	.0139	123	.0183	112	.0179	111	.0180
		200	.0083	124	.0181	125	.0140
				210	.0119		
				220	.0091		
				226	.0066		
				232	.0086		
				338	.0118		
PANEL D							
100	.0350	110	.0160	109	.0184	102	.0196
200	.0250	133	.0095	205	.0122	110	.0096
		213	.0106			192	.0078
		224	.0100				
		328	.0099				
PANEL E							
115	.0218	111	.0292	110	.0204	108	.0232
125	.0120	125	.0140	196	.0127	125	.0100
215	.0082	219	.0103			200	.0082
221	.0090					326	.0092

TABLE 6  
DAMPING RATIOS (CHEM-MILLED PANELS)

GROUP 1		GROUP 2		GROUP 3		GROUP 4	
FREQUENCY HZ	DAMPING RATIO	FREQUENCY HZ	DAMPING RATIO	FREQUENCY HZ	DAMPING RATIO	FREQUENCY HZ	DAMPING RATIO
PANEL A							
70	.0570	66	.0682	75	.0233	68	.0441
		254	.0128	100	.0125	143	.0210
				250	.0130	418	.0066
				280	.0045		
PANEL B							
70	.0446	70	.0393	70	.0214	68	.0368
164	.0335			99	.0277	162	.0154
412	.0093			145	.0120	400	.0031
				160	.0141		
				192	.0182		
				288	.0078		
				410	.0039		
PANEL C							
66	.0341	397	.0057	80	.0219	68	.0588
82	.0209	440	.0023	101	.0223	402	.0050
				119	.0097	418	.0048
				136	.0118		
				179	.0056		
				202	.0079		
				299	.0067		
PANEL D							
66	.0341	67	.0373	65	.0344	65	.0462
84	.0357	254	.0266	101	.0149	216	.0185
225	.0167	401	.0137	131	.0172	416	.0084
				195	.0090		
				262	.0105		
				405	.0062		
PANEL E							
71	.0282	65	.0308	66	.0189	65	.0385
85	.0441	81	.0309	101	.0292	390	.0090
				115	.0152		
				184	.0061		
				236	.0053		
				258	.0097		
				271	.0101		
				396	.0063		

NOTE: GROUP 3 PANELS TESTED WITH WIDE BAND SIREN.



TABLE 7  
DAMPING RATIOS (CORRUGATED PANELS)

GROUP 1		GROUP 2		GROUP 3		GROUP 4	
FREQUENCY HZ	DAMPING RATIO	FREQUENCY HZ	DAMPING RATIO	FREQUENCY HZ	DAMPING RATIO	FREQUENCY HZ	DAMPING RATIO
PANEL A							
252	.0089	250	.0080	256	.0098	163	.0084
258	.0068	256	.0098			177	.0098
						190	.0105
						207	.0096
						226	.0100
						249	.0080
						269	.0084
						280	.0054
PANEL B							
225	.0078	225	.0056	215	.0081	162	.0116
232	.0054	237	.0095	224	.0056	202	.0086
238	.0084	240	.0063	227	.0066	223	.0078
250	.0090	253	.0099	243	.0072	238	.0068
258	.0068	258	.0097	256	.0088	250	.0055
270	.0046	260	.0067	264	.0076		
		264	.0076	277	.0045		
		276	.0054	282	.0035		
				415	.0048		
PANEL C							
220	.0057	242	.0093	228	.0044	162	.0116
231	.0076	260	.0085	243	.0041	180	.0111
240	.0094	265	.0066	264	.0057	207	.0084
248	.0060	275	.0064			212	.0067
251	.0080					224	.0061
258	.0068					238	.0094
265	.0075					263	.0095
270	.0046					281	.0044
274	.0046						
PANEL D							
225	.0056	222	.0079	222	.0068	188	.0066
238	.0063	228	.0066	228	.0077	195	.0077
255	.0059	233	.0054	235	.0053	222	.0078
		249	.0050			239	.0073
		259	.0087			253	.0060
						261	.0106
PANEL E							
230	.0054	228	.0066	200	.0113	183	.0089
253	.0059	233	.0075	222	.0135	194	.0077
258	.0058	243	.0065	229	.0076	209	.0126
265	.0047	251	.0050	234	.0075	232	.0060
		265	.0057	253	.0040		
				258	.0048		
				208	.0056		
				279	.0036		

NOTE: GROUP 4 PANELS TESTED WITH WIDE BAND SIREN.

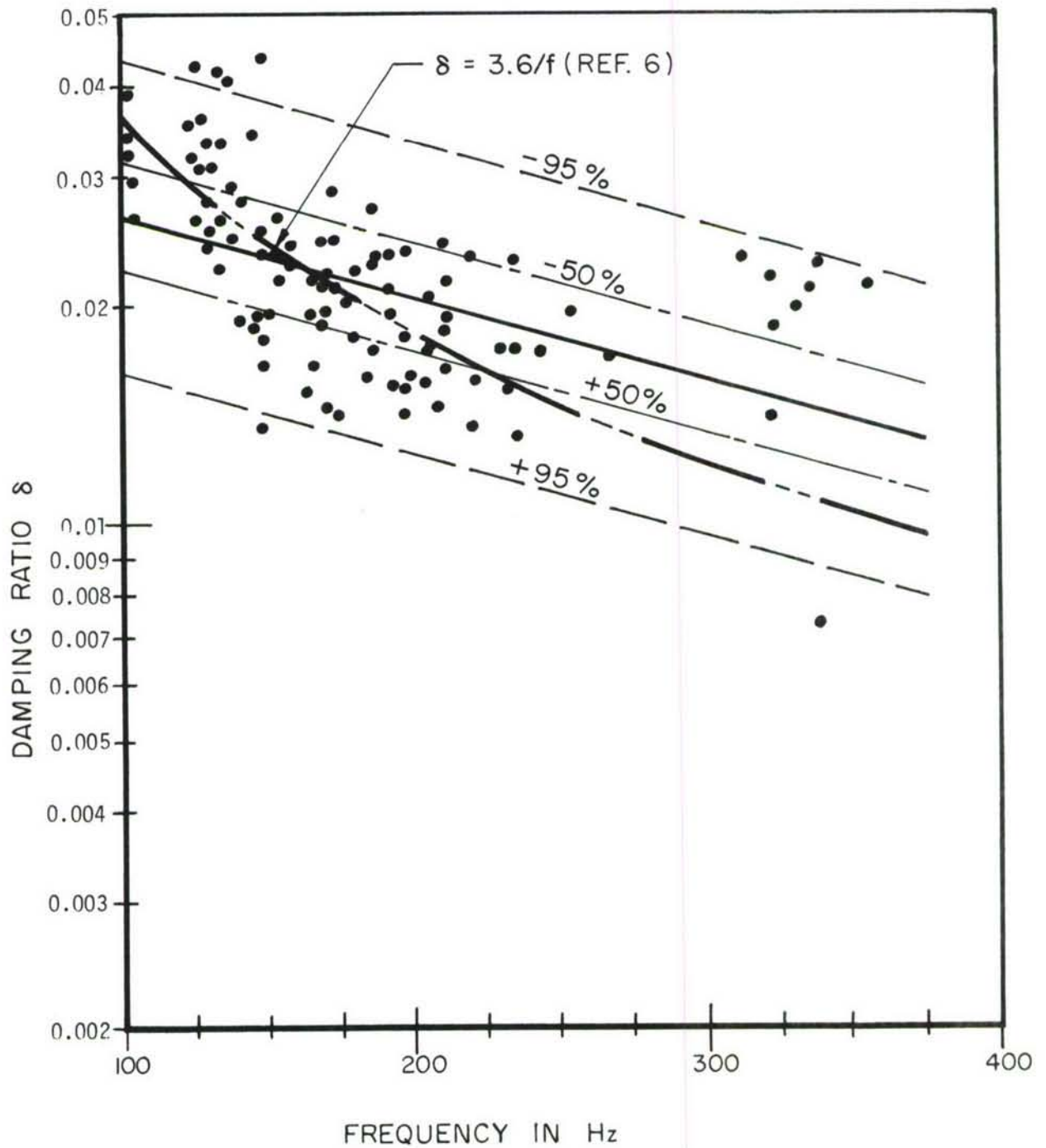


Figure 2. Damping Ratio Versus Frequency (Panel Type - Skin-Stringer)

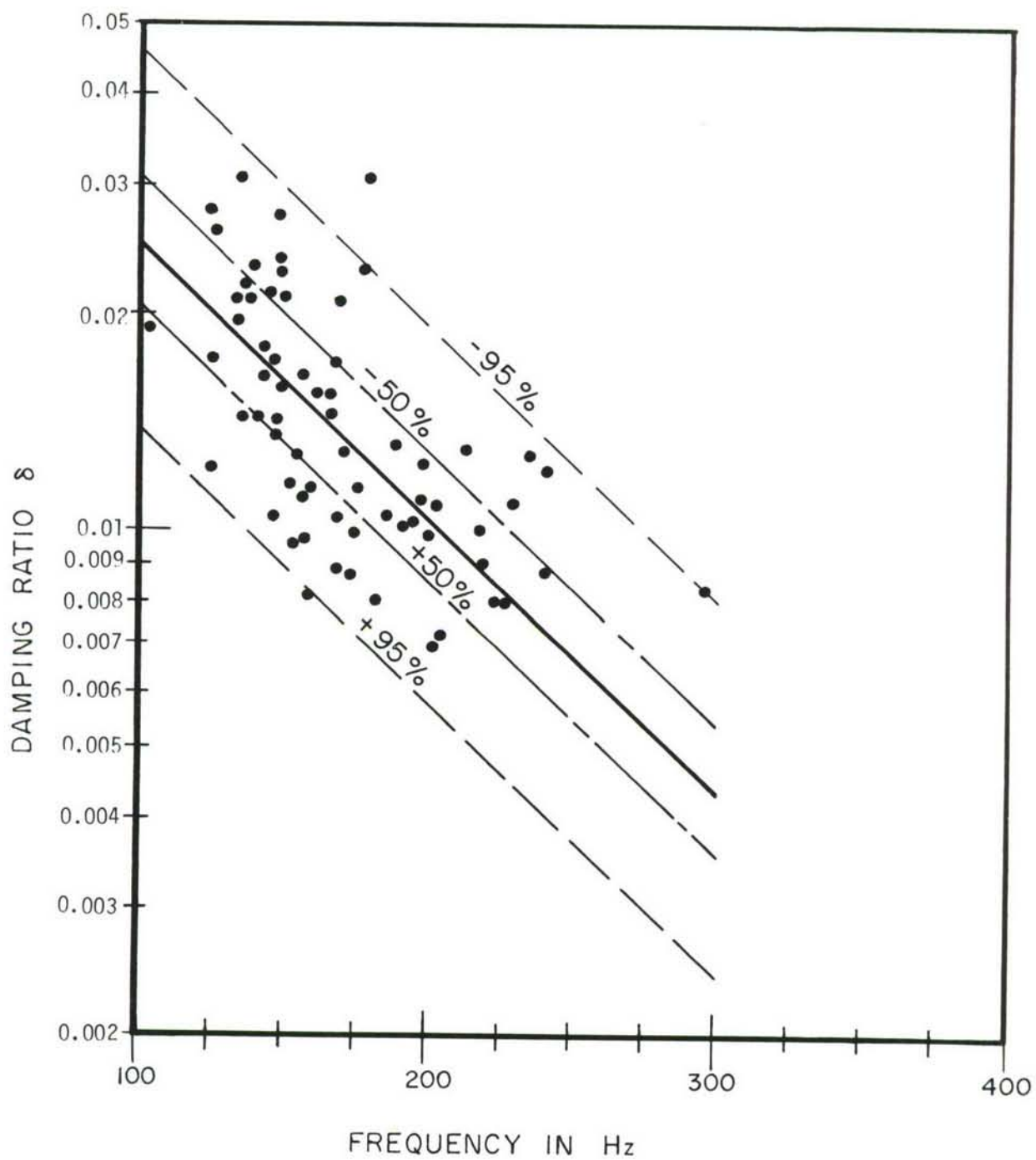


Figure 3. Damping Ratio Versus Frequency (Panel Type - Bonded-Beaded, Type I)

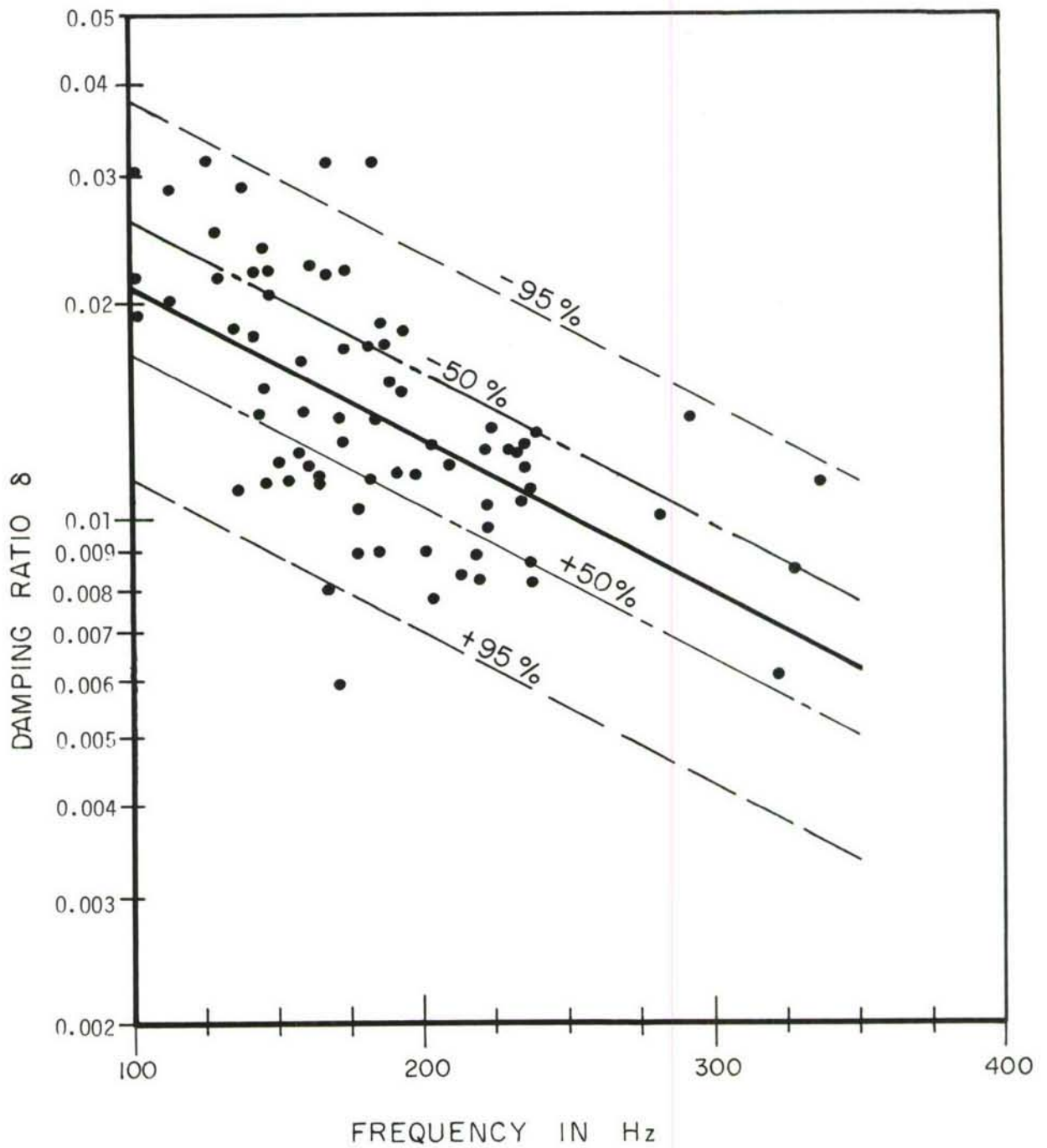


Figure 4. Damping Ratio Versus Frequency (Panel Type - Bonded-Beaded, Type II)

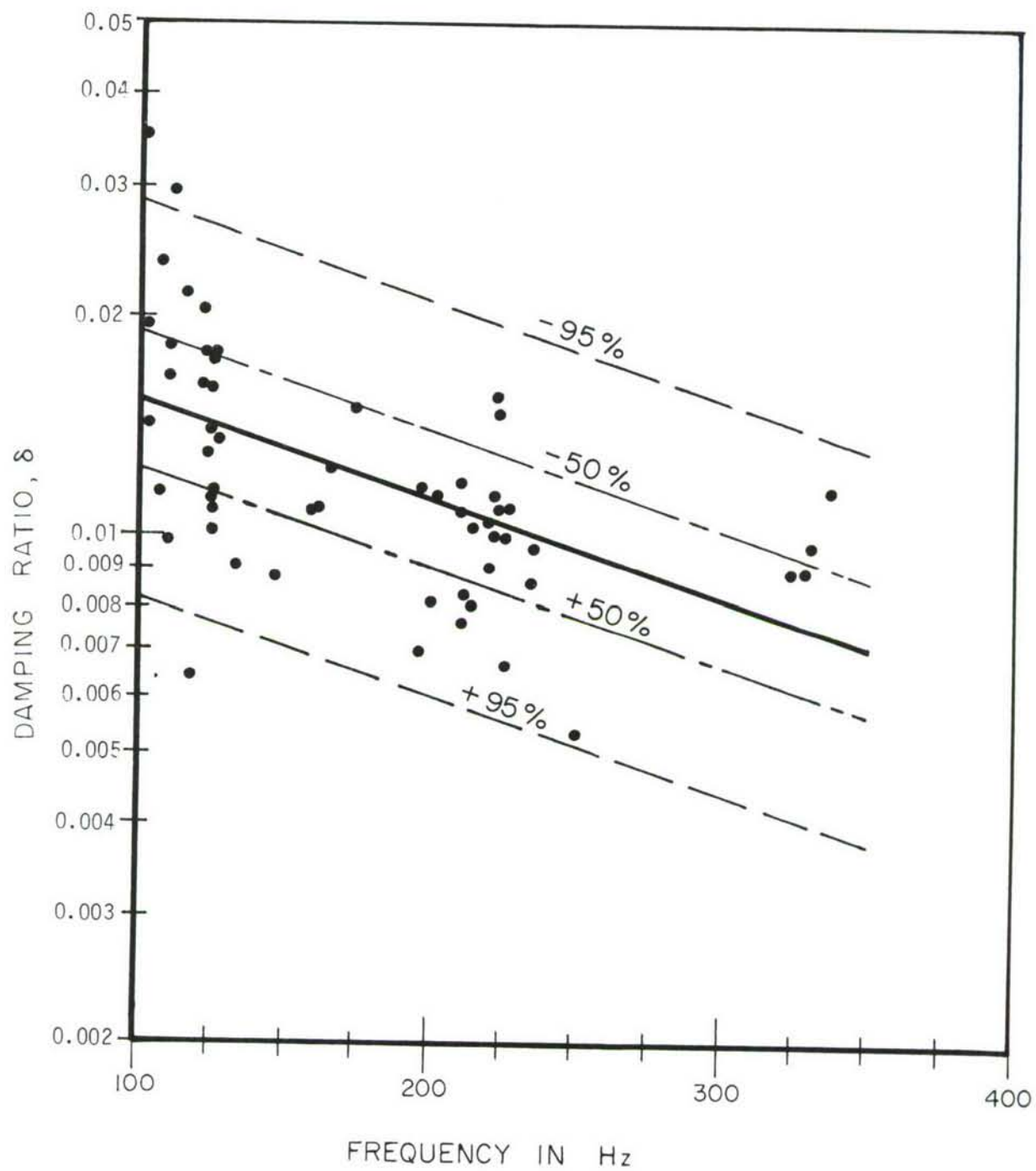


Figure 5. Damping Ratio Versus Frequency (Panel Type - Bonded-Beaded, Type III)



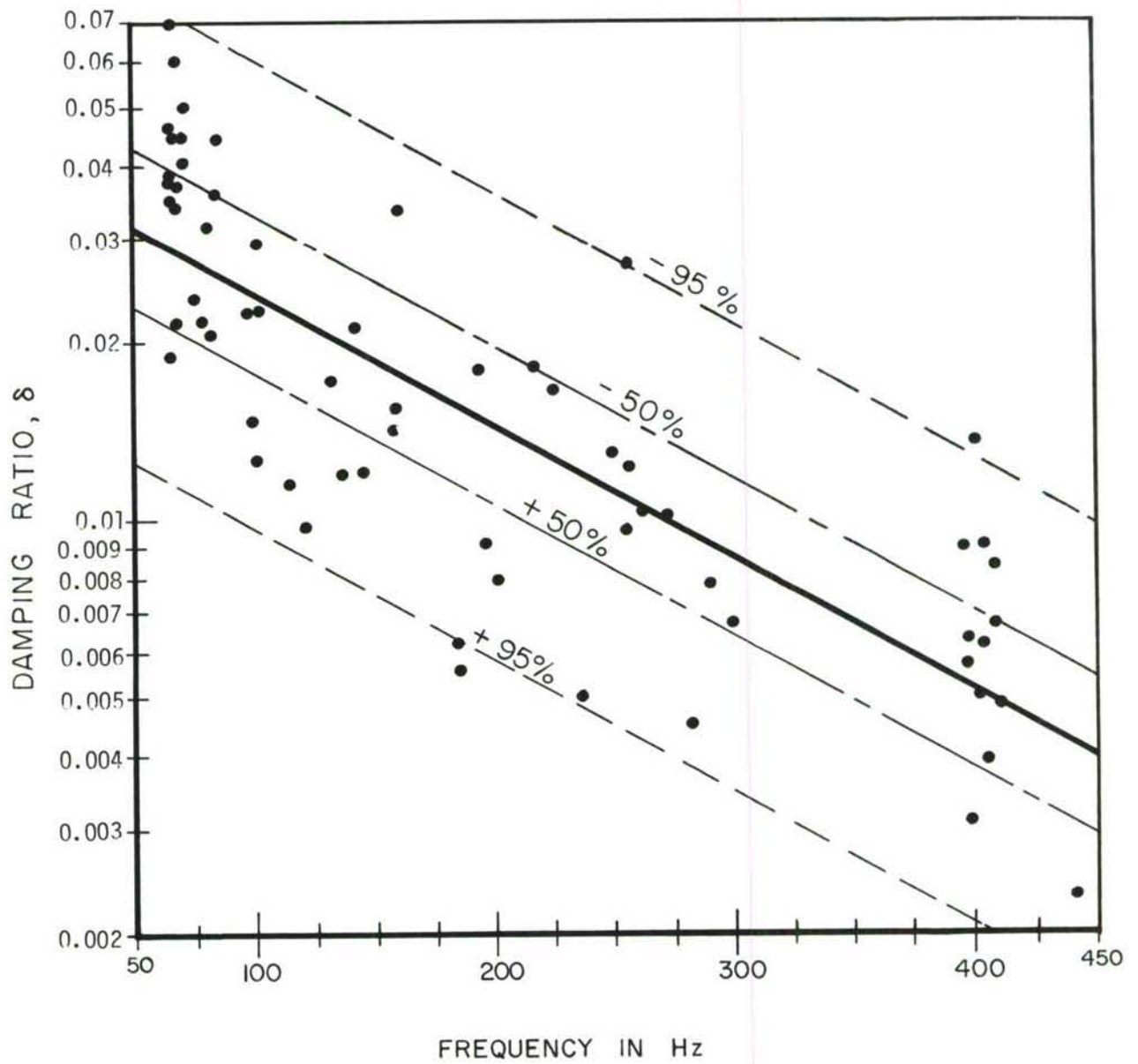


Figure 6. Damping Ratio Versus Frequency (Panel Type - (Chem-Milled))

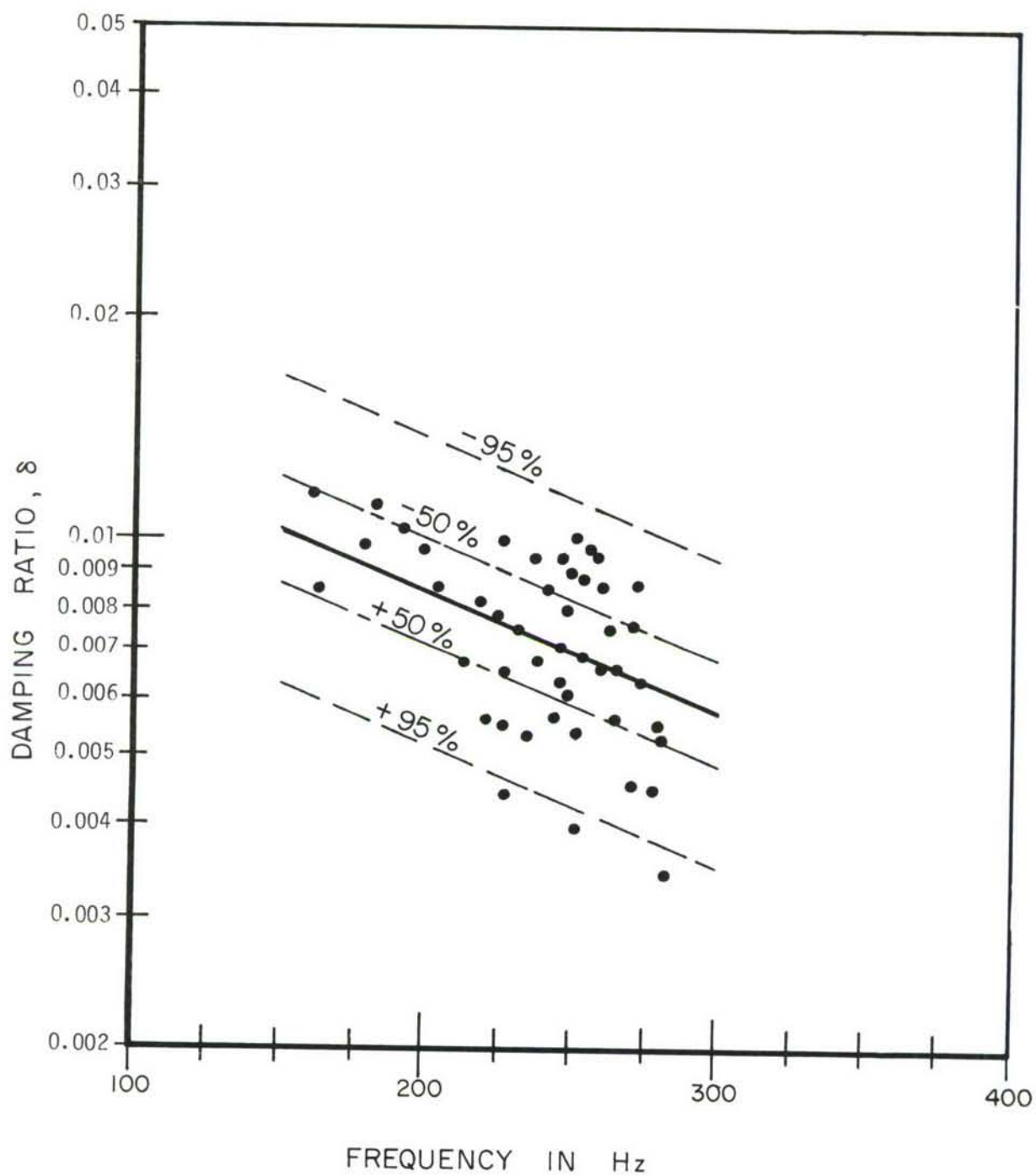


Figure 7. Damping Ratio Versus Frequency (Panel Type - Corrugated)

a. Skin-Stringer Panels

The first mode natural frequency for these panels was estimated to range between 125 to 130 Hz based upon data taken from Reference 2. Damping in this mode was estimated to range between 2.5-4.3% based upon data in Table 2. The zero crossings per second given in Table 8 range from 126 to 194 and in general are higher than the first mode frequencies which tends to show the effects of the higher modes. A large number of response peaks were present in the wide band excitation data as can be observed in Table 2. The value of the damping ratio taken from the mean curve of Figure 2 at 125 Hz is 0.026 and the median value taken from Table 2 between frequencies of 125 to 131 Hz is 0.030. Damping values for this panel type, same design, have also been reported in Reference 6 and the damping curve from this reference is plotted on Figure 2.

b. Bonded-Beaded Panels

(1) Type I

The first mode natural frequency for these panels was 143 Hz based upon data taken from Reference 3. Damping in this mode was estimated to range between 1.1-2.7% based upon data in Table 3 for frequencies from 139 to 148 Hz. Peaks in this frequency range were found on 17 of the 20 wide band response curves and showed a moderately strong correlation with the first modal frequency. On 14 of the panels tested, there were four or less response peaks up to 450 Hz. The zero crossings per second given in Subsection II-2, Table 9, range from 147 to 210 and are generally higher than the first mode

frequencies which tends to show the effects of the higher modes. The value of the damping ratio taken from the mean curve of Figure 3 at 143 Hz is 0.018 and the median value taken from Table 3 between frequencies of 139 to 148 Hz is 0.016.

(2) Type II

The first mode natural frequency for these panels was also 143 based upon data taken from Reference 3. Damping in this mode was estimated to range between 1.2 to 2.5% based upon data in Table 4 for frequencies from 138 to 148 Hz. Peaks in this frequency range were found on 12 of the 20 response curves and showed a moderate correlation with the first modal frequency. On 11 of the panels tested, there were four or less response peaks up to 450 Hz. The zero crossings per second given in Subsection II-2, Table 10, range from 121 to 315 and are higher than the first mode frequency which tends to show the effects of the higher modes. The value of the damping ratio taken from the mean curve of Figure 4 at 143 Hz is 0.018 and the median value taken from Table 4 between frequencies of 138 to 148 Hz is 0.016.

(3) Type III

The first mode natural frequency for these panels was 120 Hz based upon data taken from Reference 3. Damping in this mode was estimated to range between 1.0 to 1.8% based upon data in Table 5 for frequencies from 123 to 125 Hz. Peaks in this frequency range were found on 10 of the 20 response curves and showed only a weak correlation with the first modal frequency. The 1-5 mode was also

clearly evident in Reference 3 and occurred at a frequency of 223 Hz. Damping in this mode was estimated to range between 0.70 to 1.6% based upon data in Table 5 for frequencies from 220 to 226 Hz. Peaks in this frequency range were found on 11 of the 20 response curves and showed only a weak correlation with the 1-5 response mode. The zero crossings per second given in Subsection II-2, Table 6, range from 130 to 434 and are higher than the first mode frequency and generally higher than the 1-5 modal frequency. On 16 of the panels tested, there were four or less response peaks up to 450 Hz. The values of the damping ratios taken from the mean curve of Figure 5 at frequencies of 120 Hz and 223 Hz are 0.015 and 0.010 respectively. The median values for the frequency ranges of 123 to 125 Hz and 220 to 226 Hz are 0.014 and 0.010 respectively.

c. Chem-milled Panels

The first mode natural frequency for these panels was 66 Hz based upon data taken from Reference 4. Damping in this mode was estimated to range between 1.9 - 6.8% based upon data in Table 6 for frequencies from 65 - 75 Hz. Causes for the wide spread in the data are unknown but may show the damping of these panels to be sensitive to mounting conditions. Peaks in this frequency range were found on 19 of the 20 wide band response curves and showed a strong correlation with the first modal frequency. On 16 of the panels tested, there were four or less response peaks up to 450 Hz. The zero crossings per second given in Subsection II-2, Table 12, range from 66 to 79 Hz and confirmed the strong first mode panel response.



The value of the damping ratio taken from the mean curve of Figure 6 at 66 Hz is 0.043 and the median taken from Table 6 between frequencies of 65 to 75 Hz is 0.037.

d. Corrugated Panels

The first mode natural frequency for these panels was estimated at 289 Hz based upon data taken from Reference 5. Damping in this mode could not be definitely established because response peaks taken from the wide band response data were generally below this frequency value with the greatest number of peaks occurring between 225 to 275 Hz (Table 7). Vibration modes were not identified for these response peaks. These frequencies as well as the above modal frequency also poorly correlate with the zero crossings per second given in Subsection II-2, Table 13. The majority of these values were above 300 Hz. The damping ratios calculated for all frequencies for all panels were generally below 1%. For an estimated mean response frequency of 240 Hz, the damping ratio taken from the mean curve of Figure 7 was 0.007.

2. PANEL STRESS AND LIFE DATA

The data recorded during the endurance testing of the panels are given in Tables 8 through 13. These include the acoustic loading, spectrum level in dB, panel stress in psi, zero crossings per second, life, and panel failure locations. The rms version of the principal stress has been calculated from strain readings taken from a rosette gage located on the facing sheet at the panel center except for the skin-stringer panel, where the rosette was located at the edge of the

TABLE 8  
SKIN-STRINGER PANELS

PANEL NR	OVERALL SPL DB	SPECTRUM LEVEL dB	PRINCIPAL STRESS PSI	STRESS CENTER LONG SIDE (PSI)	STRESS CENTER SHORT SIDE (PSI)	ZERO CROSSING 1/SEC	LIFE MILLION CYCLES	FAILURE LOCATION
A-1	154.5	128.1	2532	2085		129	2.44	RIVET LINE
B-1	155.0	126.9	3097	2294		126	1.68	RIVET LINE
C-1	154.1	129.6	3708	2156		176	2.34	RIVET LINE
D-1	155.0	121.6	2479	2492		164	1.54	PANEL EDGE
E-1	154.8	121.1	2559	2385		179	1.68	PANEL EDGE
A-2	151.0	123.7	1966	1348		183	5.60	RIVET LINE
B-2	151.6	124.0	1989	1685		160	4.90	RIVET LINE
C-2	151.7	123.0	2131	1706		194	14.78	RIVET LINE
D-2	151.4	126.8	2230	1595		132	1.98	RIVET LINE
E-2	151.2	126.0	2593	1703		143	5.28	RIVET LINE
A-3	148.9	121.5	1092	1269		181	22.81	RIVET LINE
B-3	149.4	120.6	2342	1179		148	9.32	RIVET LINE
C-3	148.5	120.9	1696	1429		186	23.44	RIVET LINE
D-3	149.6	124.8	1843	1528		129	9.42	RIVET LINE
E-3	149.3	124.5	809	1258		135	17.01	RIVET LINE
A-4	147.1	120.0	1770	772		164	22.53	RIVET LINE
B-4	147.6	119.5	1460	1122		132	86.29	RIVET LINE
C-4	146.4	199.0	1041	728		182	>130.00	NO FAILURE
D-4	147.5	117.7	1842			142	32.55	RIVET LINE
E-4	147.4	113.7	1482	794		152	25.86	RIVET LINE

NOTE: ALL PANELS TESTED WITH THE WIDE BAND SIREN

TABLE 9  
BONDED-BEADED PANELS TYPE I.

PANEL No	OVERALL SPL DB	SPECTRUM LEVEL dB	PRINCIPAL STRESS PSI	STRESS CENTER LONG SIDE (PSI)	STRESS CENTER SHORT SIDE (PSI)	ZERO CROSSING 1/SEC	LIFE MILLION CYCLES	FAILURE LOCATION
A-1	157.0	131.4	1657	1778		210	5.67	BEAD END
B-1	158.0	130.5	1866	2561		196	5.29	BEAD END
C-1	157.5	132.2	1561	1259		183	4.61	BEAD END
D-1	158.0	128.0	2418	1155		148	3.73	BEAD END
E-1	157.0	127.9	2354	2052		156	3.93	BEAD END
A-2	152.5	129.4	936	1540		177	9.50	BEAD END/PANEL EDGE
B-2	153.5	128.4	941	2002	891	200	18.36	PANEL EDGE
C-2	152.5	130.1	977	1412		147	16.25	PANEL EDGE
D-2	153.5	125.9	1170	1496		168	10.03	BEAD END/PANEL EDGE
E-2	152.0	125.9	983	1454		155	10.04	BEAD END/PANEL EDGE
A-3	151.5	128.4	954	1496		185	19.81	PANEL EDGE
B-3	151.5	128.5	812	1208	729	175	66.46	PANEL EDGE
C-3	151.5	128.6	836	865		166	14.46	PANEL EDGE
D-3	151.5	124.1	912	1188		150	19.44	PANEL EDGE
E-3	152.5	125.4	95	2441		155	6.51	BEAD END
A-4	149.5	125.4	898	1496		176	109.25	PANEL EDGE
B-4	150.0	124.5	902	1295	917	198	>125.00	NO FAILURES
C-4	149.0	125.6	746	1372		168	33.81	PANEL EDGE
D-4	150.0	129.9	626	972		195	42.12	PANEL EDGE
E-4	150.0	121.9	937	917		160	72.86	PANEL EDGE

TABLE 10  
BONDED-BEADED PANELS TYPE II.

PANEL NR	OVERALL SPL DB	SPECTRUM LEVEL dB	PRINCIPAL STRESS PSI	STRESS CENTER LONG SIDE (PSI)	STRESS CENTER SHORT SIDE (PSI)	ZERO CROSSING 1/SEC	LIFE MILLION CYCLES	FAILURE LOCATION
A-1	157.0	131.4	2268	1090		213	3.07	PANEL SKIN
B-1	158.0	130.2	1771	1372		246	1.77	PANEL SKIN
C-1	157.5	132.4	1769	1250		212	2.67	PANEL SKIN
D-1	158.0	128.3	1754			233	3.36	PANEL SKIN
E-1	157.5	128.3	1614	1059		187	2.69	PANEL SKIN
A-2	152.5	129.4	1578	917		259	22.61	PANEL SKIN
B-2	153.5	128.9	1322	1258		310	21.20	PANEL SKIN
C-2	152.5	130.1	1302	1000		256	17.51	PANEL SKIN
D-2	153.5	126.9	1583	613		193	13.20	PANEL SKIN
E-2	152.0	127.9	1758	771		265	18.13	PANEL SKIN
A-3	151.5	128.1	1291	1259	1122	213	12.15	BEAD END/PANEL EDGE
B-3	151.0	128.9	1331	944	944	246	18.58	PANEL SKIN
C-3	150.0	129.4	1248	335	613	212	34.02	PANEL EDGE
D-3	151.5	126.0	1238		410	233	64.47	PANEL EDGE
E-3	150.5	127.9	1194	866	750	187	40.82	PANEL SKIN
A-4	149.5	126.4	1241	817		259	119.98	PANEL EDGE
B-4	150.0	125.1	994	794		310	>140.	NO FAILURES
C-4	149.0	126.9	1003	398		256	108.36	BEAD END
D-4	150.0	129.9	1033	771		193	>140.	NO FAILURES
E-4	150.0	124.3	904	562		265	116.68	PANEL EDGE

NOTE: GROUP 3 PANELS TESTED WITH WIDE BAND SIREN.



TABLE II  
BONDED-BEADED PANELS TYPE III.

PANEL NR	OVERALL SPL DB	SPECTRUM LEVEL DB	PRINCIPAL STRESS PSI	STRESS CENTER LONG SIDE (PSI)	STRESS CENTER SHORT SIDE (PSI)	ZERO CROSSING 1/SEC	LIFE MILLION CYCLES	FAILURE LOCATION
A-1	160.8	135.6	4157	4467		133	.95	BEAD END
B-1	162.2	132.4	3826	4340		344	1.19	BEAD END
C-1	159.8	136.9	4164	1995		229	1.08	BEAD END
D-1	161.0	133.4	4201	3072		182	.64	BEAD END
E-1	160.0		4864					BEAD END
A-2	155.8	128.1	4386	3350		336	3.02	BEAD END
B-2	156.8	129.5	3298	3652		307	1.38	BEAD END
C-2	156.0	128.9	3330	2371		330	8.12	BEAD END
D-2	154.8	128.1	3840	3072		341	1.64	BEAD END
E-2	153.5	125.5	3517	3548		434	4.09	BEAD END
A-3	151.5	122.9	3087	3073		234	5.48	BEAD END
B-3	151.8	125.4	2203	1333		340	>110.	NO FAILURES
C-3	153.8	124.4	2502	2175		253	34.06	BEAD END/PANEL EDGE
D-3	150.0	124.1	2059	1778		253	45.54	BEAD END/PANEL EDGE
E-3	150.0	122.1	3177	1778		265	34.34	PANEL EDGE
A-4	147.0	124.6	2039	1454		143	5.66	PANEL EDGE
B-4	148.5	126.9	1213	596	972	163	34.33	PANEL EDGE
C-4	147.0	124.9	1294	771		160	112.70	PANEL EDGE
D-4	146.0	123.6	1876	841		130	58.50	BONDING FAILURE
E-4	146.2	121.9	1432	1155		250	76.88	PANEL EDGE



TABLE 12  
CHEM-MILLED PANELS

PANEL No	OVERALL SPL DB	SPECTRUM LEVEL dB	PRINCIPAL STRESS PSI	STRESS CENTER LONG SIDE (PSI)	STRESS CENTER SHORT SIDE (PSI)	ZERO CROSSING 1/SEC	LIFE MILLION CYCLES	FAILURE LOCATION
A-1	154.0	134.0	4017	2114		67	.53	PANEL CENTER
B-1	155.5	134.0	4301	1830		70	2.23	PANEL CENTER
C-1	154.5	134.5	4710	1778		76	1.32	PANEL CENTER
D-1	154.5	137.5	6747	2985		71	.57	PANEL CENTER
E-1	155.5	136.5	3411	3162		79	.63	PANEL CENTER
A-2	151.0	132.5	3367	1631		68	3.55	PANEL CENTER
B-2	151.0	131.5	3613	1631		71	4.47	PANEL CENTER
C-2	151.0	132.0	4268	1454		74	4.66	PANEL CENTER
D-2	151.5	134.5	4576	2304		70	1.26	PANEL CENTER
E-2	153.5	135.5	4784	2585		78	.98	PANEL CENTER
A-3	141.5	124.0	2163	1059		68	>49.	NO FAILURES
B-3	141.5	122.5	1175	521		67	>49.	NO FAILURES
C-3	143.0	125.5	2636	917		75	>54.	NO FAILURES
D-3	143.0	127.0	2662	1000		69	9.65	PANEL EDGE
E-3	144.0	126.5	2056	917		74	19.11	PANEL EDGE
A-4	154.5	120.5	2053	298		66	6.89	PANEL EDGE
B-4	155.0	122.5	1830	298		72	7.52	PANEL EDGE
C-4	154.0	121.5	1429	326		75	7.56	PANEL EDGE
D-4	154.0	123.0	2429	290		78	10.90	PANEL EDGE
E-4	154.0	123.0	1931	119		77	11.64	PANEL EDGE

NOTE: GROUP 3 PANELS TESTED WITH WIDE BAND SIREN.

TABLE 13  
CORRUGATED PANELS,

PANEL NR	OVERALL SPL DB	SPECTRUM LEVEL DB	PRINCIPAL STRESS PSI	STRESS CENTER LONG SIDE (PSI)	STRESS CENTER SHORT SIDE (PSI)	ZERO CROSSING 1/SEC	LIFE MILLION CYCLES	FAILURE LOCATION
A-1	159.7	140.9	656	1541	1631	338	1.86	REAR SKIN
B-1	161.7	142.6	647.9	460	531	304	1.64	FRONT SKIN
C-1	160.5	142.4	693.5	1939	917	314	2.26	REAR SKIN
D-1	159.5	140.4	668.1	729	794	336	4.23	INTERIOR FAILURES
E-1	157.5	133.4	633.9	2918	398	424	>24.5	NO FAILURES
A-2	156.0	135.2	340.7	613		228	47.53	INTERIOR FAILURES
B-2	157.0	133.3	578.6	365	376	300	11.66	FRONT SKIN
B-2	154.0	134.3	540.5		649	294	19.63	INTERIOR FAILURES
D-2	154.5	136.8	459.1	391	501	295	94.06	INTERIOR FAILURES
E-2	154.2	135.4	294.8	631	501	350	110.59	INTERIOR FAILURES
A-3	156.5	134.1	419.7	326	109.1	318	56.10	FRONT SKIN
B-3	159.0	136.6	387.9			340	52.63	INTERIOR FAILURES
C-3	157.5	132.0	261.0	345	546	360	>259.2	NO FAILURES
D-3	156.0	135.4	378.5			326	184.84	INTERIOR FAILURES
E-3	155.5	133.9	268.4			340	>244.8	NO FAILURES
A-4	153.7	125.4	440.8			318	125.0	PANEL EDGE
B-4	154.7	125.1	262.6	593	297	340	>170.0	NO FAILURES
C-4	154.0	123.6	317.1			326	>180.0	NO FAILURES
D-4	153.7	125.6	354.9	619		326	>163.0	NO FAILURES
E-4	153.7	123.9	453.9	1411		340	>170.0	NO FAILURES

NOTE: GROUP 4 PANELS TESTED WITH WIDE BAND SIREN.

stiffener at the panel center. Equations given in Reference 7 were used to calculate these values. The panel edge stress was calculated from strain readings taken from gages located at the panel edge at the center of the long and short side.

Panel life in cycles versus spectrum loading in dB has been plotted for all panels in Figures 8 through 13. A least squares fit curve was fitted to the data for all panels.

Panel life in cycles versus panel principal rms stress in psi has also been plotted in Figures 14 through 19. A least squares fit curve was also fitted to these data. These curves are not true S-N (cycles-to-failure) diagrams in the sense that failure stress is plotted versus the number of cycles to failure. The stress plotted is the rms version of the principal stress at the panel center as described above and not the failure stress usually plotted in a random S-N curve. These curves are for comparison purposes and show the relationship of the panel center stress to the number of cycles the panel experienced before a failure occurred at some point in the panel. It was not normally possible to strain gage the panels at the failure location.

### 3. DESCRIPTION OF PANEL FAILURES

Fatigue failures were induced in about 88% of all panels tested. Tables 8 through 13 give the number of load reversals the panels experienced before failure detection and a description of the failure location. All failures were detected visually and checked with the aid of a dye penetrant. Panel tapping was also used for the corrugated panels in an attempt to determine face sheet debonding or

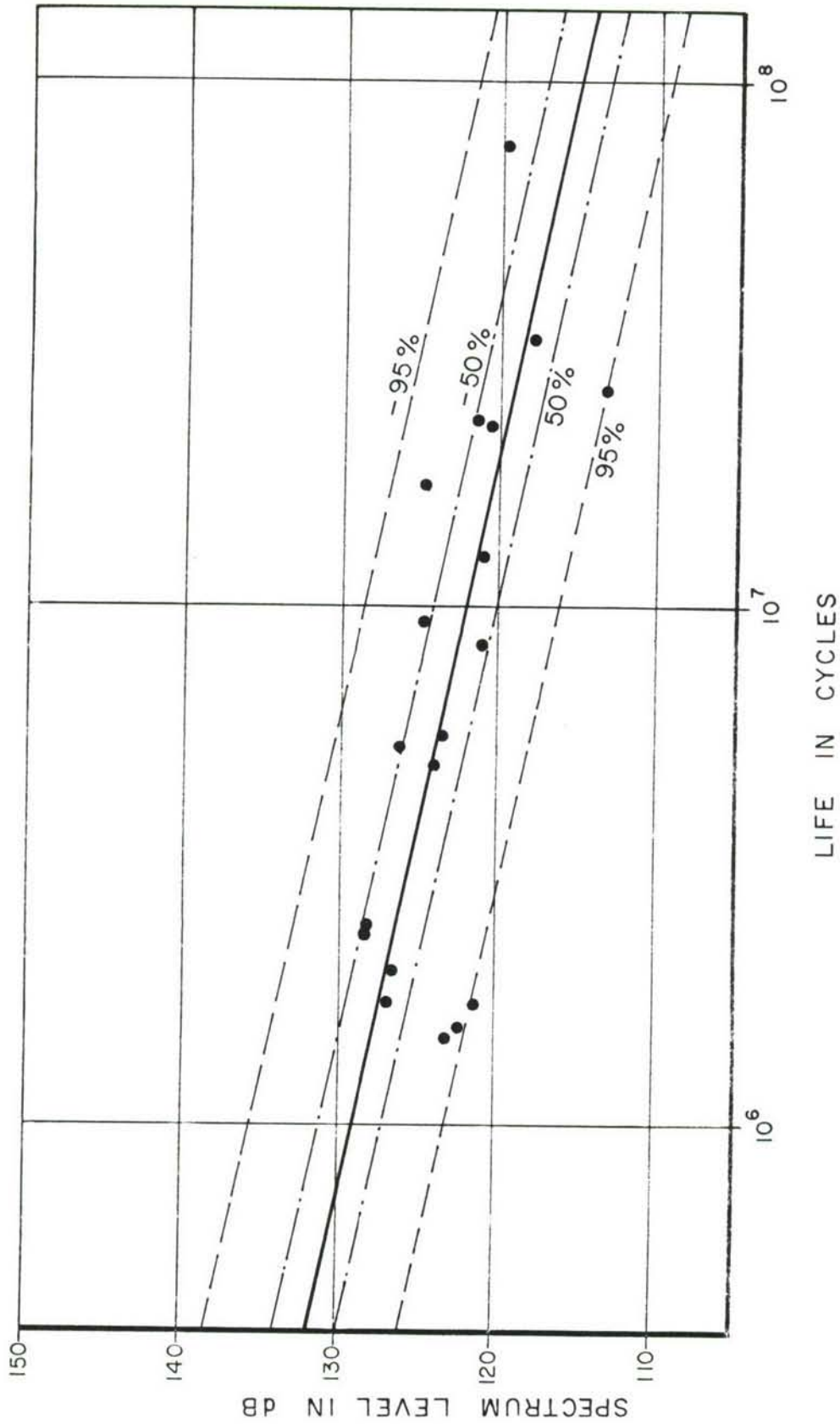


Figure 8. Spectrum Level - Life Relation (Panel Type - Skin-Stringer)

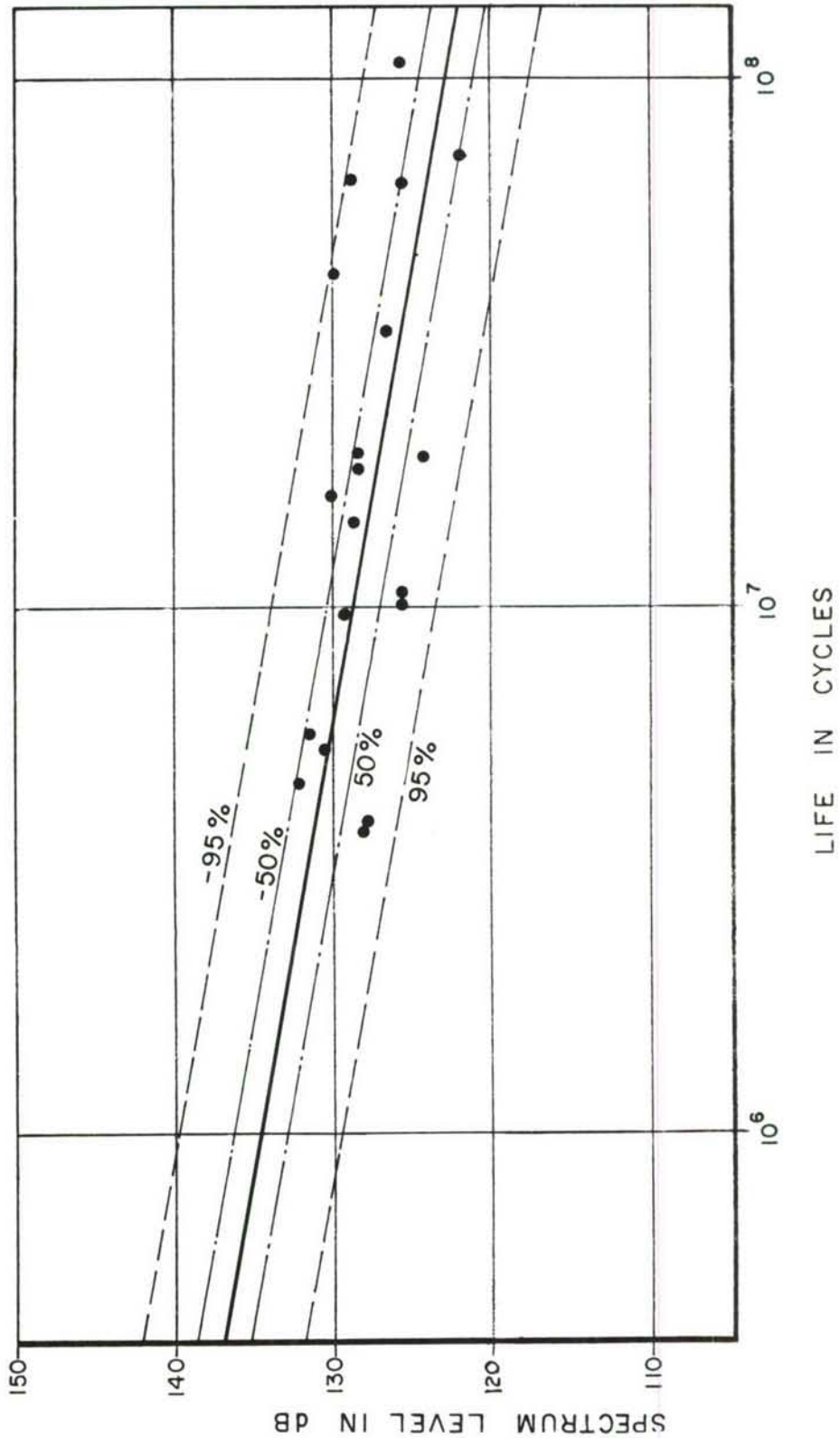
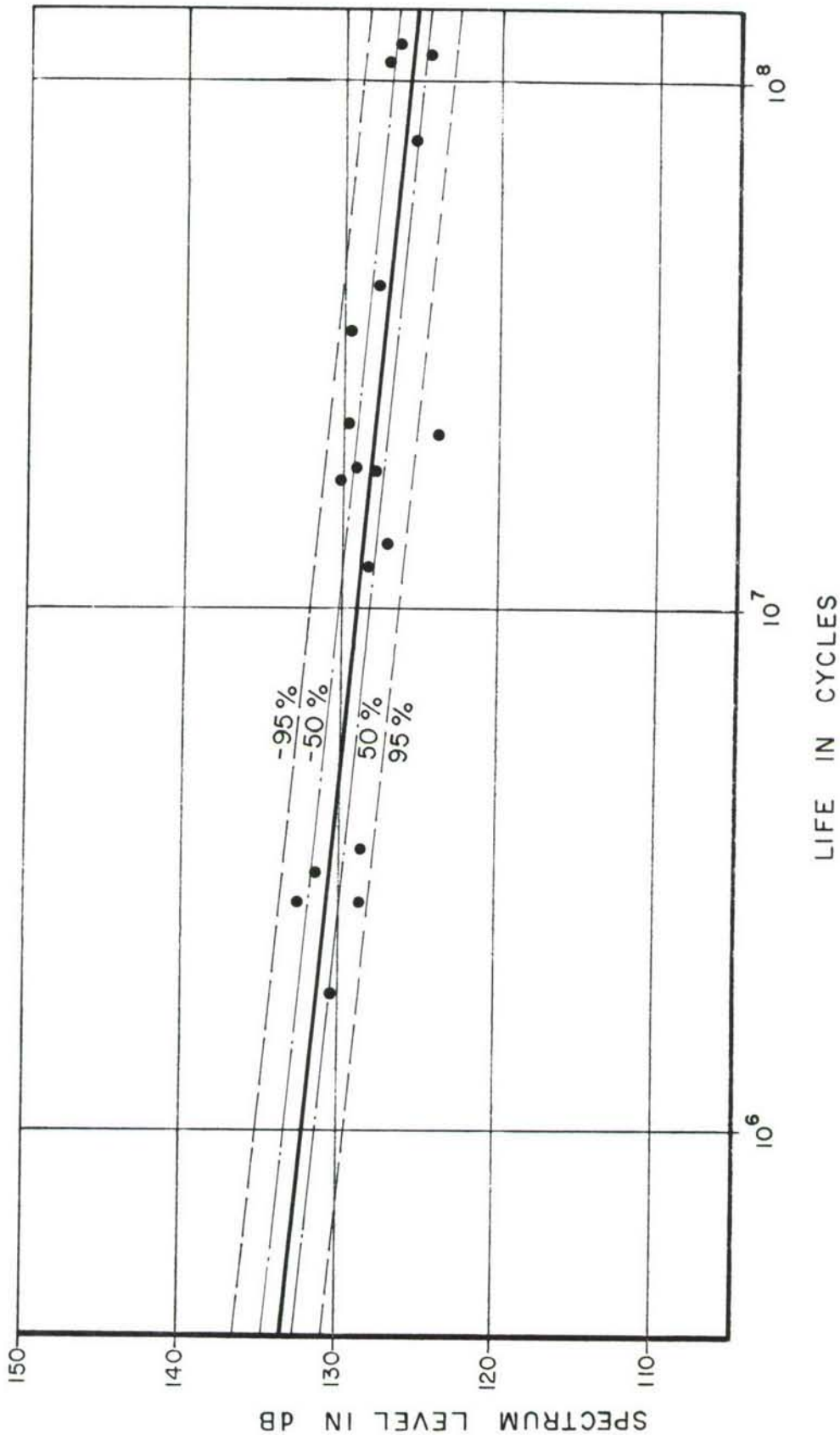


Figure 9. Spectrum Level - Life Relation (Panel Type - Bonded-Beaded, Type I)





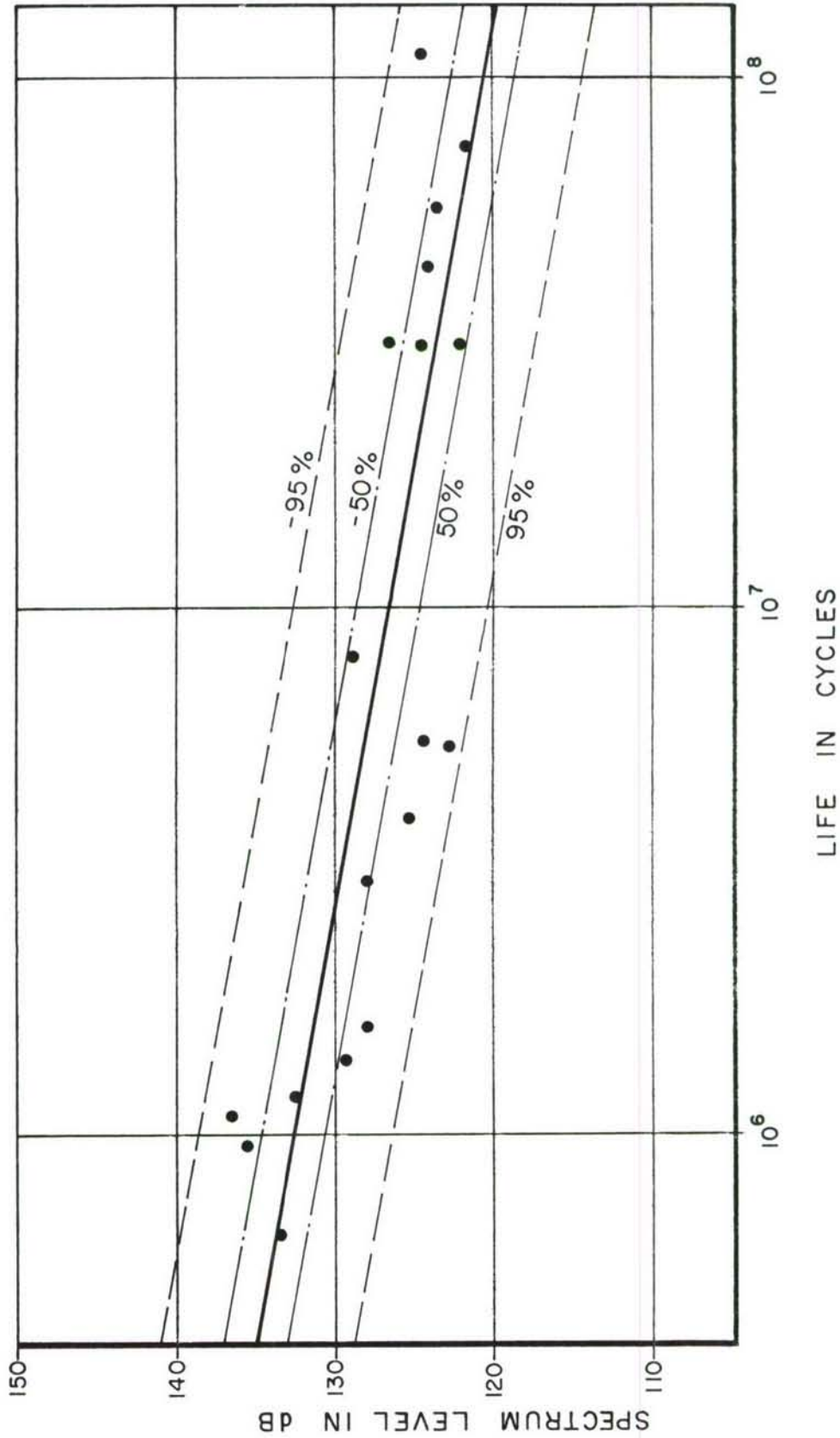


Figure 11. Spectrum Level - Life Relation (Panel Type - Bonded Beaded, Type III)

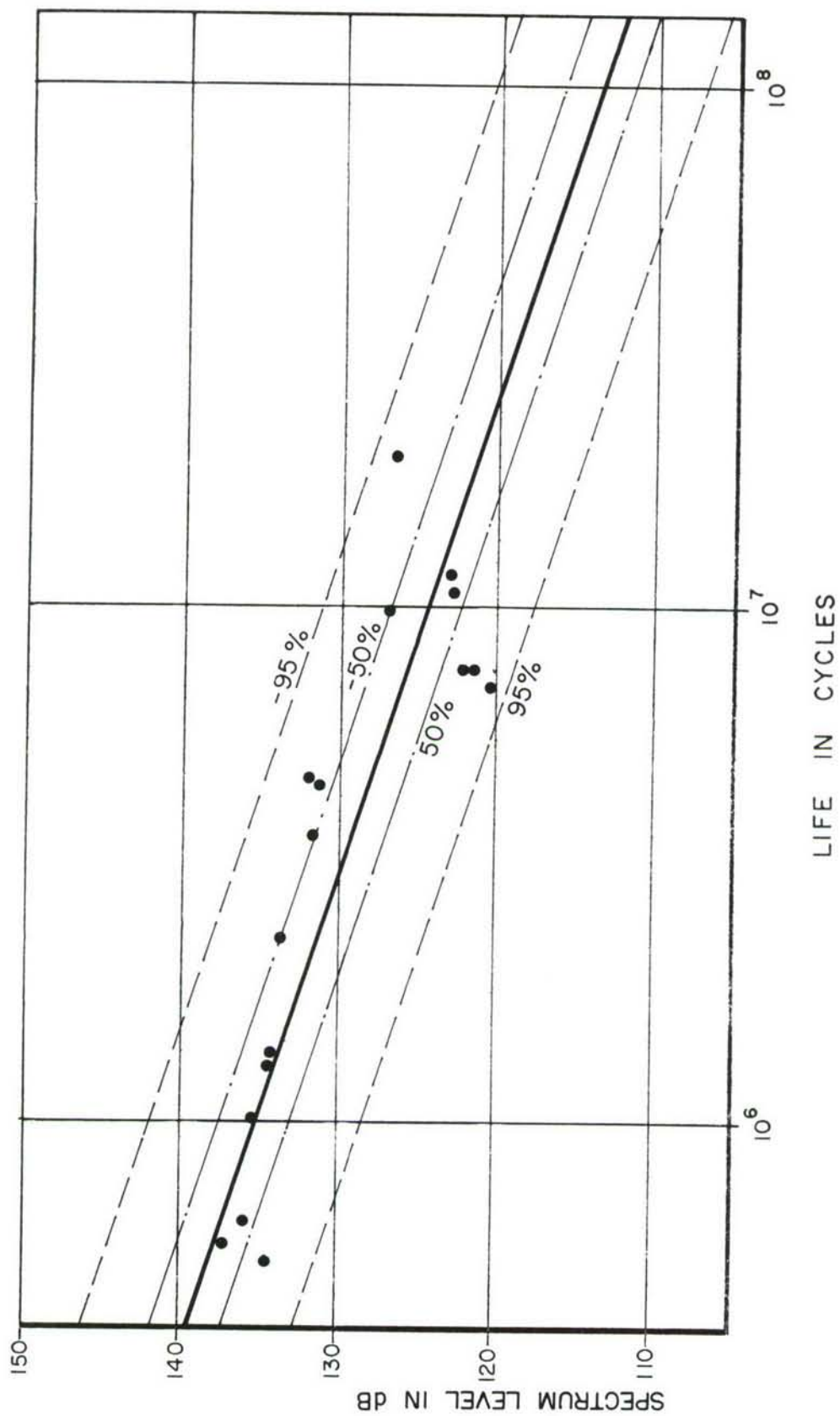


Figure 12. Spectrum Level - Life Relation (Panel Type - Chem-Milled)

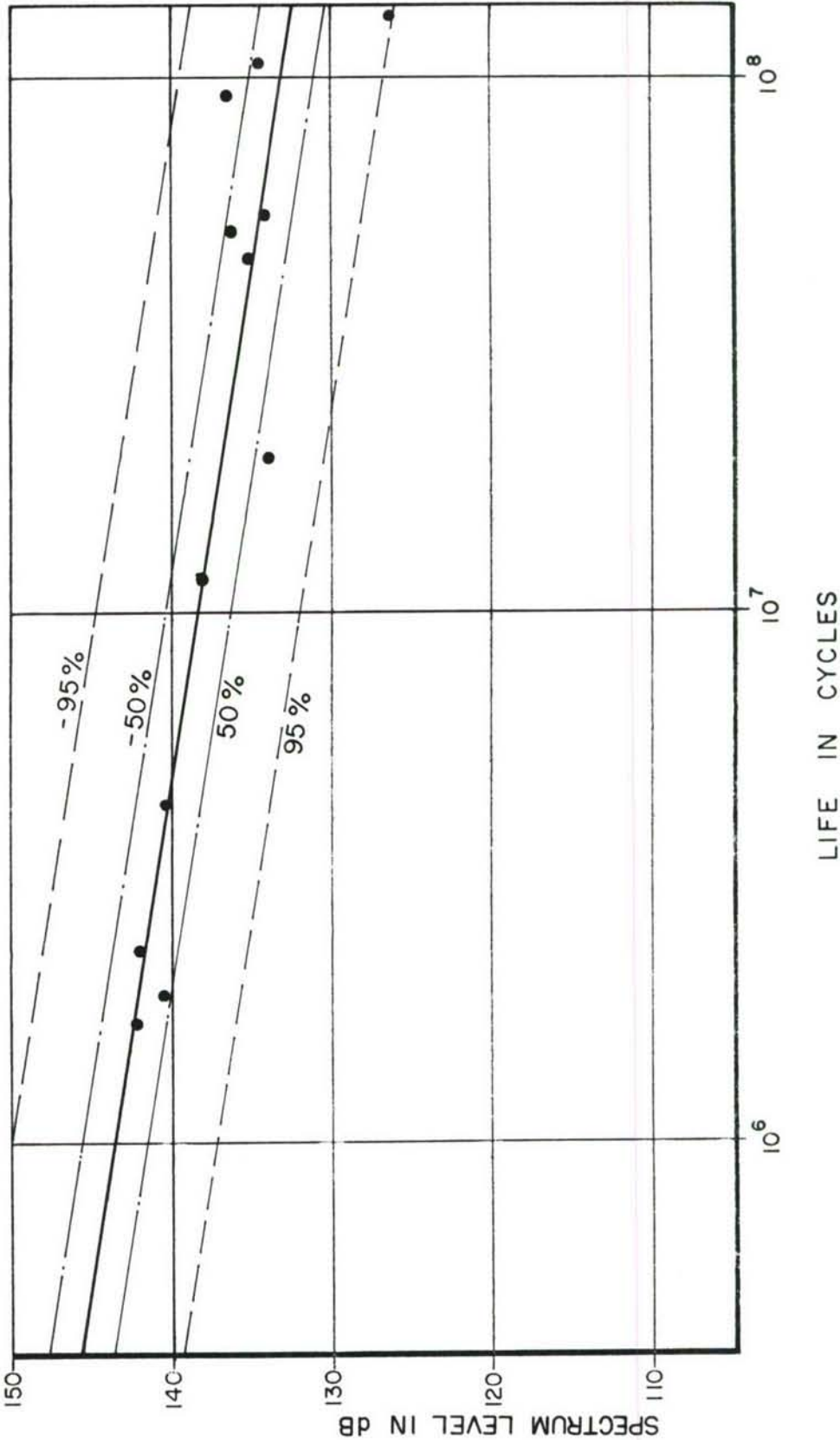


Figure 13. Spectrum Level - Life Relation (Panel Type - Corrugated)

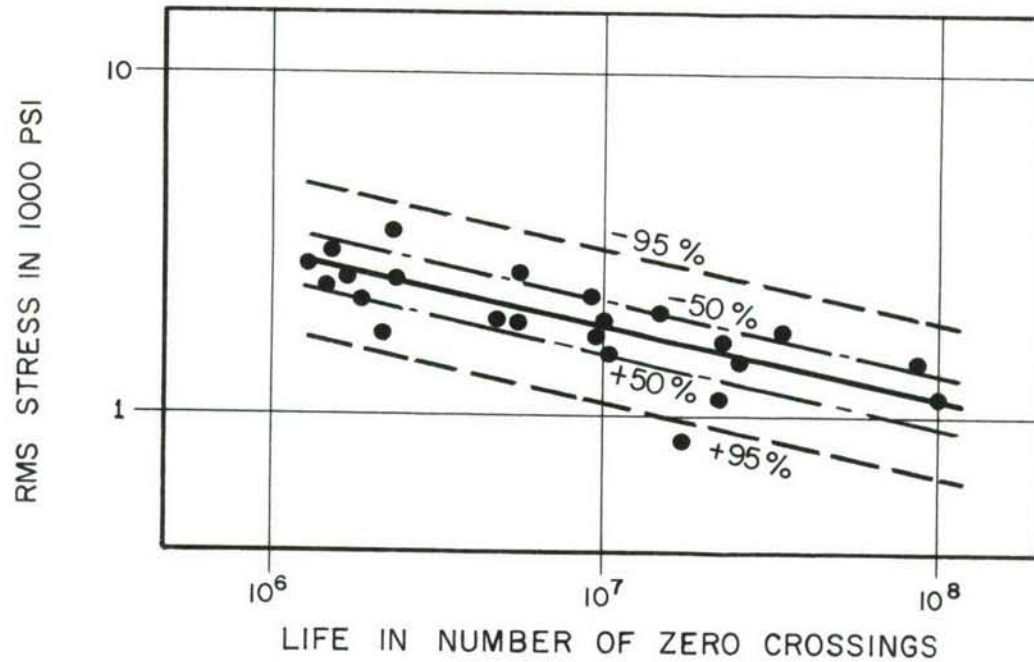


Figure 14. RMS Stress - Life Relation (Panel Type - Skin-Stringer)

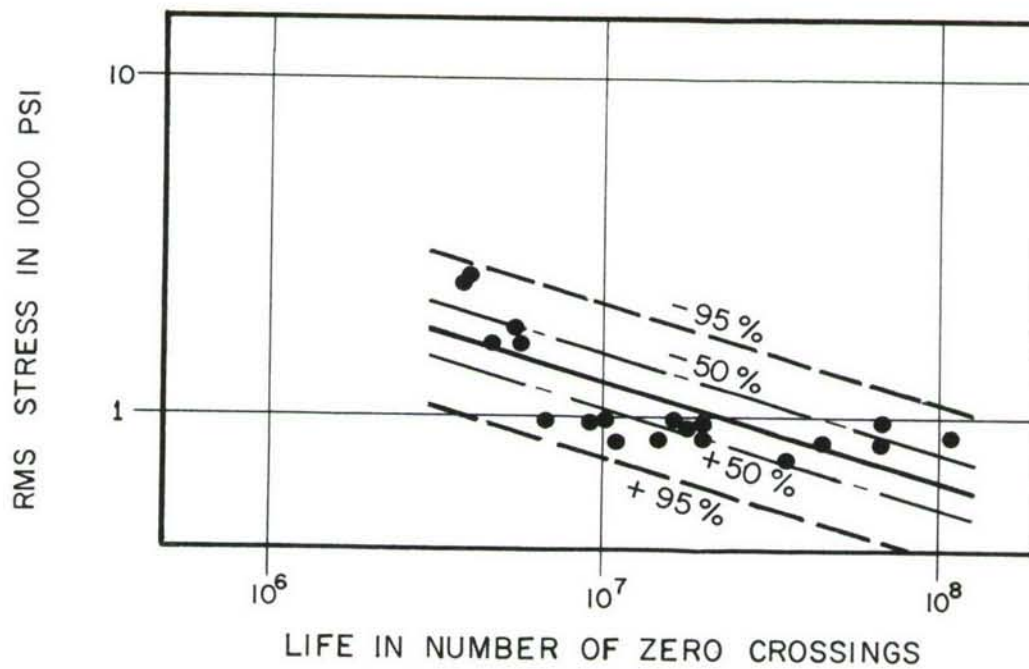


Figure 15. RMS Stress - Life Relation (Panel Type - Bonded-Beaded, Type I)



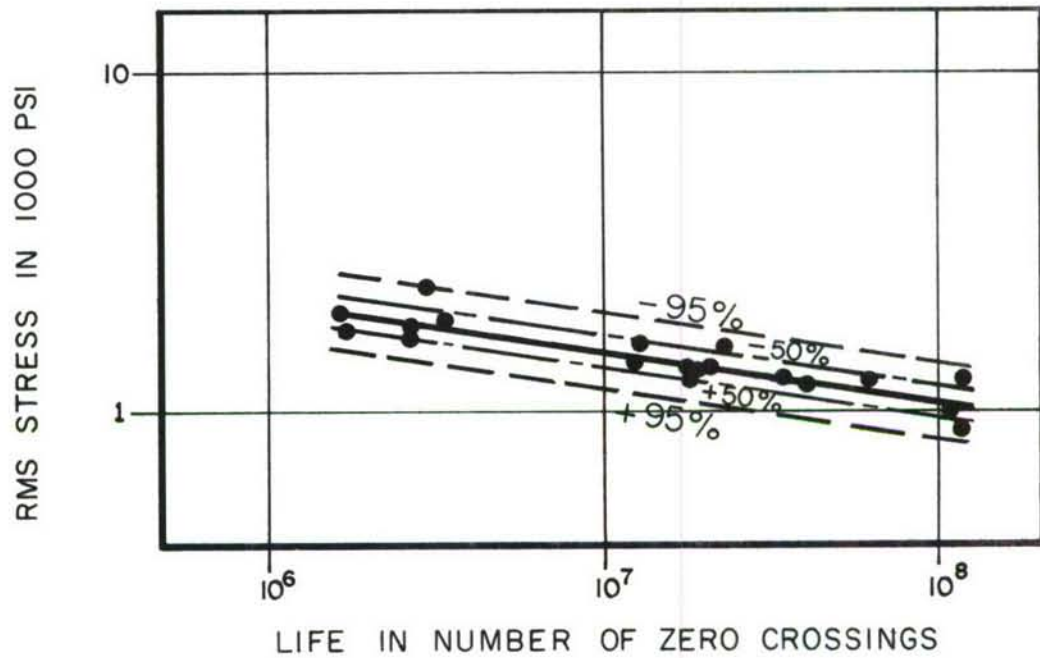


Figure 16. RMS Stress - Life Relation (Panel Type - Bonded-Beaded, Type II)

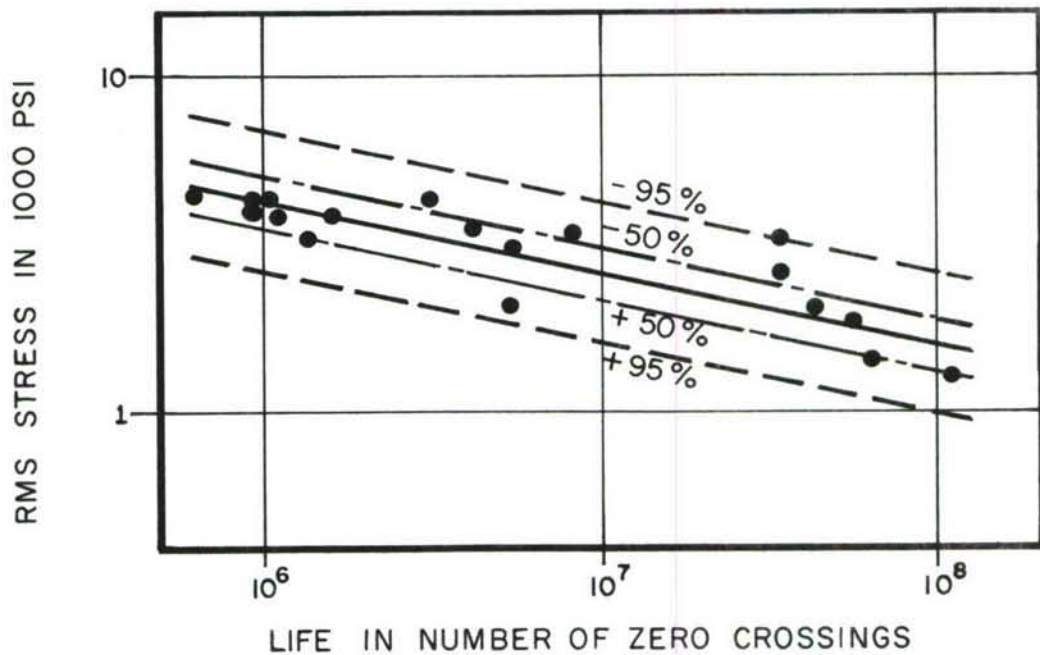


Figure 17. RMS Stress - Life Relation (Panel Type - Bonded-Beaded, Type III)

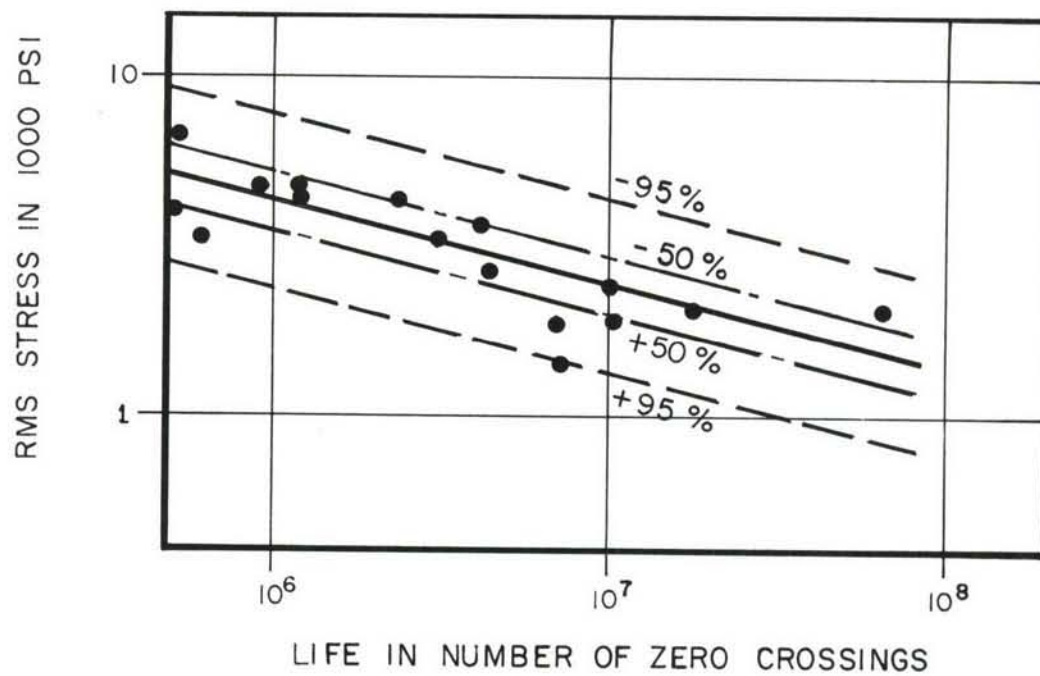


Figure 18. RMS Stress - Life Relation (Panel Type - Chem-Milled)

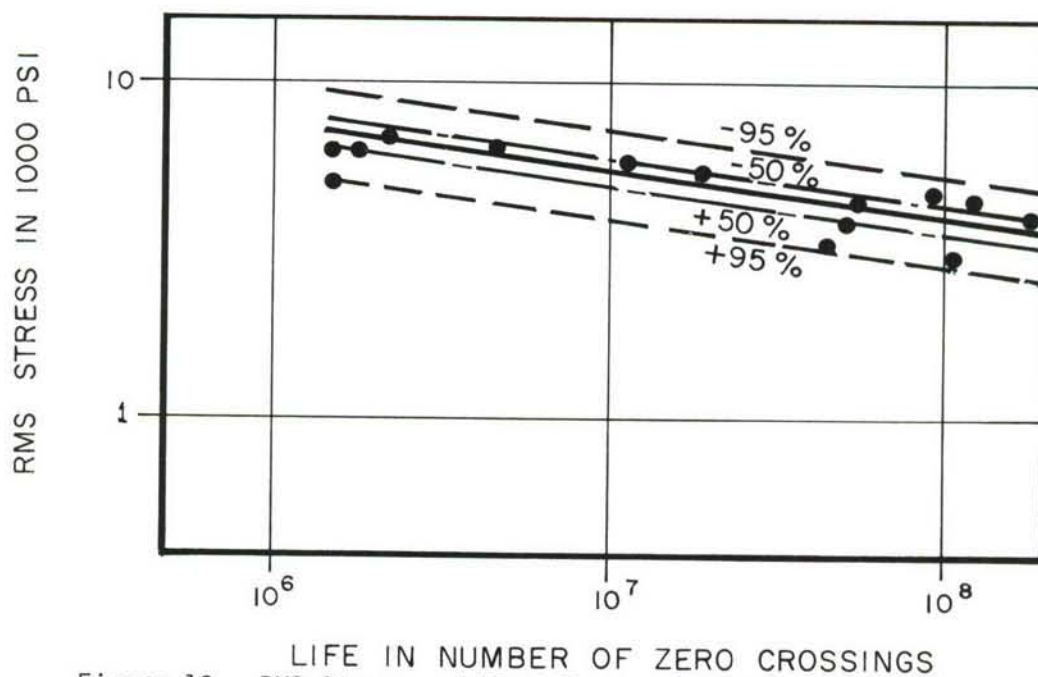


Figure 19. RMS Stress - Life Relation (Panel Type - Corrugated)

core failure. In all but four cases where no failures were detected, load reversals were in excess of  $10^8$  cycles.

Panel edge failures were not considered desirable since they primarily are a function of the edge design and not a function of the panel design. Failures near stress concentrations around panel edge attachments are a common occurrence in structures subjected to high intensity noise loadings. For determining the sonic fatigue resistivity of the panel design, failures away from the panel edge are considered the most valid, though difficult to obtain in some cases. However, since panel edge failures occur in practice and the edge design of these panels was typical of bolted panel attachments, they were counted as legitimate failures.

a. Skin-Stringer Panels

For the skin-stringer panel, the typical failure originated and propagated between the rivets. This is the normal failure mode of riveted panels without additives between the skin and stringers. Of the nineteen failures recorded, seventeen took place along the rivet line and two at the panel edge. One panel accumulated more than  $10^8$  cycles without failure. Figure 20 shows a sequence of photographs taken at increasing test time. These cracks between the rivets were typical and the photos show how the cracks propagate between rivets. For the case shown, in a period of six hours the crack grew from 4 to 13 rivet pitches.

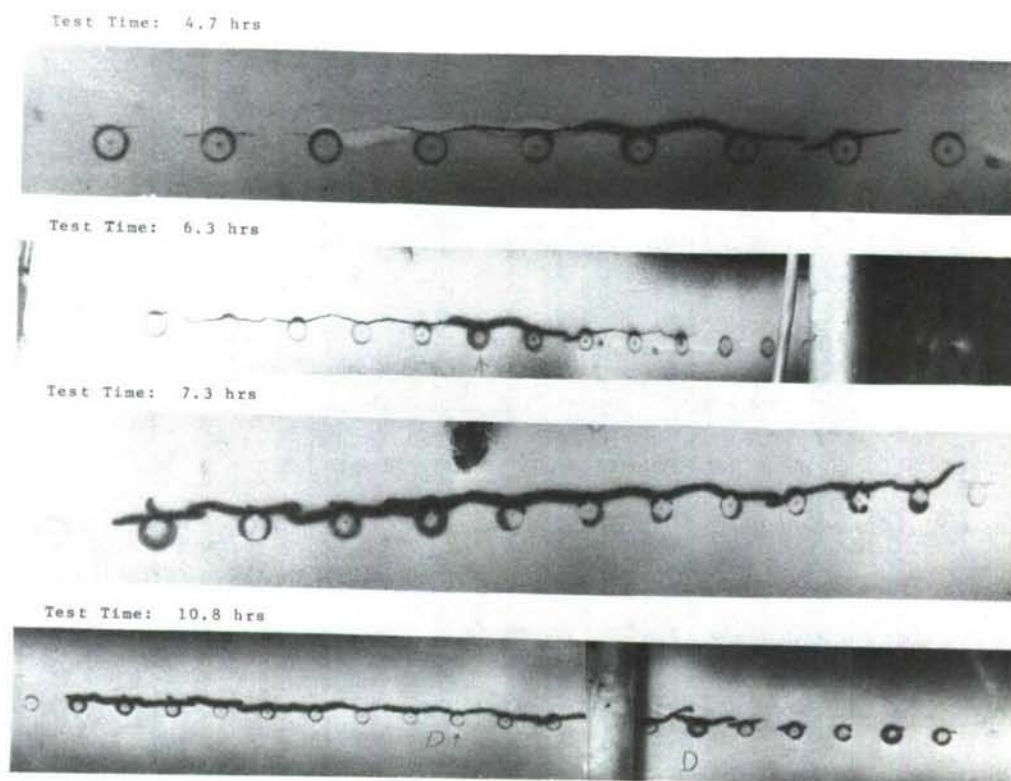


Figure 20. Typical Failure in Skin-Stringer Panels

b. Bonded-Beaded Panels

There were two typical failure locations in the Type I and Type III panels. These panels had a ratio of skin to bead thickness of one. The typical failures were in the bead end and at the panel edge. Figure 21a shows typical bead end failures. From this group of 40 panels, 17 failures were in the bead end, 15 failures at the panel edge, and five panels had failures occurring approximately at the same time in the bead end and at the edge. The majority of the bead end failures (16) occurred at a spectrum level above 125 dB whereas only nine of the edge failures and three of the combined failures occurred at a spectrum level greater than 125 dB.



For the Type II panels, where the skin to bead thickness ratio was less than one, only one dominant failure mode existed. This was in the skin. Figure 21b shows a photo of a skin failure. The other failures occurred at the bead end and panel edge. Twelve of the failures were in the skin, four at the panel edge, one in the bead and one combined bead and edge. Again, the panel edge failures took place at a spectrum level below approximately 126 dB.

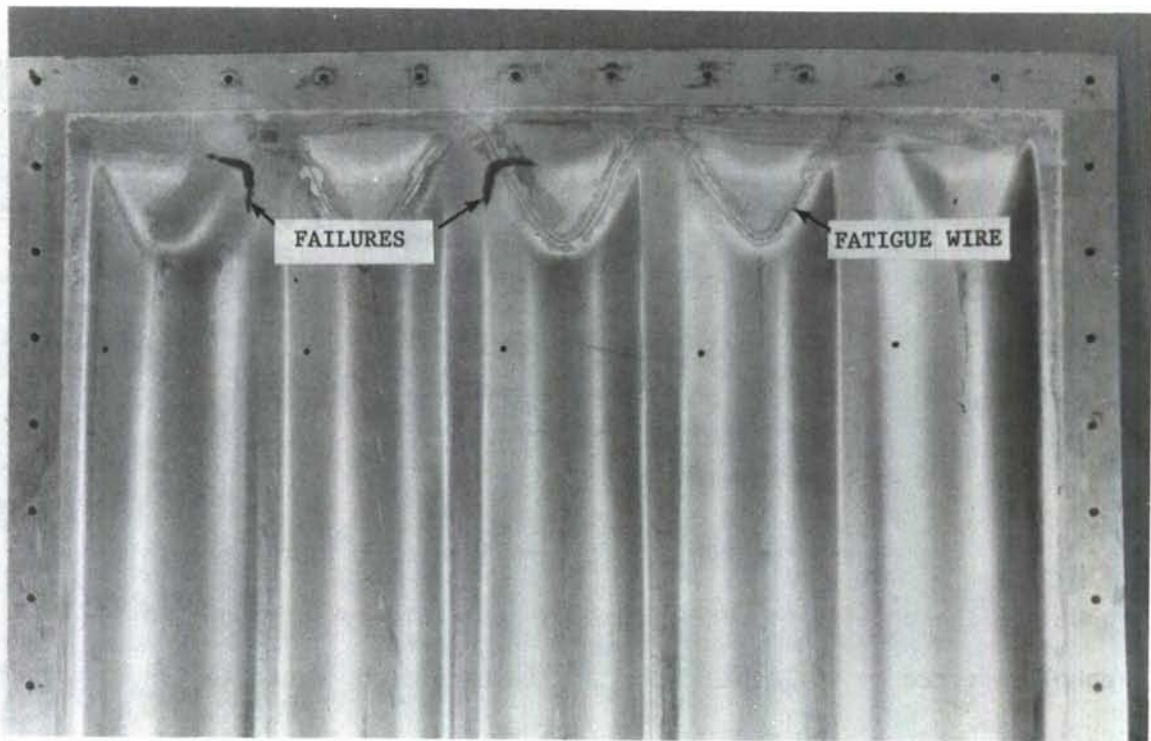
#### c. Chem-milled Panels

There were two typical failure locations in the chem-milled panels. These failures were located in the interior part of the panel referred to as "center" and at the panel edge close to the fastener holes. Figure 22 shows both the center cracks and the edge cracks. The interior cracks started in the bend radius of the land and propagated into the land and into the 0.030 inch thick skin. The edge failures started under the head of the fasteners. There were ten failures in the panel center and seven edge failures. The center failures developed under the higher spectrum levels and the edge failures all occurred at spectrum levels below 127 dB.

#### d. Corrugated Panels

Only thirteen failures were detected in the 20 corrugated panels tested. The panels failed in several ways and no typical failure mode could be identified for these panels. Seven failures developed in the panel interior, three in the front skin, two in the rear skin and one at the panel edge. One type of failure was in the skin at the end of the corrugations. Another in the front skin where the crack was one corrugation width removed from the panel





A. Typical for Type I and Type III Panels



B. Typical for Type II Panel

Figure 21. Failures in Bonded-Beaded Panels

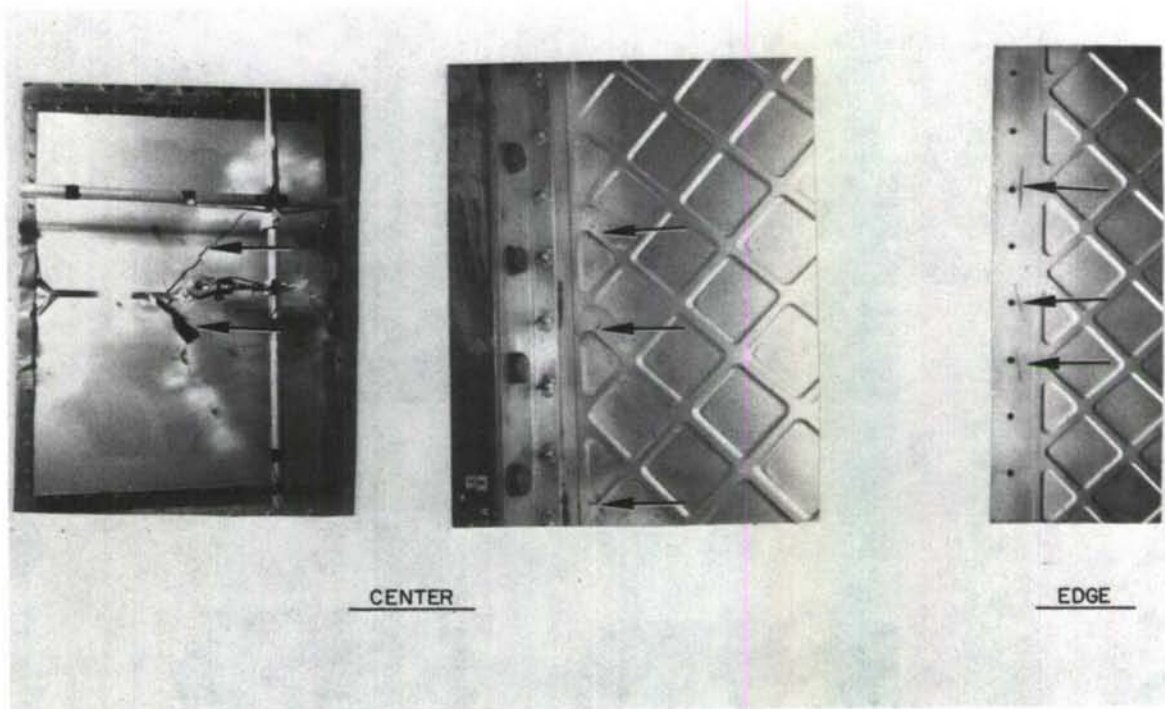
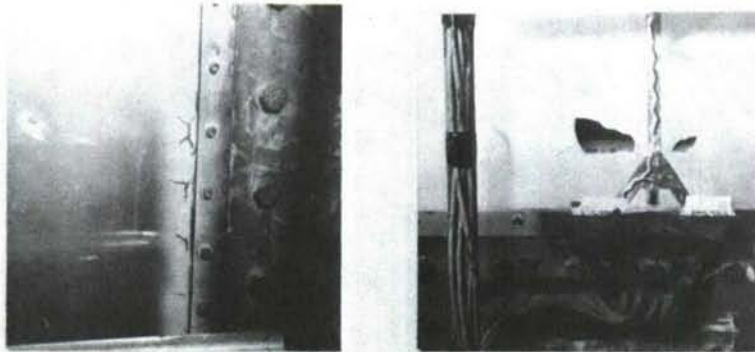
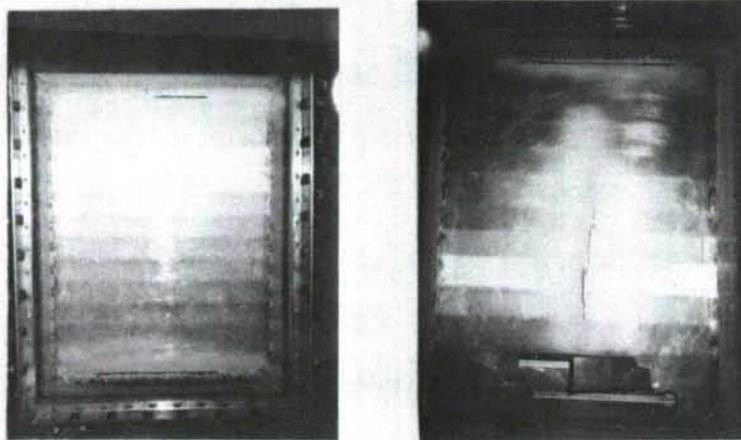


Figure 22. Typical Failures in Chem-Milled Panels

edge. Some panels with failures in the rear skin had cracks running both parallel and perpendicular to the corrugations. The various types of failures are shown in Figure 23. Interior failures were detected by a change in stress output and also by using a "coin tapping" technique where the panel was tapped with a metal object and the response was observed by listening to the ring and thereby determining locations of interior damage.



FRONT FAILURES



BACK FAILURES

Figure 23. Failures in Corrugated Panels

## SECTION III

## DESIGN CHART FOR THE BONDED-BEADED PANELS

The general approach taken to develop sonic fatigue design charts for the bonded-beaded panels consisted of a semi-empirical method which utilized a single-degree-of-freedom random response equation (Miles Formulation) to predict the dynamic stress combined with a finite element approach for determining natural frequencies and static stress values. See Reference 8 for a similar approach. A multiple regression technique was used to formulate the frequency and static stress equations using the computer generated data from the finite element models. These equations related the panel static stress and frequency to the panel geometric parameters. The finite element models were adjusted by using panel test data to give the calculated values close agreement to the measured values. The computer program was needed to give the additional panel data, not obtainable from the test program because of a lack of panel designs, required to develop the design chart. After the above expressions were obtained they were substituted into Miles equation to formulate an equation to predict the mean square dynamic stress due to the acoustic load. The multiple regression technique was again used to regress the measured dynamic stress and acoustic load from the panel testing program against the above developed parameters to give a proportionality factor based upon test data. This final equation was used in the design chart to predict stress. To obtain panel life,



the S-N curve from the panel testing program was used as part of the design chart. The above procedure is detailed in the following paragraphs.

## 1. THEORY

Miles (Reference 9) proposed the use of Equation 1 for a single degree-of-freedom system to compute the mean square stress:

$$\sigma^2(t) = \frac{\pi}{4\zeta} F G(F) \sigma_0^2 \quad (1)$$

$F$  = the natural frequency of the first mode in Hz

$G(F)$  = spectral density of the acoustical excitation at the frequency  $F$

$\sigma_0$  = static stress caused by a uniform unit static pressure load

$\zeta$  = damping ratio. (First Mode)

This equation is widely used in sonic fatigue analysis, but is limited by the following assumptions:

1. Only one response mode affects the fatigue life of the structure (first mode of a panel clamped on all edges is assumed).
2. The vibration mode shape is identical to the deflected shape under a uniform static pressure load.
3. Acoustical pressures are in phase over the complete panel.
4. The spectral density of the acoustical loading is constant in the neighborhood of the fundamental frequency of the panel.

## 2. ANALYSIS

Stress and frequency analyses were performed on the bonded-beaded panels to determine the stress in the center of the panel, the maximum stress at the bead end, and the response frequency.



Finite element models for the Type I and Type III panels were developed for the stress and frequency case. See Reference 10 for details of these models. The stress and vibration analyses were made with the NASTRAN finite element program version L15.5. This general purpose program is compatible with the CDC 6600 computer and is widely accepted by organizations dealing with stress and vibration calculations.

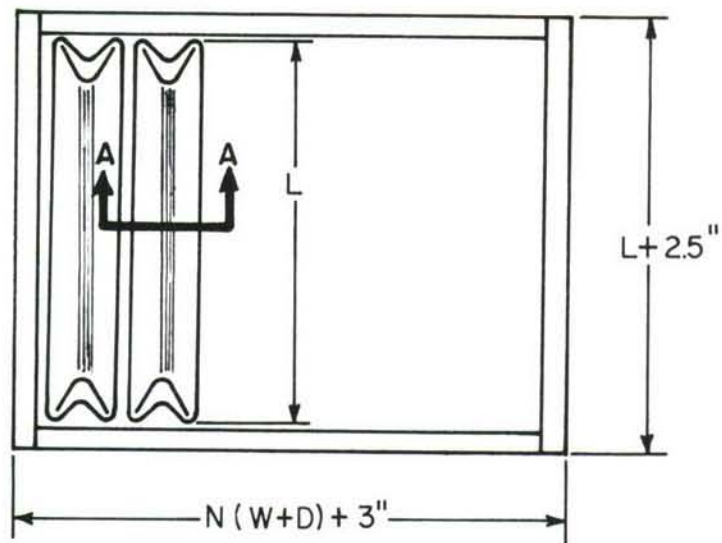
The basic panel dimensions used in developing these models are given in Table 14 with the nomenclature shown in Figure 24. The material properties used during the calculations were

$$E = 10.3 \times 10^6 \text{ psi and } \mu = 0.33$$

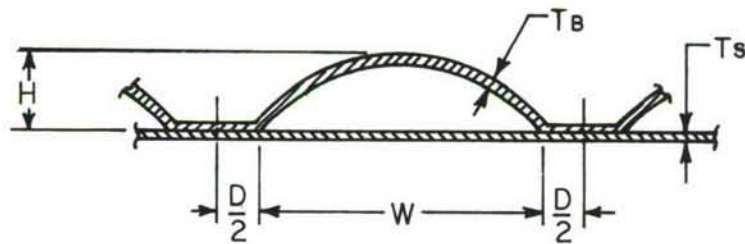
TABLE 14  
PANEL DIMENSIONS USED FOR DEVELOPMENT  
OF FINITE ELEMENT MODELS

<u>PANEL TYPE</u>	<u>I (Basic Design)</u>	<u>II</u>	<u>III</u>
W	3.5	3.5	3.5
H	0.8	0.8	0.8
L	21.0	21.0	27.0
T <sub>S</sub>	0.032	0.020	0.032
T <sub>B</sub>	0.032	0.045	0.032
D	1.0	1.0	0.7
N	6.0	6.0	5.0

The models were designed in such a manner that the stress in the center of the panel and the response frequency approximately agreed with the experimental results.



$N$  = NUMBER OF REPEATING BEAD SECTIONS.



SECTION A-A

Figure 24. Bonded-Beaded Panel Nomenclature

By varying one dimension at a time, the influence of the dimensional variation on the stress and response frequency of the panels was determined. These variations are given in Table 15 for panel cases A through S.

TABLE 15  
RESULTS OF NASTRAN CALCULATIONS

PANEL ID	W	L	H	T <sub>s</sub>	T <sub>B</sub>	D	N	FREQ (Hz)	PANEL CENTER STRESS (PSI)	STRESS ON BEAD END (PSI)
A	3.5	21.5	0.8	0.032	0.032	1.0	6	194	2035	13680
B	3.5	21.5	0.8	0.032	0.020	1.0	6	148	2939	13569
C	3.5	21.5	0.8	0.032	0.045	1.0	6	271	1792	10575
D	3.5	21.5	0.8	0.045	0.032	1.0	6	194	1842	11246
E	3.5	21.5	0.8	0.020	0.032	1.0	6	193	2418	17019
F	3.5	27.5	0.8	0.032	0.032	1.0	6	134	2766	20934
G	3.5	37.0	0.8	0.032	0.032	1.0	6	129	4142	34999
H	3.5	21.5	0.7	0.032	0.032	1.0	6	194	2287	15152
I	3.5	21.5	0.9	0.032	0.032	1.0	6	194	1834	12455
J	2.9	21.5	0.8	0.032	0.032	1.0	6	194	1945	13122
K	4.1	21.5	0.8	0.032	0.032	1.0	6	193	2303	14139
L	3.5	21.5	0.8	0.032	0.032	0.6	6	194	1970	14326
M	3.5	21.5	0.8	0.032	0.032	0.8	6	194	2007	13915
O	3.5	21.5	0.8	0.032	0.032	1.0	5	194	2075	13632
P	3.5	21.5	0.8	0.032	0.032	1.0	7	194	2064	13646
R	3.5	21.5	0.8	0.020	0.045	1.0	6	269	1745	13646
S	3.6	27.5	0.8	0.032	0.032	0.8	5	134	2700	24282

The influence of panel design variations on stress and frequency often make a regression analysis the only practical way to obtain a workable relationship between the design parameters and the stress or frequency. In practical design work, it is difficult to use a large computer program or a complicated generalized theory. Multiple regression techniques are easy to use with the availability of the computer programs developed as for example in Reference 11. The BMD02 computer program used during these analyses computes a sequence of multilinear regression equations in a stepwise manner. At each step one variable is added to the regression equation. Also calculated was the multiple correlation factor for each equation which indicates the degree of correlation between the dependent and independent variables.

#### a. Static Stress

The computer program referenced above was used to determine a relationship between the static stress at the center of the panel and the panel parameter ratios given in Table 16. The panel stress and the data required to compute the ratios were obtained from Table 15 where the stress results were from the NASTRAN calculations. The relationship of Equation 2 was determined:

$$\sigma_c = 1.67 \left( \frac{W}{L} \right)^{0.470} \left( \frac{H}{L} \right)^{-0.854} \left( \frac{T_S}{L^4} \right)^{-0.066} \left( \frac{T_B}{L} \right)^{-0.642} \left( \frac{N D}{L} \right)^{0.072} \text{ PSI } (2)$$

The multiple correlation coefficient was calculated to be 0.967.

TABLE 16  
REGRESSION COEFFICIENTS

<u>PANEL RATIOS</u>	<u>REGRESSION COEFFICIENTS</u>
W/L	0.470
H/L	-0.854
$T_S/L^4$	-0.066
$T_B/L$	-0.642
ND/L	0.072

b. Natural Frequency

The same technique as above was also used to find the relationship between the panel parameter ratios and the panel response frequency. Panel ratios and regression coefficients are given in Table 17. The relationship of Equation 3 was obtained:

$$F = 44,725 \left(\frac{W}{L}\right) (L) \left(\frac{T_S}{L^4}\right) \left(\frac{T_B}{L}\right) (Hz) \quad (3)$$

The multiple correlation coefficient was calculated to be 0.960.

TABLE 17  
REGRESSION COEFFICIENTS

<u>PANEL RATIOS</u>	<u>REGRESSION COEFFICIENTS</u>
W/L	-0.025
L	0.094
$T_S/L^4$	0.064
$T_B/L$	0.728



## c. Dynamic Stress

The dynamic stress is now computed by substituting Equations 2 and 3 into Equation 1:

$$\sigma_D = K_D \frac{W^{0.458} L^{0.786} D^{0.072} N^{0.072}}{H^{0.854} T_S^{0.034} T_B^{0.278}} \sqrt{\frac{G(F)}{\zeta}} = K_D \cdot X \cdot \sqrt{\frac{G(F)}{\zeta}} \quad (4)$$

$$\text{where } X = \frac{W^{0.458} L^{0.786} D^{0.072} N^{0.072}}{H^{0.854} T_S^{0.034} T_B^{0.278}}$$

To obtain the value of  $K_D$ , the measured values of dynamic stress were regressed against the values of  $X \cdot \left(\frac{G(F)}{\zeta}\right)^{0.5}$ . The values of  $X$  and  $K_D$  obtained are given in Table 18.

TABLE 18

VALUES OF X AND  $K_D$ 

<u>PANEL</u>	<u>X</u>	<u><math>K_D</math></u>
Type I	78.28	322.06
Type II	72.34	219.37
Type III	91.74	322.06

Substituting these values into Equation 4, the final equations for the dynamic stress become:

For bead end failures:

$$\sigma_D = 322.06 \frac{W^{0.458} L^{0.786} D^{0.072} N^{0.072}}{H^{0.854} T_S^{0.034} T_B^{0.278}} \sqrt{\frac{G(F)}{\zeta}} \quad \text{psi} \quad (5)$$

For skin failures:

$$\sigma_D = 219.37 \frac{W^{0.458} L^{0.786} D^{0.072} N^{0.072}}{H^{0.854} T_S^{0.034} T_B^{0.278}} \sqrt{\frac{G(F)}{\zeta}} \quad \text{psi} \quad (6)$$

Equations 5 and 6 were used to construct the design chart given in Figure 25.

Panel center stress has been used for the design chart parameter for all panel types regardless of the failure location. Panel Types I and III bead end failures and panel Type II skin failures were grouped respectively for the stress-life curves given in the design charts of Figure 25. Design chart relationships can be generated using panel center stress as a parameter in lieu of panel failure stress if the assumption is made that a constant relationship exists between panel center stress and panel failure stress in the test panel and actual aircraft panel. This assumption requires that the design of the test panel duplicates the actual aircraft panel in any detail that affects the panel stress concentration factors and that test panel failures must duplicate actual aircraft panel failures.

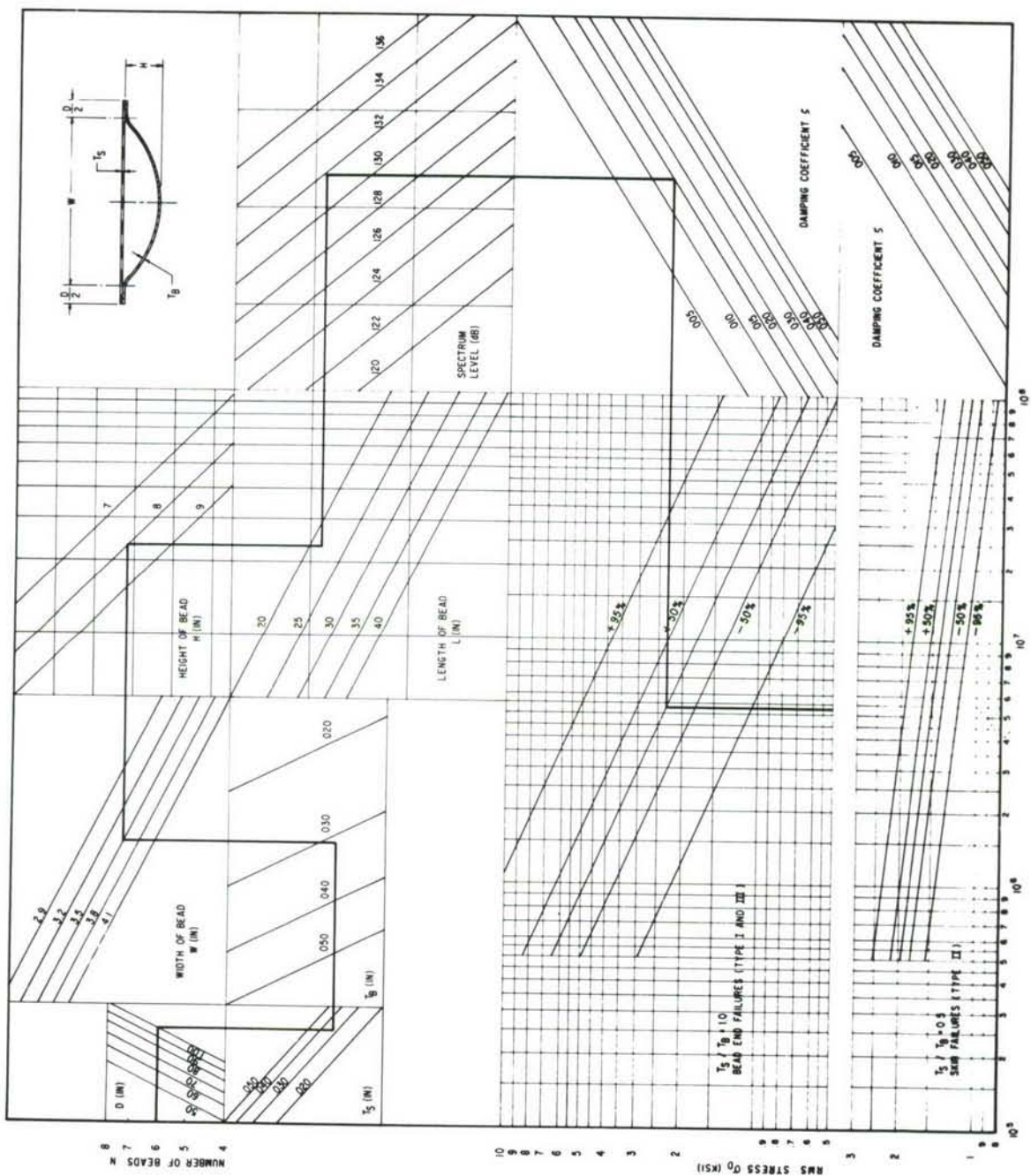


Figure 25. Design Chart for Bonded-Beaded Panel

## SECTION IV

## CONCLUSIONS

The sonic fatigue data presented in this report were obtained to (1) verify and extend existing design information for four types of lightweight aircraft panels and (2) to compare the experimentally obtained S-N curves of panel configurations with a weight to area ratio of 1 lb/sq ft, when tested under similar loading conditions. A high level of confidence in the results was obtained due to the number of specimens tested in a group, the total number of specimens tested, and the highly controlled acoustic environment.

All test specimens were fabricated using aircraft manufacturing techniques and inspection specifications. The fatigue failures and lifetimes obtained should be indicative of the variability in life to be expected under service conditions.

#### 1. PEAK FREQUENCY RESPONSE VARIATIONS

Based upon the discussion of the frequency peaks, the experimental technique, and data analysis described in Section II-1 and Appendix B-2, the following conclusions were formed for the disagreement in these peak frequencies.

- a. Mode shape data recorded at 100 dB pure tone versus wide band noise with spectrum levels ranging from 15 to 40 dB higher.
- b. Coupling between modes may have affected the location of the frequency peak in Tables 2 through 7.
- c. Zero crossings given in Tables 8 through 13 were obtained by a different technique.



## 2. PANEL DAMPING RATIO COMPARISON

The least squares fit curves drawn for the damping ratios data are compared in Figure 26 for all panel types.

Determination of damping ratios for similar panel types is recommended by selecting the value from the mean curves in Figure 26 for the desired frequency and panel configuration.

## 3. COMPARISON OF THE FOUR DESIGNS

### a. Skin-Stringer Panels

The skin-stringer panel test results are used as the baseline data for comparison with test results from other panel types and hence these panels are discussed with the other designs.

After the tests were completed, an additional use of the data was envisioned to incorporate the test results into the data, for example, from Reference 12, 13, or 14. The rivet line failures were considered valid data for design chart use; however, the stresses were measured at the edge of the stringer, a distance of 0.5 inch from the rivet line. An attempt was made to develop a numerical factor to transfer the stress measured over the edge of the stringer to the rivet line, but this did not prove entirely successful. The rms stress-life relationship for the AFFDL data has been replotted in Figure 27 by applying an approximate stress concentration and stress transfer factor to the Figure 14 data resulting in the curve shown. Comparing this curve with data from the above references resulted in different stress-life relationships. The AFFDL test panels had three



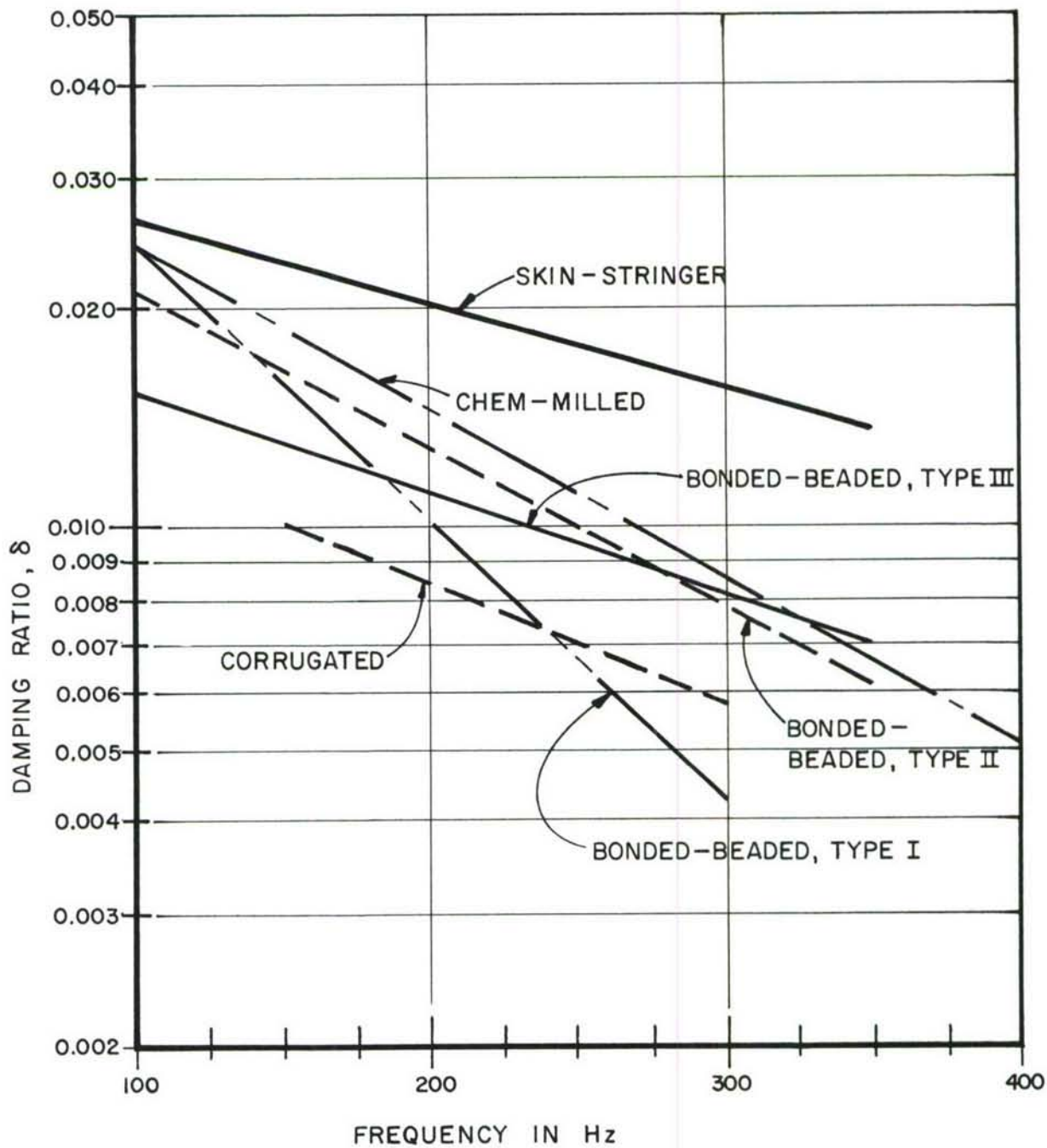


Figure 26. Comparison Between Damping Ratios for All Panel Configurations

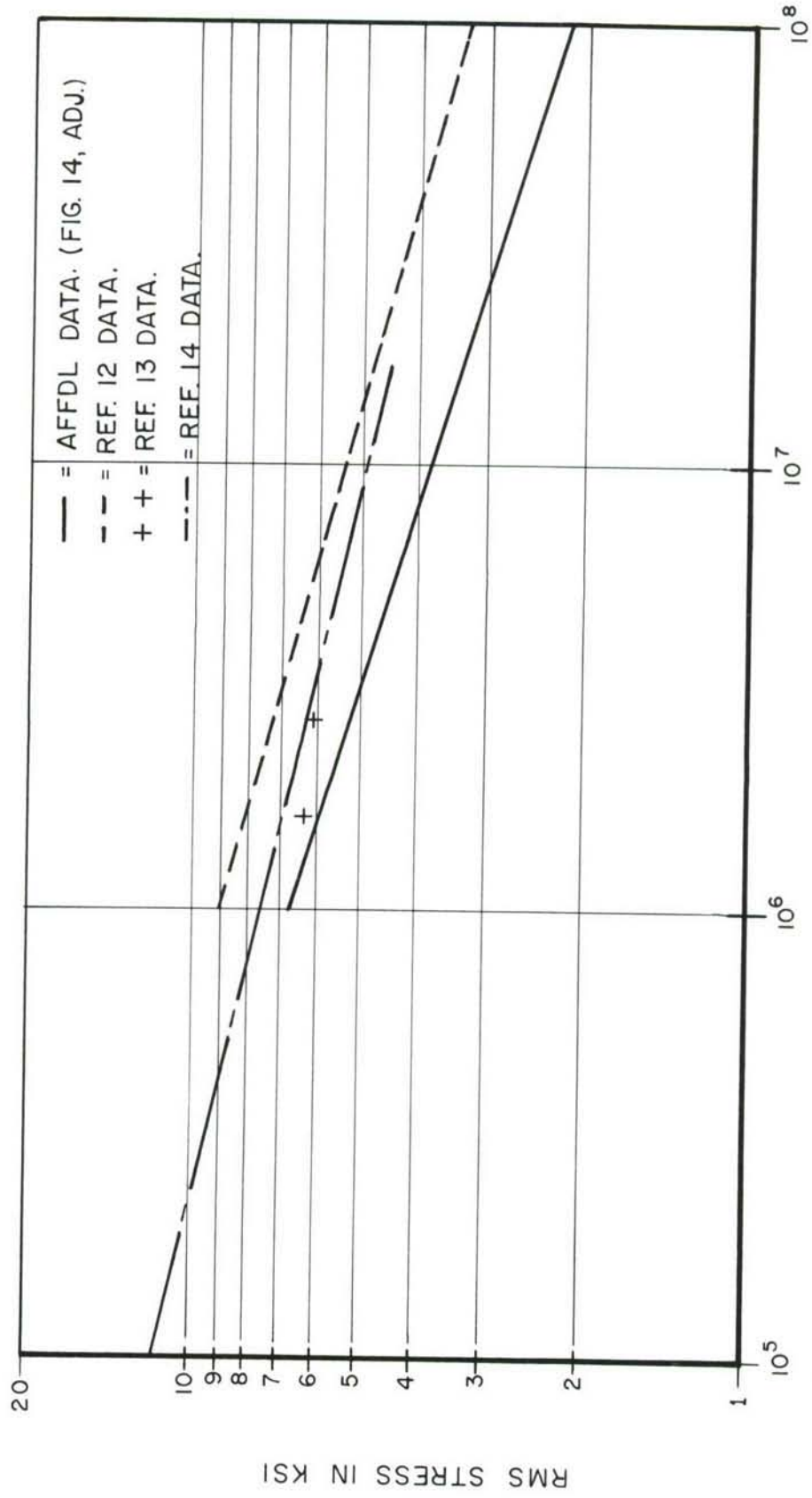


Figure 27. S/N Curves for Skin-Stringer Panels

bays with the skin riveted to the panel mounting frame and the frame in turn bolted to the test fixture. The stringer ends were prevented from rotating and the skin was attached to a more rigid boundary than during the Reference 12 tests. A fatigue failure was defined as a failure occurring anywhere in the panel.

The Reference 12 test panels had nine (3 X 3) or twelve (3 X 4) bays. Strain gages were bonded to the skin at the rivet line. A fatigue failure was defined only as a failure occurring in the center bay section. The center bays in these panels had more flexible boundaries which resulted in smaller stress concentrations in the skin near the stringers than the AFFDL panels. The resultant fatigue life of the panels would therefore be longer for a given nominal stress value.

Reference 13 tests were performed on three riveted panels. There were three bays in each panel, but in this case, the stiffeners were not prevented from rotating. The ends of the stringers were not tied to the frame. The skin was clamped to the test fixture. The fatigue failures occurred at the upstream line of rivets in three panels and at the upstream panel junction with the test fixture in two of the panels. Strain gages were bonded to the skin on the rivet line and at the edge of the stiffener. As with the AFFDL tests, the ratio between the amplitudes of the strain response of the two gages varied with sound pressure levels (SPL) and with each particular panel.

Regression lines for the Reference 12 data are also presented in Figure 27. Data for two Reference 13 panels are also indicated.

These points fall between the Reference 12 and the AFFDL regression lines. It was theorized that during the AFFDL test, the skin bent around the stiffeners, while during the Reference 13 tests, the stiffeners twisted with the skin since they offered less resistance to torsion. This low torsional restraint caused the skin to have a more even stress distribution near the stiffener resulting in longer life than the AFFDL panels.

Reference 14 also reports sonic fatigue tests on skin-stringer panels similar to those tested by the AFFDL. Figure 27 shows the regression line for the average stress at the knee of the center stringers where the strain gages were located. This line (Reference 14) was between the Reference 12 and AFFDL regression lines. During the Reference 14 tests all but one of the fatigue failures occurred in the skin at the stringer knee. These panels used an adhesive in the joint and the failure line followed the sharp edge of the adhesive bead which formed a stress concentration.

The conclusion reached was that the Reference 12 stress equation be used in lieu of equations based on the AFFDL, Reference 13, Reference 14, or a combination of these data. Future sonic fatigue tests should use a similar test arrangement as used in the Reference 12 test. Only the center bays should be considered for fatigue analysis to best simulate typical aircraft boundaries. This technique was also recommended in Reference 15.

The range of stresses for each panel type calculated from the measured strains versus the acoustic input spectrum loading is



plotted in Figure 28. These stresses are not clearly high or low for any one panel type but tend to be of the same order of magnitude.

Figure 29 shows that for the same panel life, the nominal center stresses in the bonded-beaded Type I panels are lower than the stresses for the other configurations.

b. Bonded-Beaded Panels

A total of 60 bonded-beaded panels with two skin to bead thickness ratios and bead lengths were tested at varying sound pressure levels. The bead end and panel skin failures were considered valid data for use in the design chart developed in Section III of this report. The results showed that the length of the bead does not influence the slope of the stress-life curve when plotted on log-log paper. The influence of the skin-bead thickness ratio was pronounced. See Figure 30.

The panel life, panel depth, and manufacturing costs provide the designer with various trade-offs. See Figure 31. The bonded-beaded panels have a superior sonic fatigue resistance compared to the skin-stringer configuration (see Figure 32); however, the bonded-beaded panels are more expensive to manufacture. The additional advantage of the bonded-beaded panels is their shallower depth compared to the rib-stringer design which can become a controlling factor if space limitations exist.

c. Chem-milled Panels

A total of twenty identical panels were tested at essentially four loading levels. The ten failures in the chem-milled areas



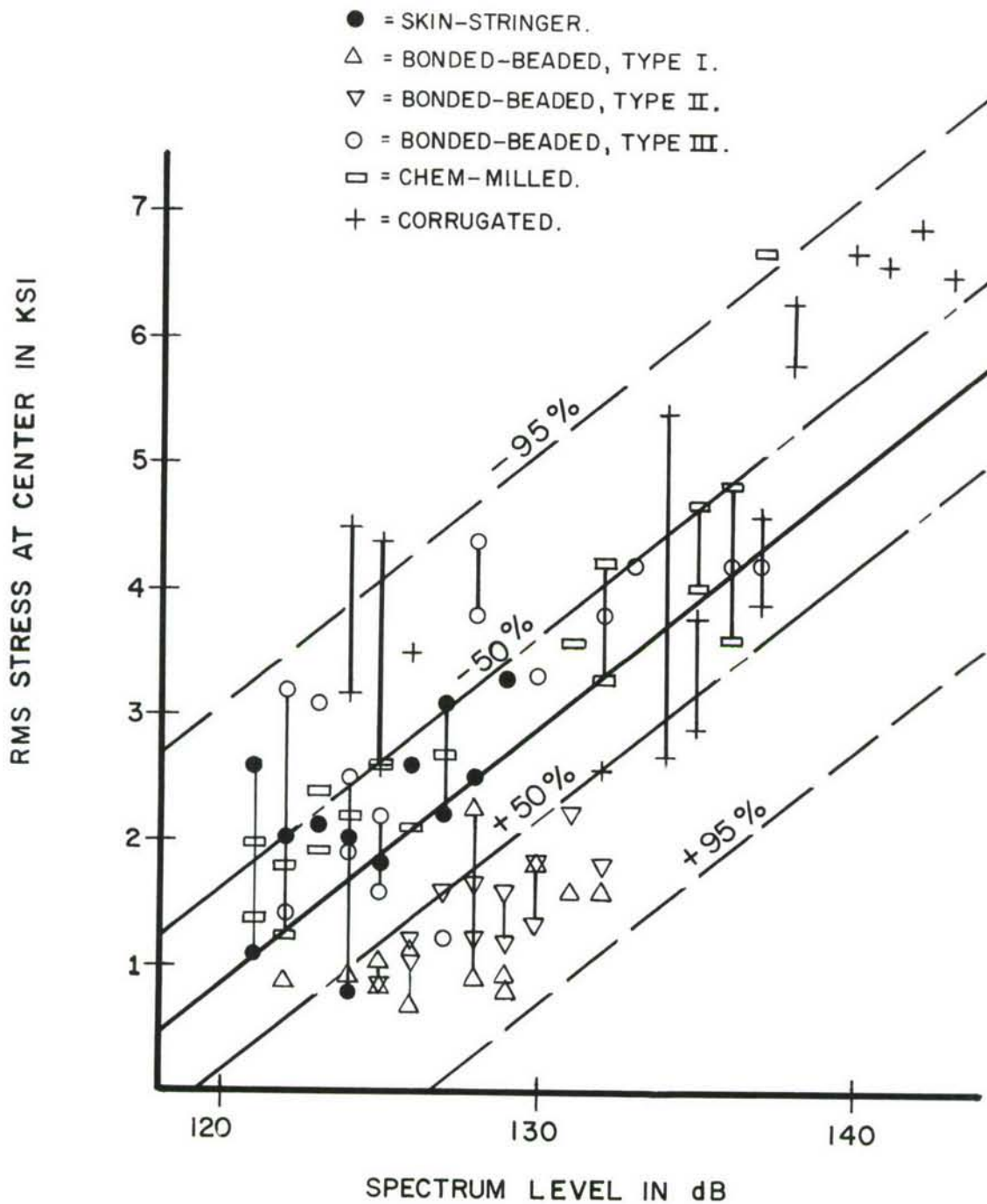


Figure 28. Stress Range Versus Acoustic Loading

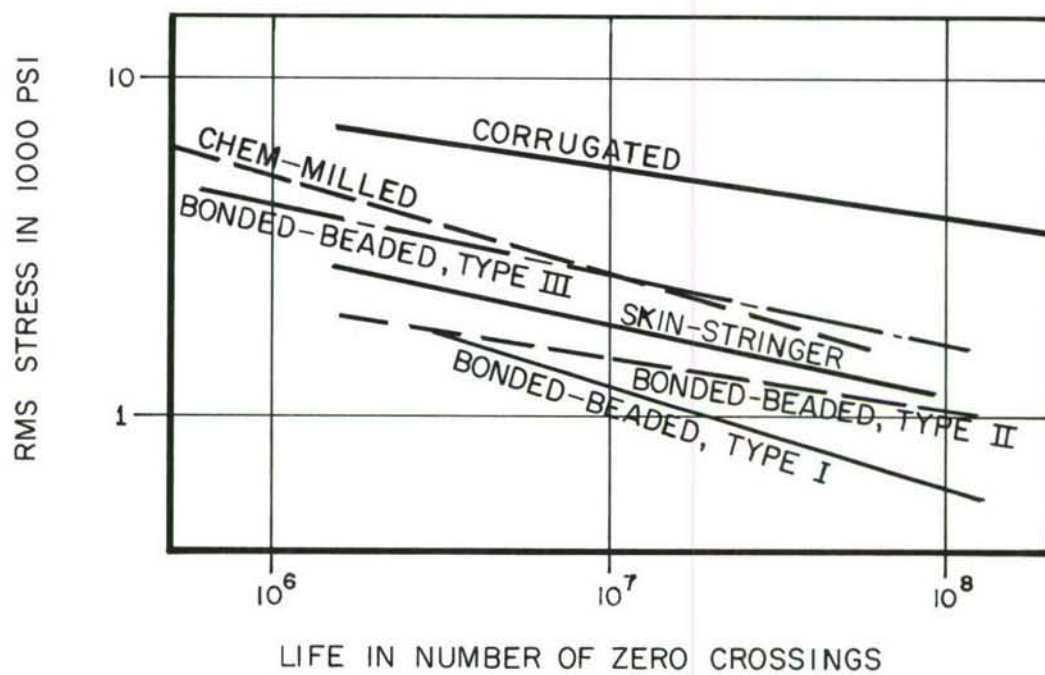


Figure 29. RMS Stress - Life Relation  
(Comparison Between All Panel Types)

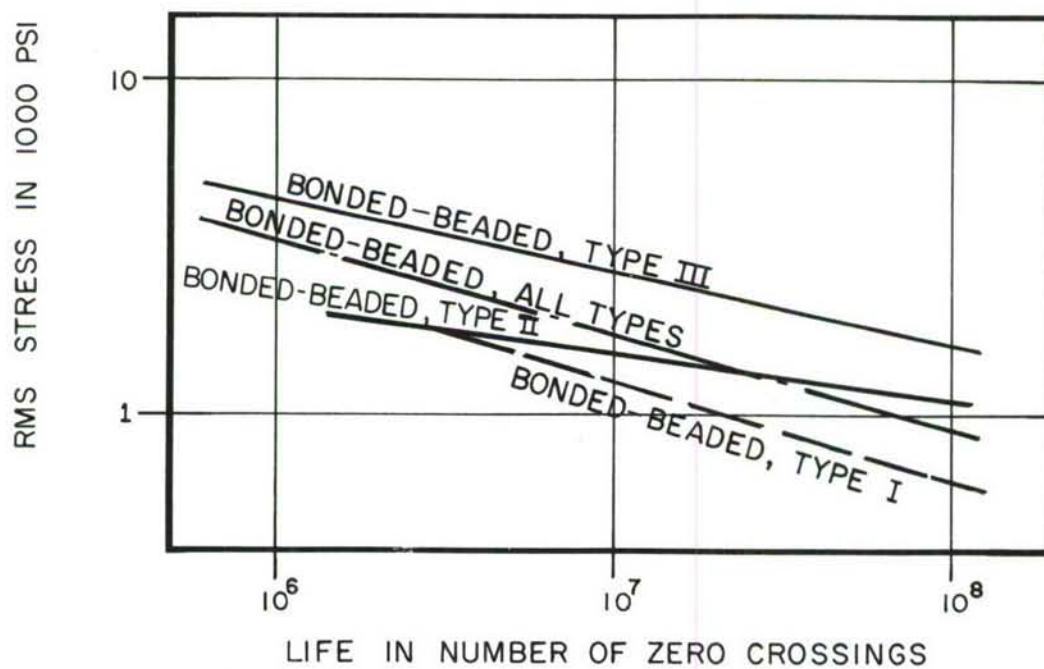
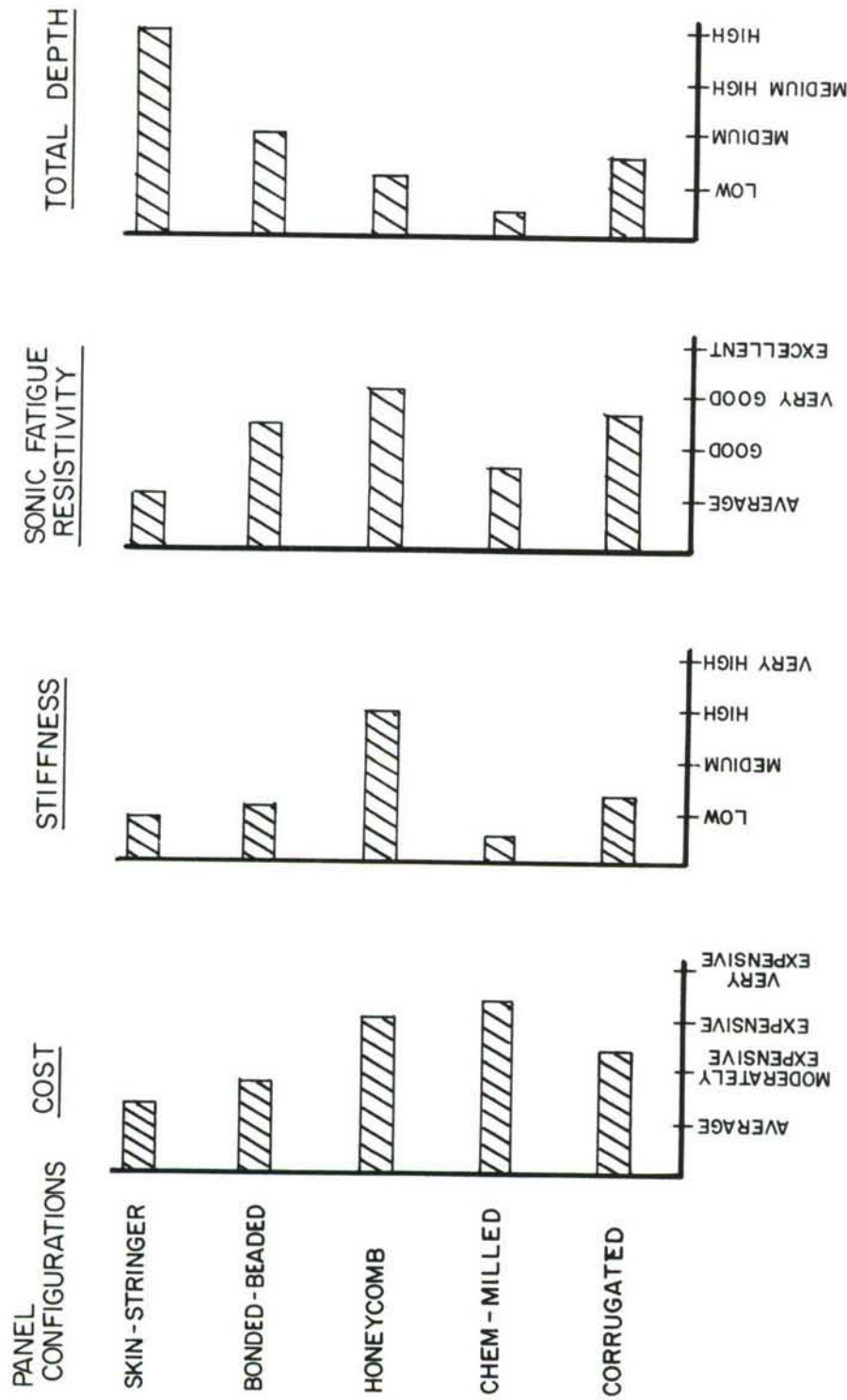


Figure 30. RMS Stress - Life Relation (Comparison,  
Bonded-Beaded Panels)



NOTE: ALL DESIGN PARAMETERS BASED ON PANELS  
WITH SURFACE DENSITY OF 1LB/FT<sup>2</sup>.

Figure 31. Panel Selection Criteria

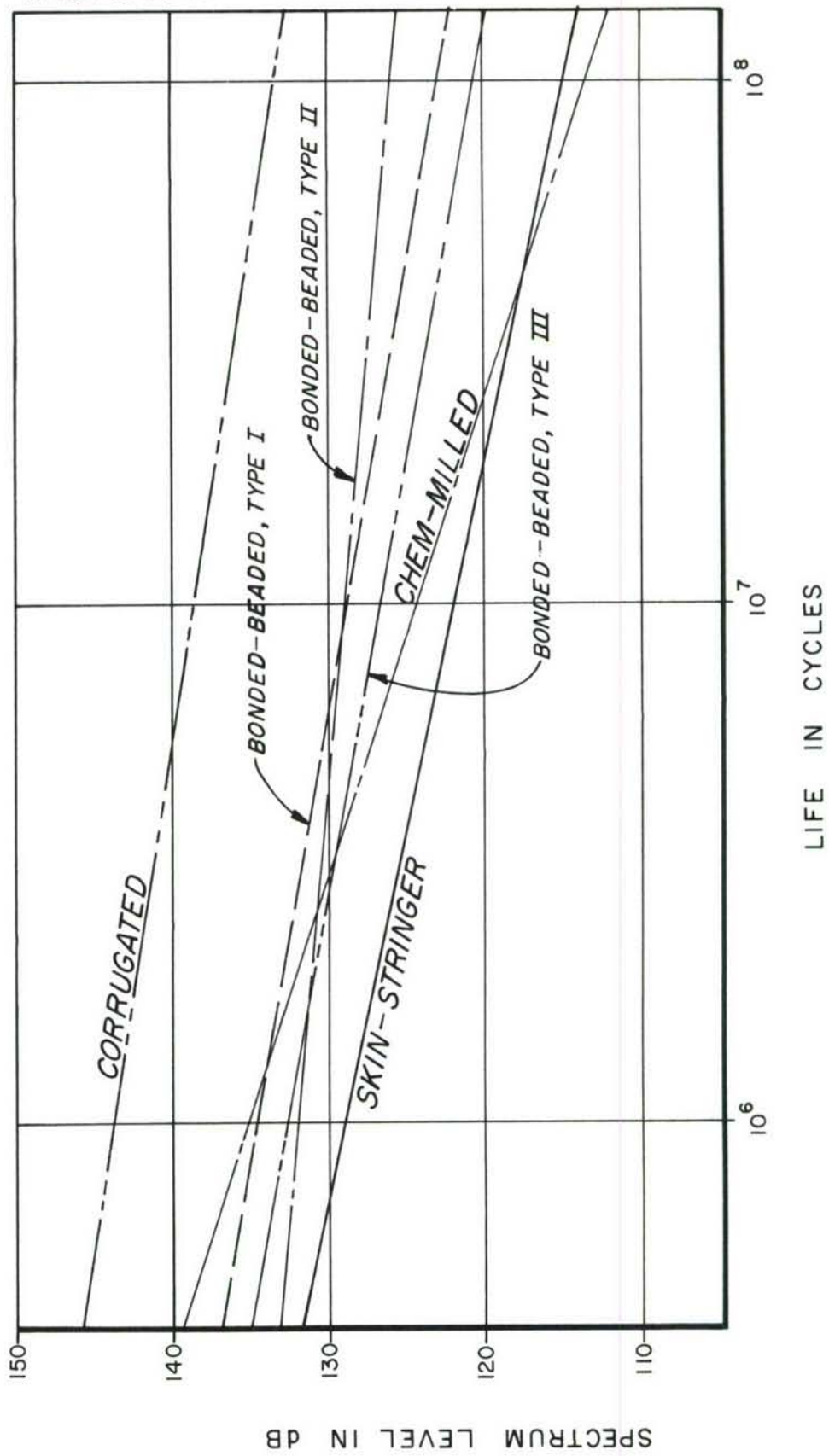


Figure 32. Spectrum Level - Life Relation

were considered valid data for use in design chart development. Additional sonic fatigue life data on other chem-milled panels are not available. These additional data are required before a design chart for the chem-milled panels can be constructed. Design data are needed for additional panels over a range of geometric parameters. This would require additional sonic fatigue testing. The results of the panel life comparisons are given in Figure 32. The chem-milled panels have superior sonic fatigue resistance compared to the skin-stringer panels, but were rated below the bonded-beaded panels. The chem-milled panels were judged to be more expensive to manufacture than either the skin-stringer or bonded-beaded (see Figure 31). The advantage of the chem-milled panels is their shallow depth which can become the controlling factor if space limitations exist.

#### d. Corrugated Panels

The corrugated panels show superior sonic fatigue resistance compared with all other panel types tested under this program. See Figure 32. These panels were also the stiffest of those tested. In general the corrugated panels were loaded by higher acoustic pressures which induced higher nominal stresses in the panels for the same number of stress reversals required to produce a panel failure.

These panels have a superior sonic fatigue resistance; however, small internal material failures and delaminations are difficult to detect. High cost inspection equipment (x-ray or ultra-sonic equipment) is required to determine the location of internal failures.



The manufacturing cost of corrugated panels was judged relatively high compared with the cost of skin-stringer panels. The advantages of the corrugated panels are the stiffness and shallow depth of the panel in comparison with the skin-stringer design.

Table 13 gives the loading, stress response, life, and failure location for the corrugated panels tested. These data are for one panel configuration. Additional sonic fatigue data on other corrugated panels are not available. These additional data are required before design charts can be developed for panels of this type and testing would be required for additional panels covering a range of geometric parameters.

## APPENDIX A

## DESCRIPTION OF TEST SPECIMENS

All of the sonic fatigue test panels used for these tests had external dimensions of 24" x 30". Since the design criterion for each panel was 1 lb/sq ft, each panel weighed  $5.0 \pm 0.2$  lbs. The variation in weight was not expected to affect fatigue life. The background which led to the various designs is given in the following paragraphs for each configuration. Specific dimensional details are given in Figures A-1 through A-5 and Table A-1.

#### 1. Skin-Stringer Panel (Figure A-1)

The two factors that mainly affected the final design of this panel were the weight and rib spacing. Based on previous experience and utilization of existing sonic fatigue skin-stringer design charts, a panel with 1 lb/sq ft density requires a rib spacing on the order of 6-9 inches. Since the overall dimensions of the panel were set at 24" x 30", the division into three bays gave the most logical bay dimension. The design of a skin-stringer panel requires that the "Z"-shaped or channel-shaped stringer be one standard metal gage heavier than the skin. Two end Z-sections were added to stabilize the stringers against excessive rolling motion. The doubler on the long side of the panel stiffens the edge, prevents cracks along the fastening line and also acts as a shim to provide a level mating surface. The doubler and stabilizing rib are bonded to the plate since protruding rivet heads would provide an uneven surface for

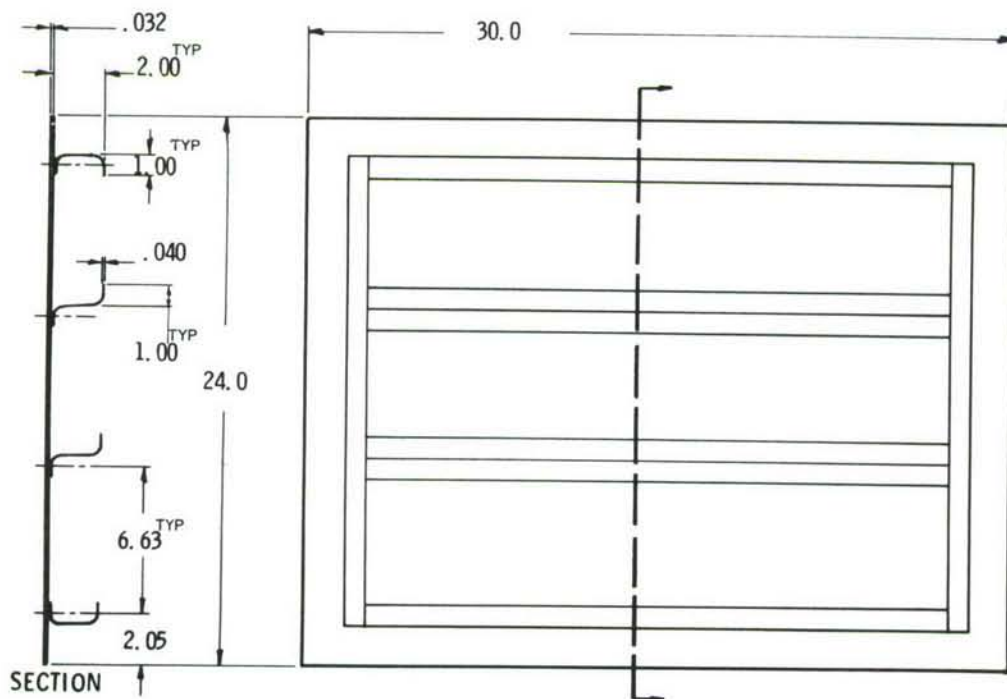
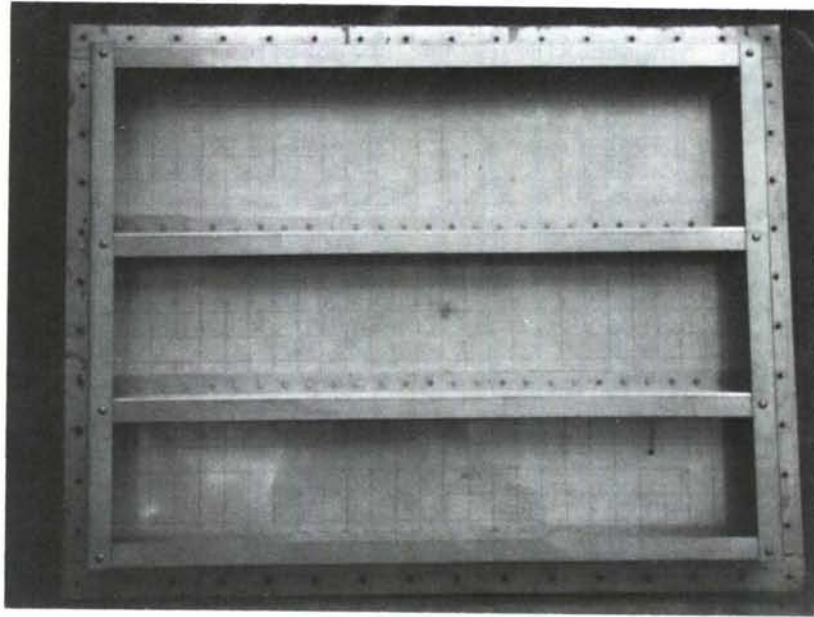


Figure A-1. Skin-Stringer Panel

fastening the panel to the test frame. Also, the bonded doubler provides more damping, better stress distribution, and is not as susceptible to cracking under the bolt heads used for fastening the panel to the support structure. It was necessary that the rib be at least 1.5 inches deep. The final rib depth of 2.0 inches was selected to obtain a total panel weight of 5 lbs.

## 2. Chem-milled Waffle Grid Panel (Figure A-2)

The basic design parameter for this panel was weight, but other factors were of importance. Based upon past experience, the major dimension of a single grid in the pattern should lie between 2 and 4 inches. It was also necessary to design the lands with enough height to insure adequate panel stiffness. Chem-milling requirements fixed the land width in the order of 0.2 inch and a cell thickness of not less than 0.015 - 0.020 inch. A minimum edge thickness of 0.090 inch was used in all the panel designs to maintain section properties. Combining all these requirements in conjunction with the 5.0 pound weight requirement resulted in the proposed design.

## 3. Bonded-Beaded Panels (Figures A-3 and A-4)

There are many parameters to vary in designs of this type of panel and it is difficult to determine the most important. From previous sonic fatigue tests on bonded-beaded panels and certain production limitations, the following guidelines were used in the design.

- a. The beads should be double ended to prevent failures at the bead end. See Figures A-3 and A-4.



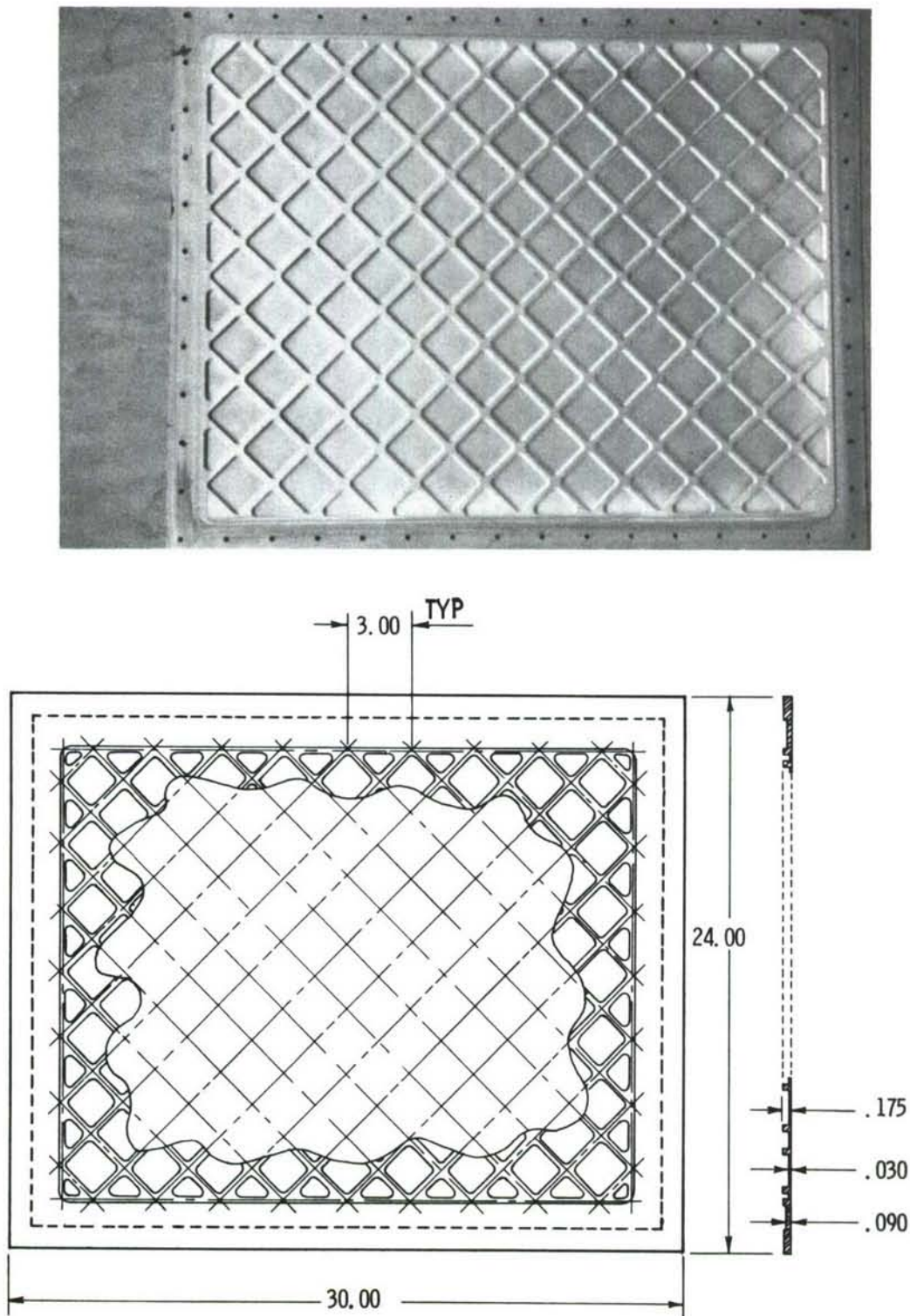


Figure A-2. Chem-Milled Panel



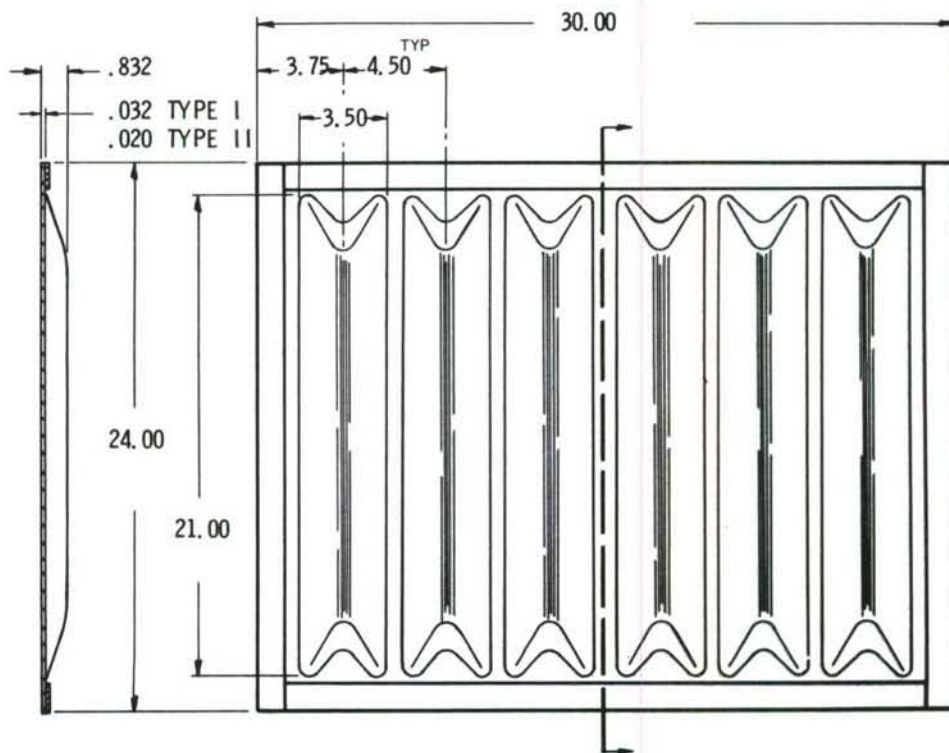
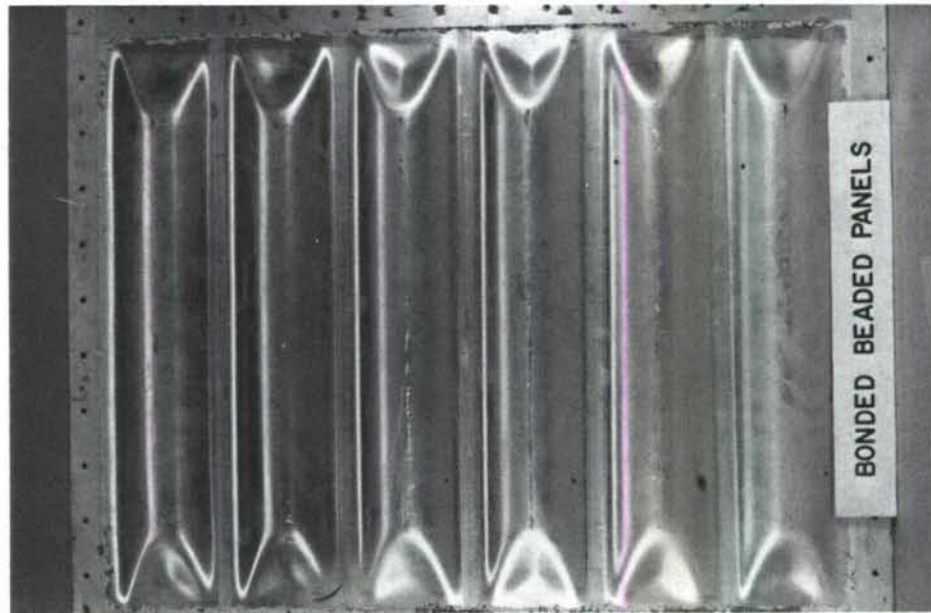


Figure A-3. Bonded-Beaded Panel Type I and Type II

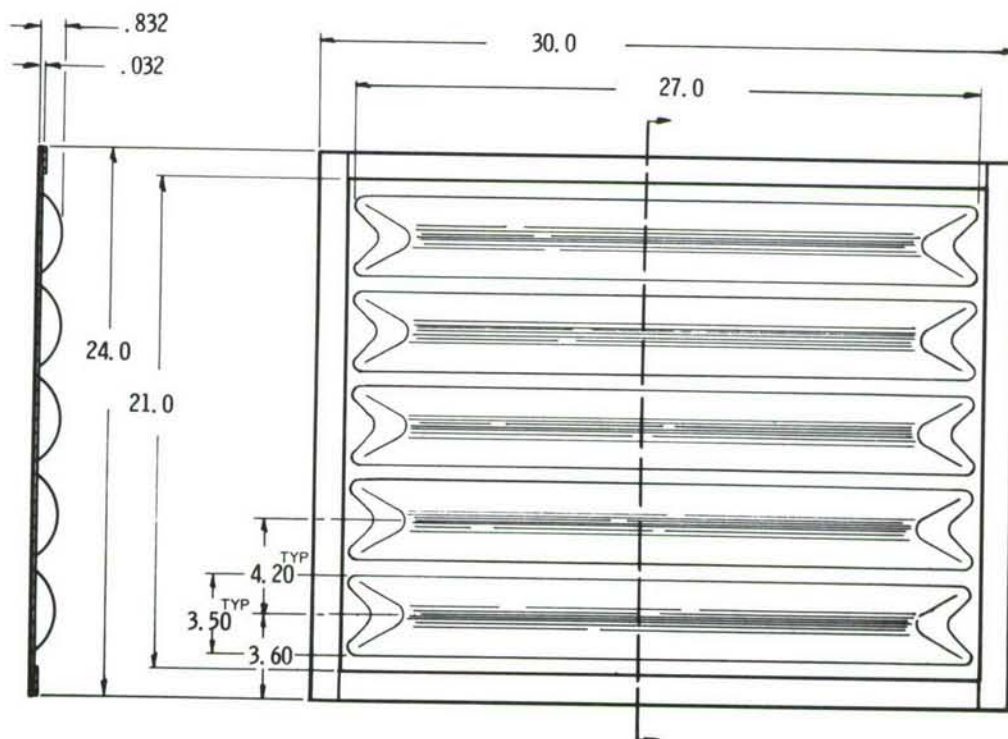
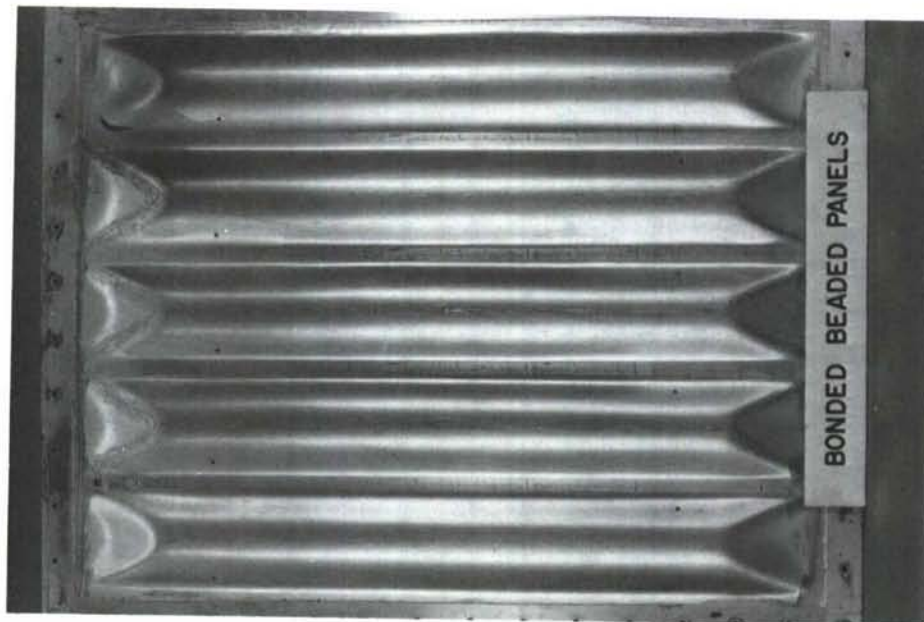


Figure A-4. Bonded-Beaded Panel Type III

b. Edge doublers should be provided to prevent attachment failures.

c. The depth of bead should be as great as possible to maintain panel stiffness; however, due to fabrication limitations and material ductility, the bead height to width ratio must be limited to 1:4.5.

d. From previous experience it was necessary to keep bead width on the order of 3 to 4 inches or less.

e. It is desirable to keep the beads as close together as possible; however, this is limited to one-half inch due to fabrication limitations.

f. Past results have shown that when bead thickness and panel thickness have been equal, most of the fatigue failures occur on the bead at the panel center when proper bead end design was utilized and when sufficient edge thickness was used.

After consideration of all the above items, the bead to panel thickness ratio and bead length were considered the most important variables to be considered in tests of limited scope. Since failures usually occurred in the bead of an otherwise well designed panel, the bead thickness was increased in the Type II design (see Table A-1) while keeping total panel thickness constant. The panel size of 24" x 30" offered a convenient means for varying bead length by changing the bead orientation in the Type III design. This variation would also indicate which direction the beads should be orientated on a rectangular panel. Using the above considerations and

TABLE A-1

## DETAIL TEST SPECIMEN DIMENSIONS

PANEL TYPE	PANEL DEPTH (in.)	SKIN THICKNESS (in.)
Skin-Stringer Stiffener Thickness (in.)	2.0	0.032
Bonded-Beaded Bead Length (in.)	21	27
Skin Thickness (in.)	0.032	0.032
Bead Thickness (in.)	0.032	0.032
Number of Beads	6	5
Panel Depth (in.)	0.832	0.832
Chem-milled	0.175	0.030
Corrugated	0.80	0.020

varying parameters to obtain the 1 lb/sq ft density, the designs were completed.

#### 4. Corrugated Skin Sandwich Panel (Figure A-5)

Previous sonic fatigue tests on corrugated panels were designs having a single face sheet with spot-welded corrugations. Most of the failures recorded occurred at the spot welds. A second face sheet was added since this would increase the static strength of the panel and it was decided that the thickness of the panel should be the same as a typical honeycomb sandwich panel. In addition, the corrugation should be bonded to the face sheets for increased fatigue strength. The final design should be used in applications where high static strength (stiffness) is required in one direction of orientation. Multiple layers of fiberglass cloth were layed up on the back side of these panels in the edge region.



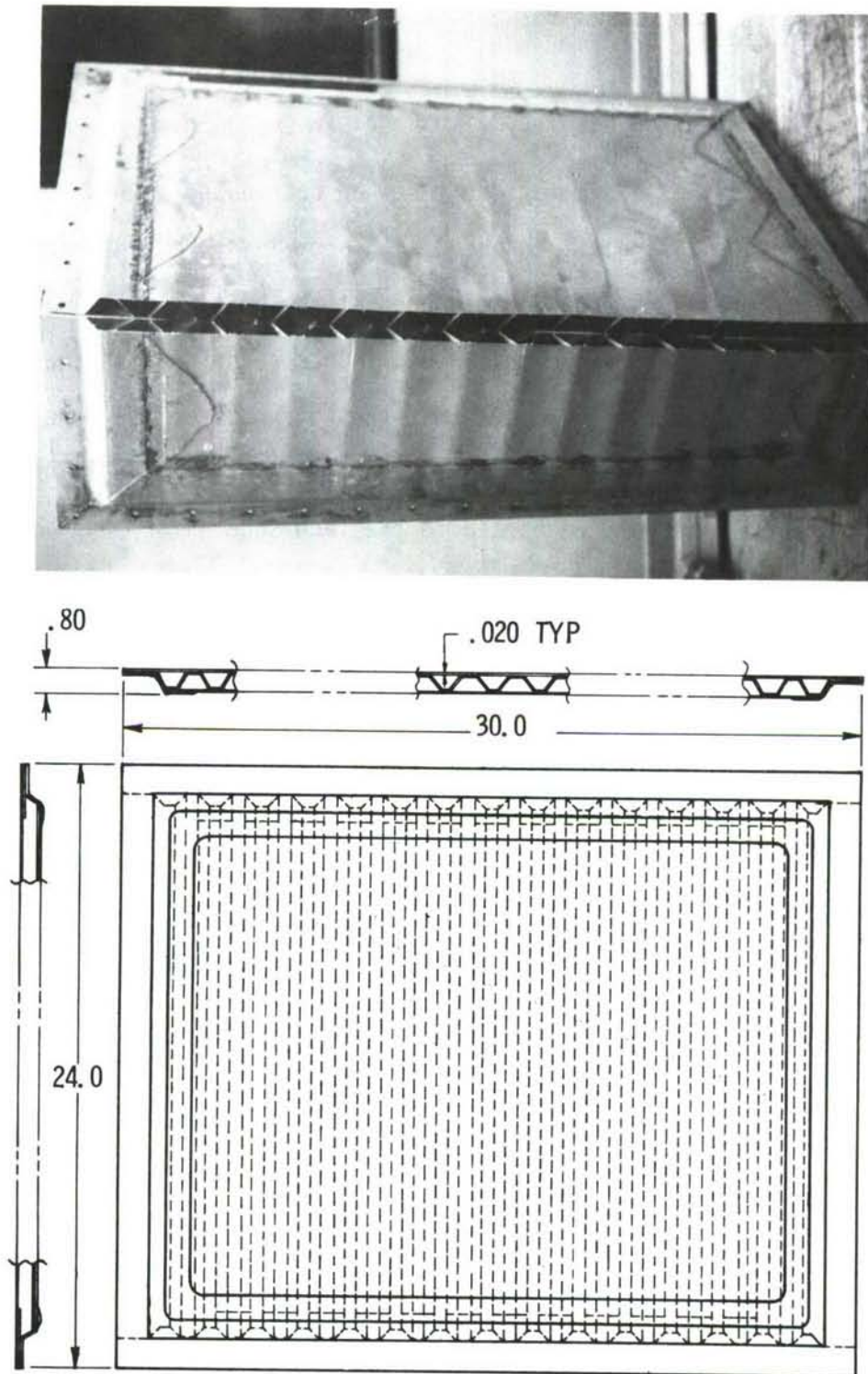


Figure A-5. Corrugated Panel

## APPENDIX B

### DESCRIPTION OF THE AFFDL WIDE BAND NOISE CHAMBER AND INSTRUMENTATION SYSTEM

#### 1. TEST FACILITY

The panels were tested in the Wide Band Noise Chamber of the AFFDL Sonic Fatigue Facility. This facility (Figure B-1) consists of three separate areas.

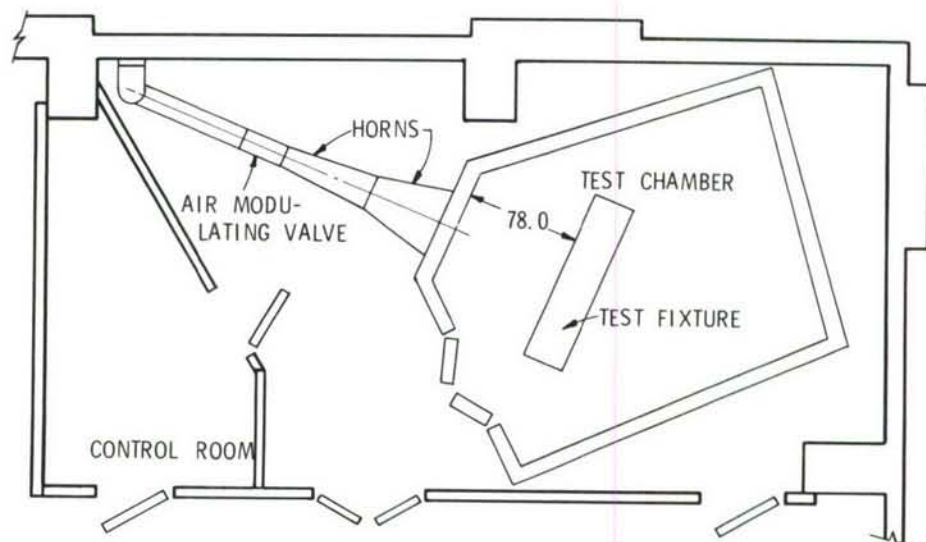


Figure B-1. Floor Plan of the Wideband Acoustic Fatigue Facility

##### a. The Reverberation Chamber

This chamber has a floor area of  $230 \text{ ft}^2$  and an approximate volume of  $2500 \text{ ft}^3$ . The room is isolated from the surrounding structure by rubber absorbers. The walls are constructed from steel sheet, three 1/16-inch thick sheets are separated by 4-inch deep channels (Figure B-2), and the space between the steel sheets is filled with fiber glass. The access opening to the chamber is  $8 \times 8 \text{ ft}$ , and can

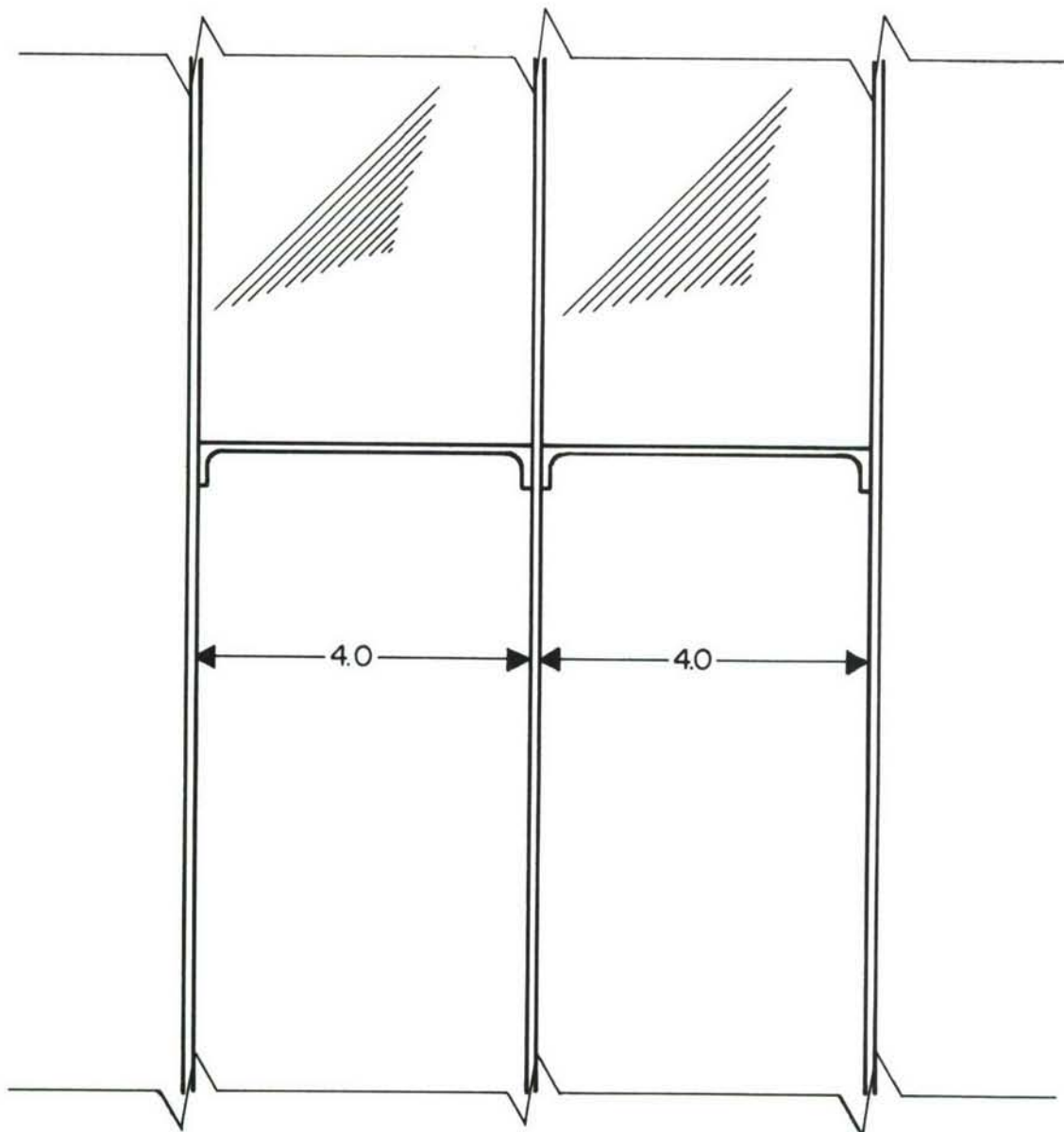


Figure B-2. Wall Detail for the Wideband Chamber

closed off with two heavy steel refrigerator type doors. The odd shape of the test chamber was chosen to improve reverberation qualities.

b. Noise Source Area

The noise sources (siren or air modulator) are located in this area. The noise source is connected to the test chamber by an exponential horn system.

c. The Control Room

The noise input to the test chamber is controlled and monitored in this room which is isolated from the noise source area by a similar type wall construction as is used for the reverberation room, the only difference being the wall facing the noise source area is perforated to improve the noise absorption in this area. The control equipment (Figure B-3) consists of a beat frequency oscillator, spectrum shaper, and amplifier for the modulator and motor controls for the siren. The noise in the test chamber is monitored by an octave band analyzer and level recorder.

d. Noise Sources

The noise in the test chamber is generated by either a random siren or air modulator.

(a) Random siren: This is the older of the two sources and was internally developed (see Figure B-4). The noise is generated by randomly interrupting the air stream from five nozzles with four counterrotating rotors. The noise spectrum generated by the siren is a function of the speed-variation of the rotors.

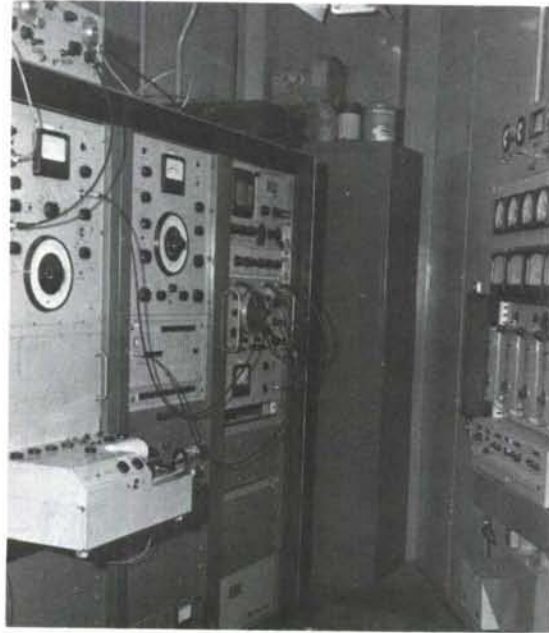


Figure B-3. Controls for the Siren and Air Modulator

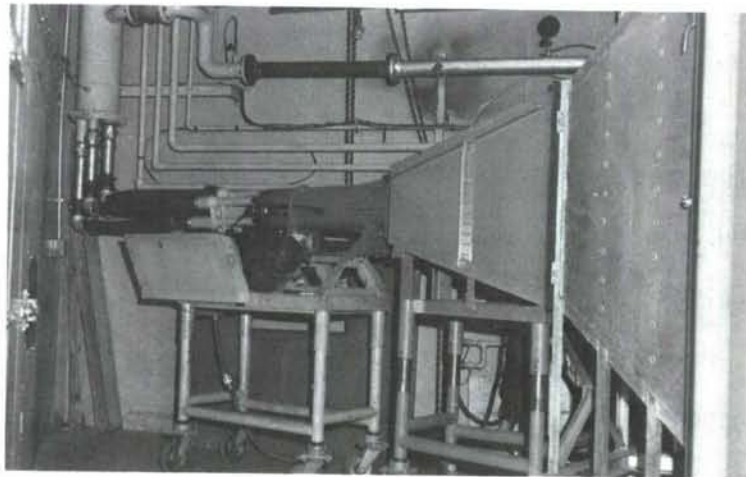


Figure B-4. Wideband Siren with Three Horn System



Tests showed that a practically flat 1/3 octave band spectrum in the 80 to 1,000 Hz range was obtained with the following rotor speeds (in the direction of the air flow): 1300 - 2000, 2300 - 3000, 3400 - 4000, and 1300 - 1800 rpm. The level of the noise produced by the siren depends on the air pressure supplied to the siren. The maximum pressure available at the siren inlet is 28 psi. This pressure produces an overall sound pressure level of 160 dB at the horn mouth of an 87 inch long exponential horn.

(b) Air Modulator: (Figure B-5) The second noise source is a Wyle air modulating valve. This system is more versatile than the siren. The valve is electromagnetically driven and interrupts

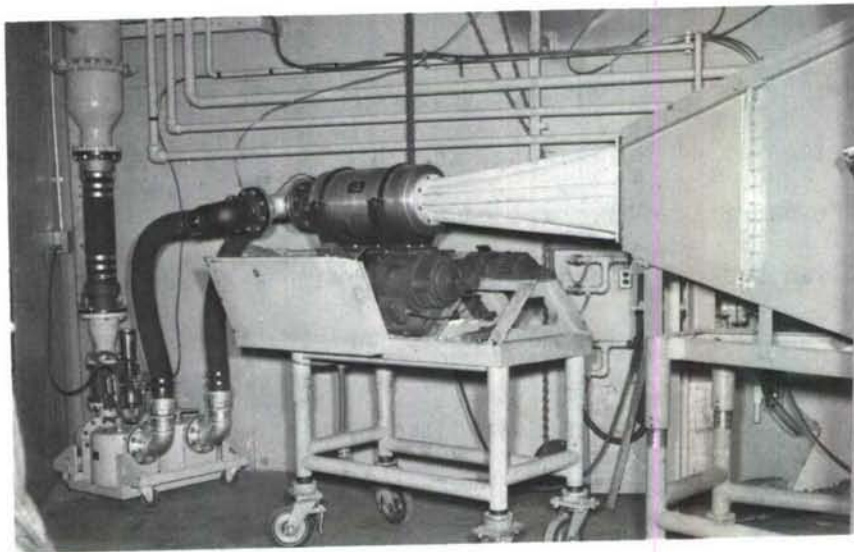


Figure B-5. Air Modulator with Two Horn System

the air flow according to an electronic signal supplied by a signal generator and amplifier system. The frequency output of the generator can be easily adjusted and the noise output can be limited to a narrow band, creating high intensity acoustic inputs in the neighborhood of the first natural frequency of the test specimens. The disadvantage of this system is that only noise in the 50 to 500 Hz range can be produced and that the higher frequencies are generated as higher harmonics of the frequencies below 500 Hz. The noise intensity in the region over 500 Hz drops sharply with increasing frequency.

e. Horn System

The first horn section, which is connected to the siren, is 43 inches long and constructed from fiber glass reinforced plastic. Its lower cut-off frequency is 200 Hz. This section is used when the frequencies below 200 Hz are not required for the test environment. The second section is 44 inches long, the third section is 40 inches long. Both are fabricated from welded aluminum. These horn sections are double walled and the cavities are filled with fine sand, which supplies the necessary mass and damping to the structure.

Most tests are performed with the combination of first and second horn sections. The cut-off frequency of this system is 120 Hz.

f. Test Fixture

The test fixture used for these tests accommodates five specimens, each with an exposed area of 30 x 24 inches. This was

accomplished by constructing an odd shaped welded fixture from 0.50 inch thick steel plates, reinforced by channels and internal braces. The back of the panels was accessible through five hatches in the back of the structure. The inside was lined with two inch thick acoustic foam to eliminate internal standing waves and reduce the internal noise levels. The fixture is shown in Figure B-6.

g. Location of the Test Fixture

Testing five test specimens with the same acoustic load required a series of tests to determine the location of the fixture in relation to the noise source. These tests were performed with the openings in the front of the fixture closed with 0.75 inch thick plywood panels. Twelve microphones were placed four inches in front of the fixture. The results of these tests showed that the optimum location was 78 inches from the horn mouth, and that a plywood wing 24 inches wide should be added to each side of the fixture to obtain an overall sound pressure variation over the surface of the fixture of less than 1 1/2 dB. This configuration was used for all the panel tests.

2. INSTRUMENTATION AND DATA ANALYSIS

Each panel was instrumented with a rosette strain gage located in the center of the panel and one single element gage was located at the center of one of the long sides and one at the center of one of the short sides. The skin-stringer panels had a gage on the edge of a stringer instead of in the center. Each strain gage element operated as a single active gage and was connected to the data module

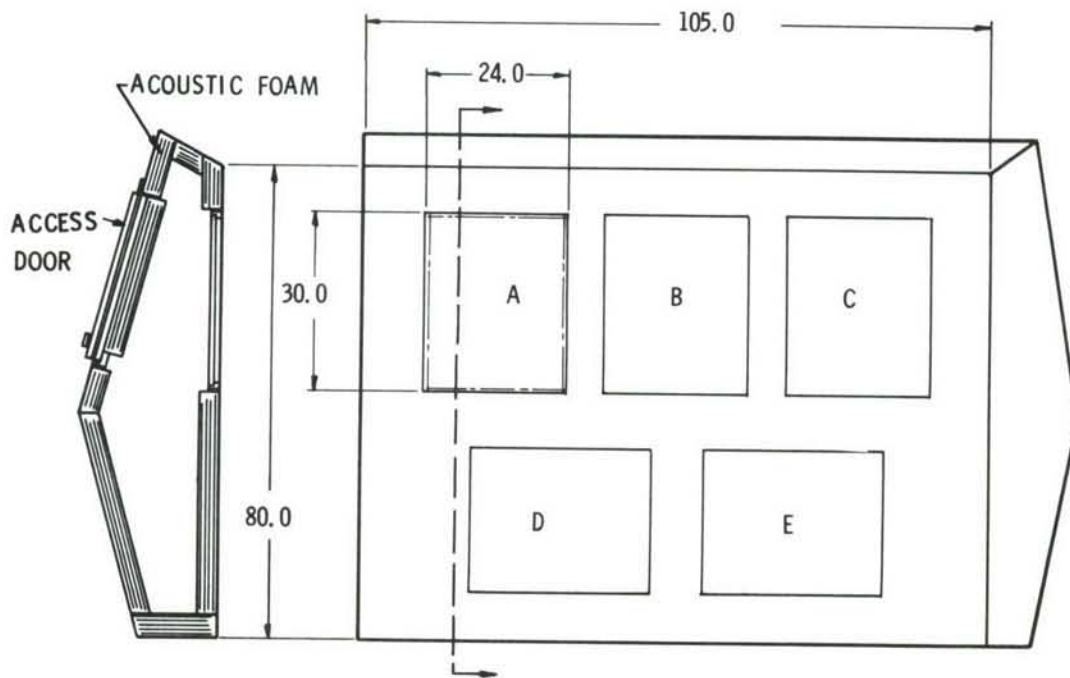


Figure B-6. Test Fixture



in a quarter bridge arrangement. High intensity piezoelectric microphones were used to measure the acoustic sound field. One was located at the sound generator horn mouth and monitored the sound pressure level and spectrum. The noise impinging on the panels was measured with a microphone mounted at the center of each panel, four inches from the surface. The data modules for strain and acoustic signal conditioning each consist of two d-c 1000 gain amplifiers with a resistive attenuator network in between. The amplifiers are operated in a fixed gain position and the attenuator is remotely controlled to change the gain in 10 dB increments. The test data were monitored on line with oscilloscopes and an octaveband analyzer to check levels and frequency content. The data to be further analyzed were recorded using 12-channel FM tape transports. The monitor microphone was connected to a separate octave-band analyzer associated with the noise generator control system. A block diagram of the data collection and monitoring system is shown in Figure B-7.

One-third octave and narrowband analysis of the test data were performed using the data reduction system shown in Figure B-8. Reel and loop tape transports were used for playback of the recordings into the data analyzers. In the analysis process, about 15 sec of data is transferred from the reel of tape, 12 channels at a time, to a tape loop which enables the analysis of a small segment of data. One-third octave analysis was performed with a multi-filter (connected in parallel) analyzer at high speed and plotted using an X-Y plotter. Narrowband analysis was performed with a digital analyzer and also plotted using an X-Y plotter.



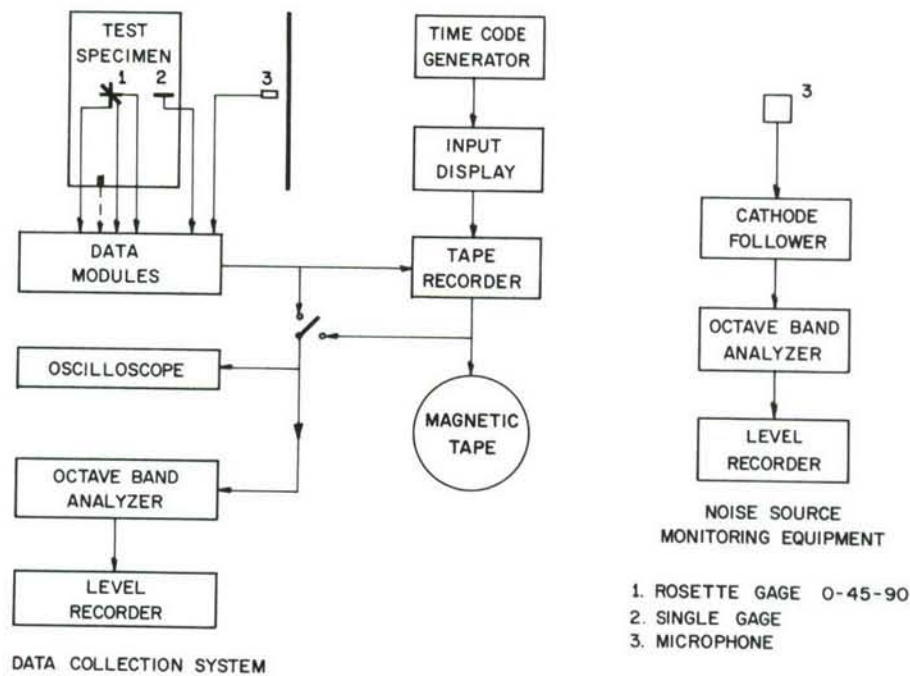


Figure B-7. Data Collection and Monitoring System

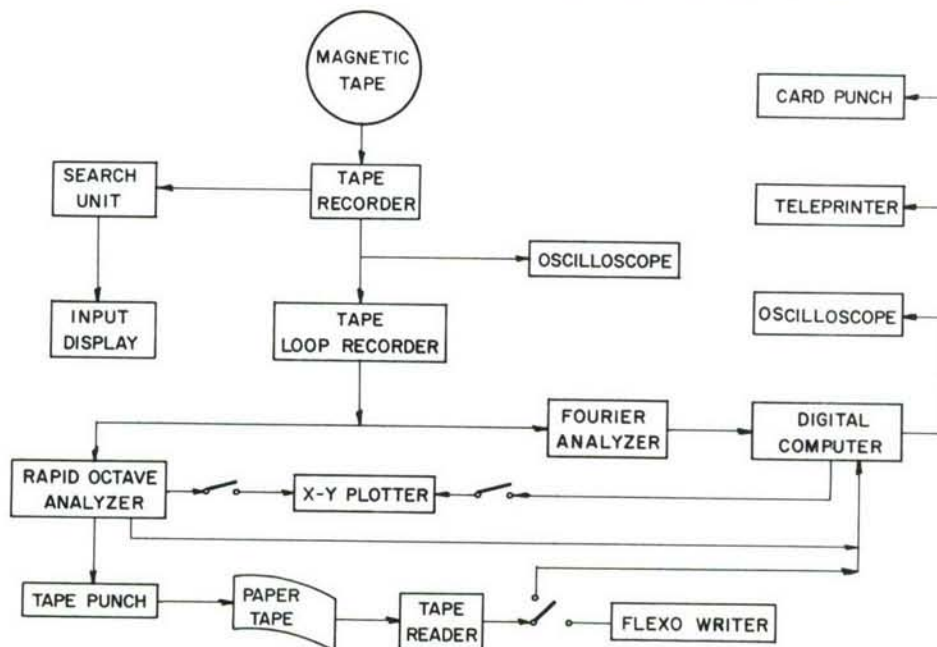


Figure B-8. Data Reduction System

## APPENDIX C

## STATISTICAL TECHNIQUES

One of the features of this program has been that sufficient data were taken to provide a reasonable degree of confidence in the indicated trends. The number of test panels was chosen to define a given point on the S-N curve with a defined reasonable degree of assurance. In References 16 and 17 it is shown that requirements for statistical confidence may be stated as

$$\epsilon = 1 - N\beta^{N-1} + (N - 1) \beta^N \quad \text{C-1}$$

where  $\epsilon$  is the degree of assurance that at least 100 $\beta$  percent of an infinite number of specimens will fail between the longest and shortest failure times encountered in a sample size N. For example, if five specimens are tested, there is an 80% assurance that the experimental data limits contain 50% of all possible cases. The equation has been calculated for  $\epsilon$  in Table C-1 for values of  $\beta$  ranging from 0.1 to 0.9 and values of N from 1 to 20. The 80% degree of assurance was considered as the minimum acceptable for this program.

$\beta$		.10	.20	.30	.40	.50	.60	.70	.80	.90
N										
1		0.00	0.00	0.00	0.00	0.00	0.00	0.00	0.00	0.00
2		81.00	64.00	49.00	36.00	25.00	16.00	9.00	4.00	1.00
3		97.20	89.60	78.40	64.80	50.00	35.20	21.60	10.40	2.80
4		99.63	97.28	91.63	82.08	68.75	52.48	34.83	18.08	5.23
5		99.95	99.33	96.92	91.30	81.25	66.30	47.18	26.27	8.15
6		99.99	99.84	98.91	95.90	89.06	76.67	57.98	34.46	11.43
7		100.00	99.96	99.62	98.12	93.75	84.14	67.06	42.33	14.57
8		100.00	99.99	99.87	99.15	96.48	89.36	74.47	49.67	18.69
9		100.00	100.00	99.96	99.62	98.05	92.95	80.40	56.38	22.52
10		100.00	100.00	99.99	99.83	98.93	95.36	85.07	62.42	26.39
11		100.00	100.00	100.00	99.93	99.41	96.98	88.70	67.79	30.26
12		100.00	100.00	100.00	99.97	99.58	98.04	91.50	72.51	34.10
13		100.00	100.00	100.00	99.99	99.83	98.74	93.63	76.64	37.87
14		100.00	100.00	100.00	99.99	99.91	99.19	95.25	80.21	41.54
15		100.00	100.00	100.00	100.00	99.95	99.48	96.47	83.29	45.10
16		100.00	100.00	100.00	100.00	99.97	99.67	97.39	85.93	48.53
17		100.00	100.00	100.00	100.00	99.99	99.79	98.07	88.18	51.82
18		100.00	100.00	100.00	100.00	99.99	99.87	98.58	90.09	54.97
19		100.00	100.00	100.00	100.00	100.00	99.92	98.96	91.71	57.97
20		100.00	100.00	100.00	100.00	100.00	99.95	99.24	93.08	60.83

TABLE C-1

CALCULATED VALUES OF  $\epsilon$

## REFERENCES

1. F. F. Rudder & H. E. Plumblee, AFFDL-TR-74-112, Sonic Fatigue Design Guide for Military Aircraft, Air Force Flight Dynamics Laboratory, WPAFB, Ohio, May 1975.
2. R. C. W. van der Heyde et al, TM-73-149-FYA, Sonic Fatigue Resistance of Skin-Stringer Panels, Air Force Flight Dynamics Laboratory, WPAFB, Ohio, December 1973.
3. R. C. W. van der Heyde et al, TM-73-150-FYA, Results of Acoustic Fatigue Tests on Three Series of Bonded-Beaded Panels, Air Force Flight Dynamics Laboratory, WPAFB, Ohio, September 1974.
4. R. C. W. van der Heyde et al, TM-73-151, Results of Acoustic Fatigue Tests on a Series of Chem-Milled Panels, Air Force Flight Dynamics Laboratory, WPAFB, Ohio, December 1973.
5. R. C. W. van der Heyde et al, TM-73-152, Results of Acoustic Fatigue Tests on a Series of Corrugated Panels, Air Force Flight Dynamics Laboratory, WPAFB, Ohio, July 1974.
6. L. D. Jacobs, D. R. Lagerquist, AFFDL-TR-68-44, Finite Element Analysis of Complex Panel Response to Random Loads, Air Force Flight Dynamics Laboratory, WPAFB, Ohio, October 1968.
7. R. C. W. van der Heyde & A. W. Kolb, "Sonic Fatigue Resistance of Lightweight Aircraft Structures", Paper Nr 20, AGARD Conference Proceedings Nr 113, Symposium on Acoustic Fatigue, May 1973.
8. I. Holehouse, "Sonic Fatigue of Diffusion-Bonded Titanium Sandwich Structure", Paper No. 15, AGARD Conference Proceedings No. 113, Symposium on Acoustic Fatigue, May 1973.
9. J. W. Miles, "On Structural Fatigue Under Random Loading", J. A. S. Volume 21, November 1954.
10. C. D. Johnson, Stress and Vibration Analysis of Bonded-Beaded Sonic Fatigue Panels, (Problem 4 ASIAC), October 1972.
11. W. J. Dixon, Editor, BMD Biomedical Computer Programs, Health Sciences Computing Facility, Department of Biomathematics, University of California, January 1973.
12. J. R. Ballentine, et al, AFFDL-TR-67-156, Refinement of Sonic Fatigue Structural Design Criteria, Air Force Flight Dynamics Laboratory, WPAFB, Ohio, January 1968.
13. M. J. Jacobson, NOR 69-111, Acoustic Fatigue Design Information for Skin-Stiffened Metallic Panels, Northrop Corporation, Hawthorne, Calif., August 1969.



REFERENCES CONT'D

14. J. A. Hayes, AFFDL-TR-66-78, Sonic Fatigue Tolerance of Glass Filament Structure: Experimental Results, Air Force Flight Dynamics Laboratory, WPAFB, Ohio, December 1966.
15. E. E. Ungar, K. S. Lee, AFFDL-TR-67-86, Considerations in the Design of Supports for Panels in Fatigue Tests, Air Force Flight Dynamics Laboratory, WPAFB, Ohio, September 1967.
16. S. S. Wilks, Mathematical Statistics, Princeton University Press, Princeton New Jersey.
17. A. P. Berens et al, AFFDL-TR-71-113, Experimental Methods in Acoustic Fatigue, Air Force Flight Dynamics Laboratory, WPAFB, Ohio, March 1972.